Todaria *et al.*
Future Journal of Pharmaceutical Sciences (2024) 10:25
https://doi.org/10.1186/s43094-024-00601-9

Future Journal of
Pharmaceutical Sciences

REVIEW

Open Access

Biogenic metallic nanoparticles as game-changers in targeted cancer therapy: recent innovations and prospects

Moulika Todaria[1], Dipak Maity[2*] and Rajendra Awasthi[1*]

Abstract

Background Cancer is a significant global health issue, resulting from uncontrolled cell division leading to abnormal cell or tissue growth. Traditional chemotherapeutic techniques have investigated a wide variety of pharmaceutically active molecules despite their poor bioavailability, quick renal clearance, inconsistent distribution, and unavoidable side effects. Green synthesis, unlike chemical methods, prioritizes eco-friendliness and cost-effectiveness. Using natural sources like plant extracts, it minimizes environmental impact, reduces costs, and aligns with sustainability goals. Operating under milder conditions, it consumes less energy compared to traditional approaches. Green synthesis is a highly promising and efficient method for producing nanoparticles due to its versatility and scalability.

Main body Nanotechnology is making progress in cancer treatment because of nanoparticles' tiny size, large surface area, adaptability, and functionality, as well as their potential to induce apoptotic pathways and fast penetration or internalization into cancer cells. Biosynthesis of metallic nanoparticles using plant or microbe extracts is attracting attention to replace toxic chemicals with phytochemicals that can act as reducing, capping, or stabilizing agents and improve metallic nanoparticles biocompatibility, antitumor, and antioxidant properties. This review focuses on biosynthesized metallic nanoparticles and their anticancer effects on breast, prostate, skin, cervical, colorectal, lung, and liver cancer.

Conclusion Biosynthesis of nanoparticles for cancer therapy stands at the forefront of innovative and sustainable approaches. Despite challenges, ongoing research demonstrates the potential of biosynthesis to revolutionize cancer nanomedicine, emphasizing the need for continued exploration and collaboration in this rapidly advancing field. Overall, this review offers a comprehensive understanding of the most recent developments in biosynthesized metallic nanoparticles for the treatment of cancer as well as their potential future applications in medicine.

Keywords Biosynthesis, Metal nanoparticles, Metal oxide nanoparticles, Phytochemicals, Anticancer activity, Cytotoxicity

*Correspondence:
Dipak Maity
dipakmaity@gmail.com
Rajendra Awasthi
awasthi02@gmail.com
[1] School of Health Sciences and Technology, UPES, Dehradun 248001, India
[2] The Assam Kaziranga University, Koraikhowa, NH-37, Jorhat, Assam 785006, India

Background

Cancer is caused by the excessive proliferation of normal cells, which causes genetic instability and mutations to accumulate within cells and tissues, transforming them into malignant cells. Radiation, smoking, nicotine, toxins in drinking water, food, air, chemicals, certain metals, and infectious agents are all potential external causes of cancer, in addition to internal ones such genetic mutations, weakened immunity, and hormone imbalances [1]. Despite significant efforts by scientists to overcome

cancer, it remains difficult to effectively treat. Hair loss, exhaustion, nausea, and other symptoms are possible side effects of conventional chemotherapy, which uses chemicals to destroy cancer cells. Because of these side effects and drug resistance, it is difficult to take advantage of conventional chemotherapy for the complete treatment of cancer [2]. Nanomedicine has made significant advancements in the treatment of cancer over the past several years and is useful as a drug carrier for chemotherapeutics because of its size, shape, selective binding capability, high permeability and retention impact, surface modification, etc. This allows them to deliver drugs directly to the cancer cells while preserving healthy tissue [3]. Nanoparticles (NPs) have been explored as pharmaceutical carriers for more than three decades to increase the in vivo effectiveness of several existing anticancer molecules. The investigations conducted during 1970s explored anticancer drug-loaded liposomes [4]. NPs are widely used for the delivery of imaging agents, genes, or chemotherapeutics, exploiting their intrinsic toxicity, such as related to the release of hazardous species [5]. Inherent properties, such as antioxidant action, or activities dependent on the application of external stimuli, like hyperthermia in response to the introduction of infrared rays or magnetic fields, may account for the physicochemical characteristics that give NPs their anticancer activity [4]. Metal and metal oxide NPs are being used experimentally to directly kill tumor cells by converting applied magnetic fields into strong hyperthermia or by performing effective photodynamic therapies that can reach even internal tissues by converting in situ penetrating infrared radiation into visible light inside the tumor [6].

NPs are commonly synthesized using top-down (synthesized via size reduction) and bottom-up strategies (NPs are generated from small entities such as atoms and molecules) [7, 8]. Hazardous and poisonous chemicals, expensive laboratory equipment and infrastructure, and the ability to operate under a variety of circumstances, including high temperature and pressure, are all utilized in the various chemical and physical procedures used to create and synthesize NPs. NP synthesis is expensive, and it results in highly toxic and harmful compounds that pose a variety of biological risks. So, it is advised to create an eco-friendly process combining biological and green synthesis techniques [9].

Green synthesis of metal or metal oxide NPs involves reducing metal complexes in diluted solutions to form metal colloidal dispersions. Despite being commonly used reducing agents, sodium borohydride and hydrazine hydrate are not preferred due to their toxicity from nanoparticle contamination. Green resources including plant and microbial extracts contain compounds that can convert metal precursors into NPs. All green methods typically include combining one or more of these biological extracts with metal salt solutions. Biomolecules change the oxidation state of metal salts from positive to zero, stabilizing newly formed NPs or acting as *in situ* reducing and capping agents [10]. The formation of a monolayer around the NPs prevents them from aggregating together due to chemical and physical interactions. Khan et al. synthesized palladium NPs using a root extract from *Salvadora persica*. The extract contained polyphenols with bioreduction and stabilizing properties [11]. The quantity of natural compound present in the extract affects the size and size distribution of NPs. Khatami et al. synthesized 15-nm-sized silver NPs (Ag NPs) from dried grass. At 5 μg/mL, Ag NPs suppress cancer cell multiplication and decrease cancer cell survival by 30% [12].

Biological processes are preferred to chemical and physical ones because they are less expensive, safer for the environment, do not require extreme conditions, and do not generate harmful by-product molecules. Biological nanoparticle synthesis employing living organisms is a green technique for synthesizing NPs with desired properties. Biosynthesis allows unicellular and multicellular organisms to react [13]. Biogenic synthesis can produce large numbers of contamination free well-defined NPs. It also has a lower environmental impact than alternative physicochemical manufacturing methods [14]. Cheng et al. used zinc oxide NPs (ZnO NPs) synthesized from *Rehmanniae radix* (RR) as a target drug delivery vehicle to inhibit bone cancer (MG-63) cell proliferation. Increasing dosage caused apoptosis [15]. *Caesalpinia pulcherrima* extract-loaded Ag NPs are cytotoxic to HCT116 cell lines [16]. *Artemisia turcomanica* leaf extract-loaded Ag NPs were cytotoxic against normal fibroblast cells (L-929) and gastric cancer cells (AGS) [17]. Metal oxides are toxic for cancer cells and nontoxic for normal cells (Fig. 1A). Due to the presence of capping agent on metal oxide NPs, these bind to the surface of healthy and cancerous cells through electrostatic attraction. Ionic species, namely metal and oxygen radicals, are formed when the biosynthesized NPs dissociate. The elevated metal ion concentration prevents the growth of cancer cells by changing their metal cation homeostasis. Superoxide dismutase (SOD) eliminates the oxygen radical, resulting in hydrogen peroxide, which peroxisome catalases and phytocompounds then convert into water and oxygen. As a result, the superoxide radical is converted into antioxidants before reactive oxygen species (ROS) develop in normal cells [18].

ROS produced by oxygen radicals generates hydrogen peroxide, which causes oxidative stress and kills cancer cells. However, the lack of experimental evidence

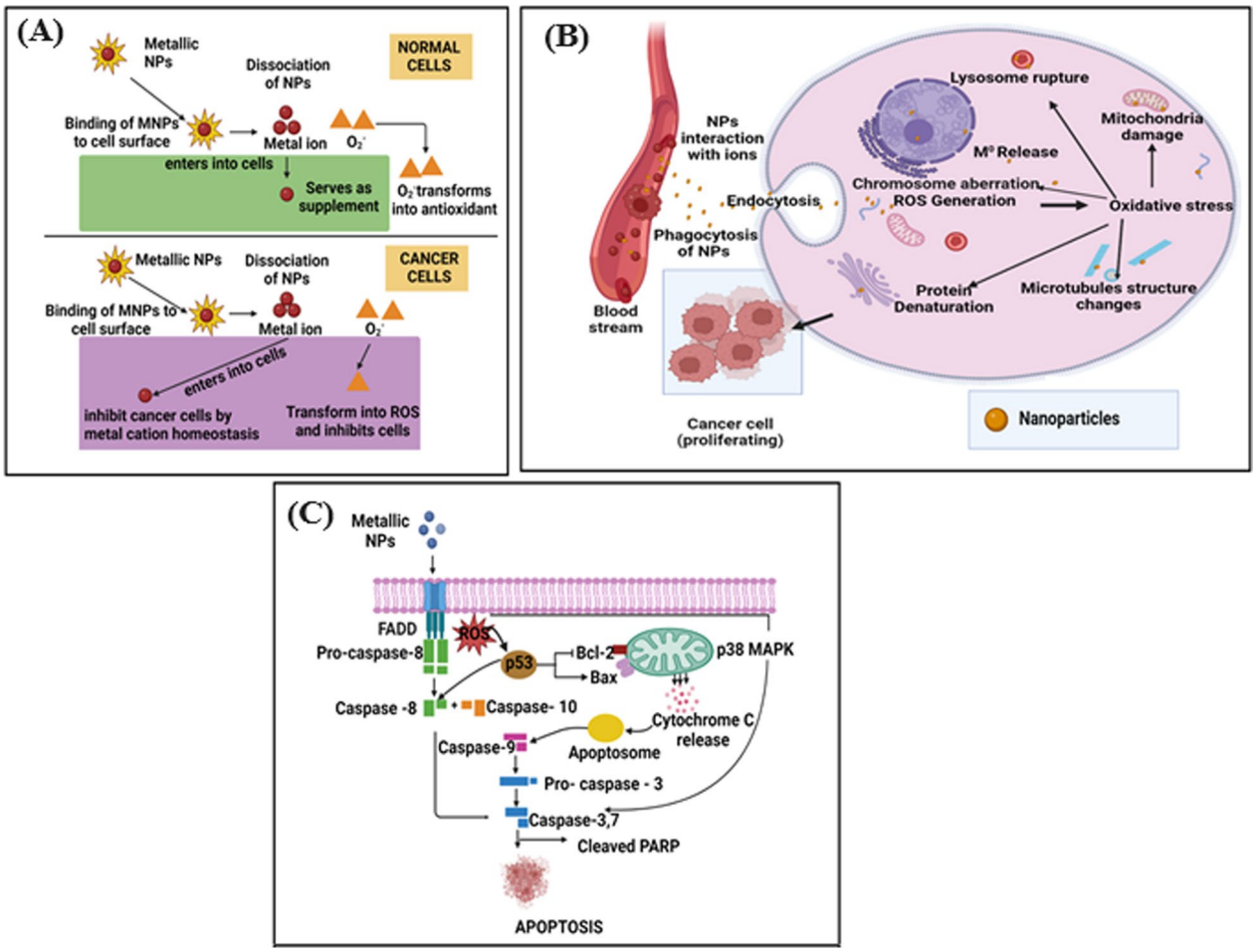

Fig. 1 **A** Effect of metallic NPs in normal and cancerous cells, **B** mechanisms of metal/metal oxide NPs for cancer cell [34], **C** proposed mechanism of apoptotic effect of metallic NPs on the cancer cells [35], (**A**: Recreated with permission © Springer Nature, **B** and **C** recreated under copyright (CC BY) from MDPI, Dovepress)

for these routes motivates more research into the lethal mechanism of photosynthesized metal oxide NPs in both healthy and malignant cells [19]. This article discusses the probable mechanism of action, the green synthesis of metallic NPs from plant extracts, and their anticancer effectiveness against different cancer cells. It also summarizes characterization methods and the most significant findings from recent studies.

Metallic nanoparticles in cancer treatment

The NPs have been used for many years in biomedical operations such as imaging and drug delivery [20]. Inorganic NPs and their numerous applications, such as cellular absorption, diagnostics, and therapy, have received significant attention in recent years. Most of the inorganic nanoparticle research is focused on materials such as gold, silica, and others. Together with a facilitator, the mesoporous silica bestows a very cutting-edge approach to imaging and drug release [21]. The activity of this facilitator is triggered with the help of external stimuli. Due to their outstanding optical, magnetic, and photothermal characteristics, metallic NPs are widely explored in biological imaging and targeted drug delivery. Gold NPs (Au NPs), Ag NPs, iron-based NPs, and copper NPs are some of the most often utilized metallic NPs. Since their size and surface qualities can be easily adjusted, Au NPs are utilized as drug carriers for intracellular targeting [22]. The visible light extinction behavior of metallic NPs makes it possible to track their trajectories in the cells.

Anti-human epidermal growth factor receptor 2 (HER2)-functionalized gold-on-silica nanoshells have been found to target HER2-positive breast cancer cells [23]. Clinical trials for the detection of nodal metastases using Combidex®, an iron oxide-based nanoformulation, are close to complete [24]. Iron deficiency anemia can be treated with Feraheme®, an iron oxide nanoformulation that contains ferumoxytol. This was approved by the FDA

in June 2009 to treat nodal metastases in prostate and testicular cancer [25, 26]. Metallic NPs cause apoptotic, autophagic, and necrotic cancer cell death through ROS generation, caspase-3 activation, mitochondrial outer membrane permeabilization, and specific DNA cleavage [27].

Metal nanoparticle delivery pathway and cell damage can be linked to interaction of NPs with ions in circulation, ingestion by phagocytic cells, opsonization or enzymic degradation, internalization via endocytosis, membrane perforating and damage of its components and function, chromosomal aberrations and changes in cell replication rate, lysosome rupture, mitochondria damage, lower growth rate, structural changes, and shorter lifespan of microtubules of the cytoskeleton, generation of ROS, oxidative stress, and subsequent processes (Fig. 1B). NPs of different sizes enter cells via distinct pathways. Smaller NPs penetrate cells via receptor-mediated uptake by interacting with the caveolin receptor on the cell membrane. Larger NPs are more likely to enter cells via clathrin-mediated endocytosis. When NPs enter a cell, they can proceed one of two ways: either they interact with cytosolic proteins in a direct fashion, or they are transported to the lysosome–endosome complex, where their surfaces are modified before they are released into the cytosol [27]. Inside the cell, NPs trigger up a chain reaction that releases ROS and initiates the release of metal ions. These metal ions tend to connect with proteins' SH groups, breaking their S–S bridges. As a result, the cell physiology is altered, resulting in activation of various signaling pathways that lead to programmed cell death [28]. Apoptosis is frequently induced by either intrinsic or extrinsic pathways. Nanomaterials can induce apoptotic signaling via both intrinsic and extrinsic pathways. In the case of intrinsic apoptosis, ROS production causes mitochondrial membrane depolarization, which results in the release of cytochrome C into the cytosol. This cytochrome C promotes the caspase-9/3 apoptotic cascade by activating pro-apoptotic proteases in apoptosis initiated by the extrinsic pathway (Fig. 1C) [29].

Ag NPs play a significant role in breast cancer treatment as well as skin wound healing therapy. In this review, most of the studies mentioned are about Ag NPs tested on breast cancer cell lines. For example, the IC_{50} value of paclitaxel is 80 g/dL, while the IC_{50} value of Ag NPs loaded with *Elaeodendron croceum* extract against MDA-MB-231 breast cancer cell line is 138.8 μg/mL [30]. *Moringa oleifera* flower aqueous extract-loaded Au NPs showed anticancer activity against A549 lung cancer cells. Au NPs (50 μg/mL) showed significant anticancer activity against lung cancer cell line [31]. ZnO NPs kill tumor cells through NADPH-dependent oxidative burst and apoptotic signaling. ZnO NPs of various sizes and specific surface areas had a similar effect on cytotoxicity and DNA fragmentation in macrophages of mice in an ap47phox- and Nrf2-independent manner. Because of their critical function in the modulation of immunological responses during inflammation and the clearing of inhaled particles, ZnO NPs trigger necrosis and apoptosis in macrophages. ZnO NPs promote the rapid induction of nuclear condensation, DNA fragmentation, and formation of hypodiploid DNA-containing nuclei and apoptotic bodies [32]. Furthermore, the delivery of cerium oxide NPs (CeO_2 NPs) might cause DNA damage, which results in tumor cell death. CeO_2 NPs enhance ROS in tumor cells, causing apoptosis without genotoxicity. The antitumor activity of CeO_2 NPs is greatly dependent on their size and shape. Both small- and large-sized NPs induce DNA damage in tumor cell lines [33].

Silver nanoparticles

Due to their unique physical and chemical characteristics, such as high electrical conductivity and optical, electrical, thermal, and biological properties, Ag NPs are gaining considerable interest in the healthcare sector [36]. Ag NP aggregates enter mammalian cells via endocytosis and can cross blood–brain barrier due to their small size. After entering an endocytic vesicle, they are intracellularly transported to the cytoplasm and nucleus [37]. The antimicrobial properties of silver have been observed since ancient times. Silver is currently employed in various applications to regulate bacterial proliferation, such as in dental procedures, catheters, and the treatment of burn injuries. Ag ions and Ag-based compounds are generally recognized for their severe toxicity to microorganisms, exhibiting potent biocidal properties [38]. Ag NPs, measuring around 32.2 nm, were manufactured using an extract derived from *Teucrium polium*. These NPs were incorporated into a film made of polylactic acid and polyethylene glycol (PLA/PEG). The resulting film serves as a biodegradable wound dressing that possesses antioxidant and antibacterial properties. The incorporation of biogenic silver NPs into PLA/PEG nanofibers resulted in the total inhibition of growth in *P. aeruginosa* and *S. aureus*, demonstrating substantial antibacterial properties [39]. The Ag NP-loaded amorphous calcium polyphosphate NPs, which were synthesized using wet chemical precipitation, exhibited effective antibacterial activity against *E. coli*, *Staphylococcus aureus (S. aureus)*, and *Enterococcus faecium* [40]. A recent study shown that the production of Ag NPs using a crude leaf extract of *Lycium shawii* exhibited a minimum inhibitory concentration (MIC) ranging from 1 mg/mL to 15 mg/mL against several microorganisms. The measured MIC clearly demonstrates the significant antibacterial properties of the

produced NPs [41]. Multiple in vitro and in vivo studies have demonstrated the anticancer effects of Ag NPs, rendering them a highly promising choice for cancer therapy [42]. At a dosage of 1.0 mg/L, enzyme-responsive Ag NPs coated with adenosine triphosphate killed 56.04% of HepG2 cell line [43]. Ag NPs produced by the one-step caffeic acid-mediated reduction are anticipated to enter cells via endocytosis and effectively suppress HepG2 cell growth through apoptosis induction [44]. The aqueous extract of *Panax ginseng* roots was used to synthesize Ag NPs with the assistance of ultrasound. The resulting NPs exhibited an IC_{50} value of 157 μg/mL against the PC14 cancer cell line. In PC14 cells, the biosynthesized Ag NPs modulated the PI3K/AKT/mTOR signaling pathway and elevated ROS levels, apoptosis, and LDH release [45]. Chen et al. studied the function and mechanism of Ag NPs in prostate cancer. Ag NPs diminished lysozyme membrane integrity, number, and protease activity. This blocked autophagy. In PC-3 cell lines, sublethal Ag NP doses can produce hypoxia and energy deficiency [46].

Gold nanoparticles

Au NPs are synthesized using chemical, physical, and biological methods. Conversion of metallic gold into nano-particulate gold by chemical reduction is a common menthod for the synthesis of Au NPs. Citrate mediated reduction method has been described by Turkevich in 1951 to synthesize stable and size controlled Au NPs. Brust and Schriffin explored sodium borohydride mediated reduction to synthesize Au NPs. In 1996 Schmid *et. al*. described seed mediated growth, the most explored chemical method, to synthesize Au NPs [47]. Surface modification of Au NPs can be done using amine and thiol groups. This has the potential to benefit biomedical applications such as targeted delivery, imaging, and sensing for electron microscopy markers [48]. Murawala et al. synthesized Au NPs with a bovine serum albumin cap and methotrexate loading that impede MCF-7 proliferation and cause G1-S phase arrest, DNA breakage, and eventually apoptosis [49]. Gum acacia (GA) was utilized successfully to synthesize gemcitabine hydrochloride (GEM)-loaded colloidal Au NPs. Cell viability was 64.8% and 51.8% for naked GEM-treated cells at doses ranging from 0.25 to 0.5 μg/mL, respectively. GEM-GA-Au NPs decreased cell viability by 51.2% and 42.8%, respectively. GEM-GA-Au NPs exhibited superior anti-proliferation effects on MDA-MB 231 human breast cancer cells compared to naked GEM [50]. In comparison with free TA-peptide, the conjugation of Au NPs and a thioctic acid-DMPGTVLP peptide (TA-peptide) conjugate led to a more substantial release of cytochrome c after the activation of caspase-3/7. However, after intratumoral injection in tumor-bearing mice, TA-peptide Au NPs exhibited superior antitumor effectiveness compared to TA-peptide [51].

Iron oxide

Over the past 20 years, iron-based NPs have gained interdisciplinary scientific interest due to their distinctive properties and nanotechnological possibilities [52]. Iron oxide NPs (Fe_3O_4/Fe_2O_3 NPs) exhibit good superparamagnetic characteristics of Fe_3O_4 and Fe_2O_3, leading to significant performance in drug delivery applications [53]. Superparamagnetic Fe_3O_4/Fe_2O_3 NPs have attracted considerable attention because of their potential use in imaging, drug delivery, and hyperthermia management. They are non-toxic, biodegradable, and biocompatible and effectively eliminated from the human body via iron metabolism pathways [54]. Unique physical and chemical properties of Fe_3O_4/Fe_2O_3 NPs (large surface area, superparamagnetic properties, and nanoscale dimensions with a spherical form and an adjustable size of less than 50 nm) make them highly efficient [55]. Fe_3O_4/Fe_2O_3 NPs have an intrinsically therapeutic impact on malignancies [56] and resist tumor cell growth in a better way when compared to untreated control cells [57]. Sun et al. synthesized multifunctional methotrexate-loaded iron oxide NPs conjugated with chlorotoxin (a targeting ligand). Due to tumor cell cytotoxicity, these NPs may be employed in cancer diagnosis and treatment [58].

Zinc oxide

Zinc oxide nanoparticles (ZnO NPs) have emerged as a promising contender for use in biomedical research, food packaging, optical, electrical, and food processing applications. ZnO NPs are harmful to cancer cells because, at low pH levels, they decompose into Zn^{2+} ions. These Zn^{2+} ions produce ROS, which kill cancer cells. Additionally, ZnO NPs have been successfully employed as a vehicle for the precise delivery of anticancer drugs into tumor cells [59]. Wahab et al. found that ZnO NPs, when utilized at very low concentrations and in a dose-dependent manner, were effective against MCF-7 (breast cancer) and HepG2 (liver cancer) cells. At 25 μg/mL, HepG2 cell viability was below 10% [60].

Copper oxide

CuO, a well-known p-type semiconductor, has long been studied for its monoclinic structure. Cupric oxide (tenorite monoclinic CuO) and cuprous oxide (cuprite cubic Cu_2O) are two crystalline forms of copper oxide [61]. Potential metal ion leaching and dissolving, as well as oxidative stress, DNA damage, lipid peroxidation, membrane damage, and mitochondrial damage have all been explored in the literature as toxicity pathways. A small amount of CuO NPs can generate large amounts of ROS

such as O_2, OH, and H_2O_2. CuO NPs cause membrane disruption and ROS generation after they enter the mitochondria [62]. Wang et al. found that CuO NPs increased the survival rate of tumor-bearing animals, inhibited the metastasis of B16-F10 cells, and significantly delayed the growth of melanoma. The data revealed that CuO NPs had minimal systemic toxicity and were promptly eliminated from the organs. When CuO NPs penetrated the cells, they preferentially targeted the mitochondria, causing cytochrome C to be released and caspase-3 and caspase-9 to be activated. Thus, CuO NPs can kill cancer cells via mitochondrion-mediated apoptosis to treat melanoma and other cancers [63].

Titanium oxide

Bioengineered titanium oxide nanoparticles (TiO2 NPs) have been shown to have good stability, chemical neutrality, hydrophilicity, oxidizing power, and electrical, optical, physical, and photocatalytic properties. Because of their powerful antibacterial and odor-removing properties, TiO_2 NPs are employed in filters and cosmetics. TiO_2 photocatalysts have been extensively explored for the killing or suppression of bacterial growth due to their excellent chemical stability and nontoxicity [64]. Plant extracts may exhibit properties of the metals or metal oxides that make up their composition in addition to the presence of phytoconstituents. These features may ultimately result in their many critical activities in the prevention or treatment of cancer. It has been shown that the tiny size of TiO_2 NPs gives them potent anticancer activity against cancer cells [65].

Biological synthesis of metallic nanoparticles

Over the past decade, there has been an increase in efforts to discover efficient, low-cost, eco-friendly, and long-lasting strategies for producing green NPs [66]. Researchers across the globe are interested in green synthesis since it is an environmentally safe technique and a fascinating study topic for the synthesis of metallic NPs for biomedical applications [67]. Using biological agents to make NPs of various sizes, shapes, compositions, and physicochemical characteristics is safe, non-toxic, and environmentally sustainable [68]. Biosynthesis of these NPs is done at mild pH, pressure, and temperature without using an external reducing agent, capping agent, or stabilizing agent [69]. Capping agents have a significant role in the synthesis of metallic NPs. The major role of capping agent is to functionalize and stabilize the NPs, along with controlling size and morphology [70]. NPs synthesized by green synthesis methods are exceptionally stable, well dispersed, and have a narrow size distribution [71].

Nucleation and production of stable metallic NPs during biological synthesis are affected by several factors such as temperature, reactant concentrations, pH, and reaction time. For example, when employing biomass from *Avena sativa* (oats) at pH 2, rod-shaped Au NPs were larger, ranging from 25 to 85 nm. In contrast, at pH 3 and 4, the Au NPs were comparably smaller, with sizes ranging from 5 to 20 nm. The functional groups present in extract were more easily accessible for particle nucleation within the pH range of 3 to 4. In contrast, a reduced number of functional groups were present at pH 2, leading to the aggregation and formation of bigger Au NPs [72]. Ag NPs were synthesized using bark extract derived from *Cinnamon zeylanicum*. The particle yield exhibited a positive correlation with the concentration of the bark extract, whereas the NPs assumed a mostly spherical morphology at pH values of 5 and higher [73]. Prathna et al. found that the combination of $Ag(NO)_3$ with *Azadirachta indica* leaf extract led to the formation of progressively bigger particles as the reaction time increased. By adjusting reaction time from 30 to 240 min, the particle size changed from 10 to 35 nm. The concentration of NPs produced at various stages of reaction was determined using inductively coupled plasma optical emission spectroscopy measurements. After 2 h, the yield of the process had significantly increased to 78%. Subsequently, there was a progressive and continuous increase in the yield [74]. The photosynthesized NPs are safer than their chemically synthesized counterparts for usage in healthcare applications since they do not contain any harmful contaminants. When applying metal in healthcare products, safety risks related to nanosize, penetration, and tissue permeability must be considered. In vitro cytocompatibility of phytonanoparticles has been documented by multiple researchers. Extensive research is still required to determine their pharmacodynamics, immunogenicity, absorption, biodistribution, excretion, and acute and chronic toxicity. Although plant-mediated nanoparticle production is often considered an environmentally beneficial approach, there is still a dearth of evidence addressing the direct and indirect ecological impacts of these particles [75].

Green synthesis using plant extract

Plants, which include grasses, ferns, trees, bushes, flowers, and other varieties of green algae and lichens, are among the most essential forms of life. NPs can help plants by acting as fertilizers, pesticides, growth regulators, and antibacterial agents. However, flora can also assist with the development of nanotechnology. Plants can be used to produce NPs in two different ways: directly through extraction or indirectly via plant-mediated biosynthesis. Agriculture, food

science, nanotechnology, and pharmaceutical science are just some of the fields that could benefit from a better understanding of the interaction between NPs and plant extracts [76]. Plant-mediated green NP synthesis is one of the most preferred approaches because it normally requires a neutral pH and can occur at room temperature [77]. Plants and plant extracts are sustainable and renewable resources for NP production, unlike prokaryotic bacteria, which require expensive methods for maintaining microbial cultures and downstream processing [7]. Using the various plant parts (Fig. 2A), such as fruits, seeds, calluses, stems, peels, leaves, and flowers, biological processes synthesize metal NPs in a range of sizes and shapes. Metal NPs are synthesized using metal precursors and plant extracts as reducing and capping agents under suitable conditions [78]. A green chemistry approach for the synthesis of metal NPs can be achieved in three stages: (i) the activation phase, in which the phytoconstituents reduce the metal ions, followed by the nucleation of reduced metal atoms; (ii) the growth phase, in which small NPs join to form larger NPs; (iii) the termination phase, in which the NPs take on their final shape [79]. Bioactive alkaloids, phenolic acids, polyphenols, proteins, carbohydrates, and terpenoids in plant extracts reduce and stabilize metallic ions (Fig. 2B) [80].

Tabebuia berteroi leaf extract is rich in polyphenol, and *Withania coagulans* plant extract is rich in flavonoids, tannins, and phenolics. These extracts have been used to reduce Fe and Pd ions to form their respective metal NPs, which are then mixed with graphene oxide to make a nanocomposite [81]. *Anisomeles indica* leaf extract reduced silver ions to spherical Ag NPs (50–100 nm) in 10 min at room temperature [82]. Lee et al. reported Au NPs synthesis utilizing sequential fractional extracts from *Ocimum sanctum* leaves. For the sequential fraction extraction of *O. sanctum* leaves, different polarity solvents (hexane, chloroform, n-butanol, and water) were utilized, and it was discovered that unique solvent fractions (extract) are responsible for the creation of morphologically varied Au NPs. Water extract produced anisotropic NPs, hexane extract produced spherical Au NPs, chloroform extract produced a circular disk-shaped structure with rough edges, and n-butanol extract produced Au NP aggregates [83]. Possible mechanisms of the anticancer effect of phytosynthesized metal or metal oxide NPs include the formation of pro-apoptotic caspases, activation of reactive oxygen species, damage to cell membranes and mitochondria, damage to DNA, and DNA fragmentation [84]. Table 1 represents various plant extracts utilized in the synthesis of metallic NPs along with their corresponding applications.

Biosynthesis of nanoparticles using microbes

Actinomycetes, bacteria, fungi, marine algae, viruses, and yeasts have all been effective in the production of NPs employing unicellular and multicellular organisms (Fig. 2C) [113]. These organisms can produce reducing and stabilizing agents in the synthesis of NPs with a wide range of shapes, compositions, and physiochemical properties (Fig. 2D) [114]. Microorganisms can synthesize metallic NPs both intracellularly and extracellularly (Fig. 2E) [115]. To produce NPs extracellularly, microbes are cultivated in the appropriate environments. The microorganism-containing enzyme-rich broth is centrifuged to synthesize NPs [116]. The intracellular synthesis of NPs is carried out via the cellular mechanism of microbial cells [117]. Several studies explored extracellular methods for producing metal NPs [118]. Kalimuthu et al. investigated the role of the nitrate reductase enzyme in the production of Ag NPs by *Bacillus licheniformis*. The enzyme is responsible for converting Ag^+ to Ag°, and they hypothesized that nitrate ions might play a role in its induction. Cofactors like NADH in NADH-dependent nitrate reductase enzymes are required for generating metal NPs. Bioreduction of Ag^+ to Ag° may be caused by the release of cofactors NADH and NADH-dependent enzymes by *B. licheniformis*, in addition to other components, especially nitrate reductase [119]. *Pseudomonas stutzeri* was treated with a concentrated Ag NO_3 solution to produce Ag NPs in the periplasm [120]. Numerous fungi strains have been described for the extracellular biofabrication of NPs using CdS, Au, Zirconia, Si, Ti, and magnetite [121]. The method of NP production varies depending on the microorganisms. However, the basic concept involves microorganisms entrapping metal ions on their surface or within their cells, followed by their reduction to NPs. Electrostatic forces are frequently used as a trapping medium [122].

Bacteria

Bacteria can precipitate metals at nanoscale level as well as regulating interaction pathways for metal ion reduction [123]. *E. coli* biosynthesized Ag NPs of 50 nm size by a reliable and cost-effective approach [124]. *Pseudomonas aeruginosa* (*P. aeruginosa*) and other species have been studied for their ability to synthesize Zn, iron, nickel, Au, and Ag NPs [125]. The NADPH-dependent reductase enzyme may be involved in the reduction of Au^{3+} to Au° and stabilization via capping molecules in the presence of *Stenotrophomonas maltophilia* [126]. Different bacterial species, as listed in Table 2, have been employed to produce metal NPs.

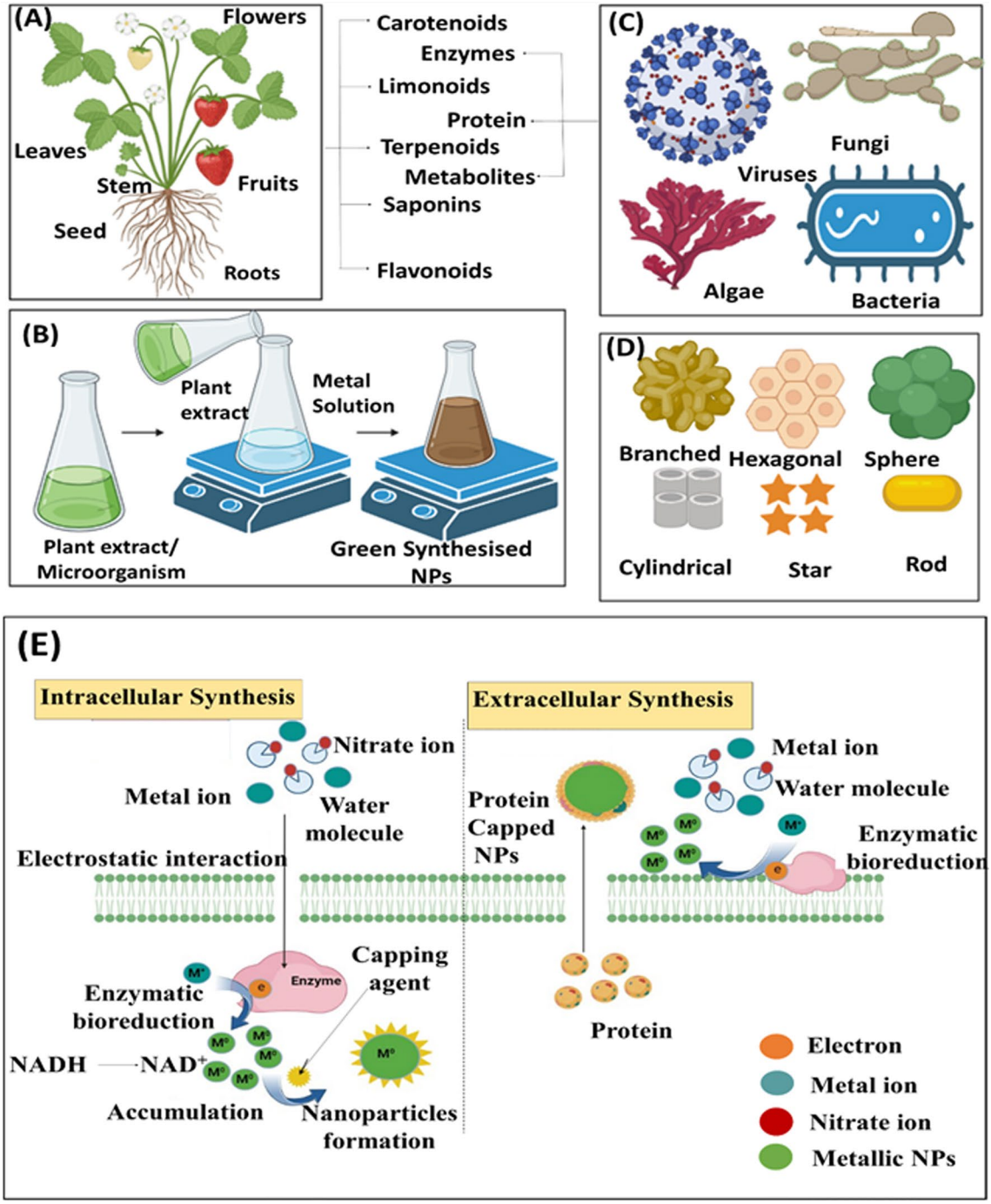

Fig. 2 Green synthesis of nanoparticles: **A** different plant parts used for nanoparticles formation, **B** general method for biosynthesized nanoparticles formation, **C** different microorganisms used for nanoparticles formation, **D** different shapes of nanoparticles that can be synthesized, and **E** possible mechanism of nanoparticle synthesis using microbes (Figure **E**: recreated with permission © Springer Nature)

Fungi

Fungi are non-phototrophic eukaryotic microorganisms with rigid cell walls [147]. Fungi are among the biological sources that are exploited in bioremediation, can mineralize, and are known as mediators in the synthesis of NPs. This is due to their ability to create huge volumes of biomass [148]. Fungi can reduce the size of metal ions to NPs via two different processes: (i) through the contact of the fungus biomass with the metal inside the fungal cell and (ii) through the interaction of the fungus filtrate

Table 1 Biosynthesized metallic NPs using various plants and their biomedical applications

MNPs/MONPs	Plant/part used	Metal precursor used	Morphology	Biomedical application	Findings	References
Fe_2O_3/Fe_3O_4	*Hyphaene thebaica* (Aqueous fruit extract)	Iron nitrate hexa hydrate	Quasi-spherical/cuboidal 10 nm	Antibacterial, antioxidant, antiviral activity	Growth of *Bacillus subtilis* (*B. subtilis*) inhibited. Fe_2O_3 NPs were effective against *Aspergillus flavus* (*A. flavus*). An increase in Fe_2O_3 NP concentration reduced viability of RD cells and L20B cells. Moderate inhibition of poliovirus-1 and poliovirus-2 was noted in the culture of virus in L20B cells	[85]
	Ficus carica (Leaf extract)	Ferric chloride hexahydrate	Multiform 43–57 nm	Antioxidant activity	At 12.118 mg/mL, synthesized NPs had antioxidant capacity that can eliminate half of the environmental 2,2′-diphenyl-1-picrylhydrazyl (DPPH) radicals	[86]
	Celosia argentea (Leaf extract)	Ferric nitrate	Spherical/hexagonal/Cubic shape 5–10 nm	Antibacterial, antibiofilm, antioxidant, anti-inflammatory, anti-diabetic, anticancer, larvicidal activity	At 150 µg/mL, antibacterial activity was detected against *E. coli* (19 mm) and *S. aureus* (25 mm). A greater rate of inhibition of biofilm activity was observed at 150 µg/mL. A higher antioxidant (97%) was recorded at 80 µg/mL and higher anti-inflammatory (93%) and anti-diabetic (87%) activities were recorded at 500 µg/mL. MCF-7 breast cancer cells showed 86% inhibition at 50 µg/mL	[87]
	Platanus orientalis (Leaf extract)	Ferric nitrate nonahydrate	Spherical 78–80 nm	Antifungal activity	Antifungal activity of iron oxide NPs against the fungus was 1.6 times higher than that of *A. niger*	[88]
	Carica papaya (Leaf extract)	Ferric Chloride	Spherical 56 nm	Antibacterial	Antibacterial activity demonstrated against Gram-positive (*S. aureus, Bacillus subtilus*) and Gram-negative (*E. coli, Enterobacter, Pseudomonas fluorescens*) bacteria	[89]

Table 1 (continued)

MNPs/MONPs	Plant/part used	Metal precursor used	Morphology	Biomedical application	Findings	References
ZnO	*Ziziphus nummularia* (Leaf extract)	Zinc nitrate	Spherical/irregular 17.33 nm	Antifungal activity	ZnO NPs demonstrated strong cytotoxic action against HeLa cancer cell line. NPs had superior antifungal activity compared to conventional azole antibiotics	[90]
	Limonium pruinosum L. Chaz. (The shoot system, leaves and stems)	Zinc acetate dihydrate	Hexagonal/cubic crystalline 41 nm	Anti-skin cancer, antimicrobial, antioxidant activity	The plant extract and synthesized ZnO NPs demonstrated the largest inhibition zone against *E. coli* measuring 29 and 31 mm, and *C. albicans* measuring 28 and 29 mm. At 1000 µg/mL, ZnO NPs and *L. pruinosum* extract showed highest DPPH activity, at 75.2% and 84.6%, respectively	[91]
	Bixa orellana (Leaf, seed, and seed coat)	Zinc acetate	Spherical/almond-like 169 – 259 nm 304 – 465 nm 278 – 654 nm	Anticancer, antimicrobial	Antibacterial activity was detected in ZnO NPs containing leaf extract against *S. aureus* and *B. subtilis*. NPs containing seed extract inhibited *E. coli*, and NPs containing seed coat extract inhibited *S. aureus*. No cytotoxicity was observed against HCT-116 cancer cells. No antifungal activity recorded against fungi, including *Penicillium sp., A. flavus, Fusarium oxysporum* (*F. oxysporum*), and *Rhizoctonia solani*	[92]
	Mentha longifolia L. (Leaf extract)	Zinc nitrate	Spherical 60–70 nm	Antiparasitic	At 400 ppm and 150 min of exposure, NPs demonstrated highest scolicidal activity and 100% mortality rate. Morphological changes and loss of viability were seen in the treated protoscolices	[93]

Table 1 (continued)

MNPs/MONPs	Plant/part used	Metal precursor used	Morphology	Biomedical application	Findings	References
CuO	*Bacopa monnieri* (Leaf extract)	Copper (II) acetate	Monoclinic crystalline 34.4 nm	Antibacterial, anti-diabetic, anti-inflammatory	Strong inhibition zones at 5 mg/mL were demonstrated for *H. salomonis* (13.50 ± 0.84), *H. felis* (15.71 ± 0.91), *H. suis* (15.84 ± 0.89), *and H. bizzozeronii* (13.11 ± 0.83). After 48 h, NPs showed 74% less edema as compared to the control group that received diclofenac (100 mg/kg)	[94]
	Momordica charantia (Fruit extract)	Copper sulfate pentahydrate	Spherical 50–57 nm	Antiviral, antifungal, antibacterial	The highest efficacy was observed against *Bacillus cereus* with a 31.66 mm zone of inhibition. Additionally, CuO NPs had therapeutic potential against R2B strain of Newcastle disease, *Streptococcus viridians*, and *Corynebacterium xerosis*	[95]
	Artemisia (Leaf extract)	Copper (II) sulfate	conceivable spherical/irregular form 38.5–48.5 nm	Antibacterial	Zones of inhibition for *B. subtilis* and *E. coli* were observed as 26.7 and 20.5 mm, respectively	[96]
	Pimenta dioica (Leaf extract)	Copper (II) sulfate	Platelet/cuboid shape 20–50 nm	Antibacterial, anticancer, anti-diabetic, antioxidant	For the L929 and DLD-1 cell lines, the IC_{50} value of CuO NPs is 89.42 mg/mL and 119.06 mg/mL, respectively	[97]
	Gomphrena globosa *Gomphrena serrate* (leaf extracts)	Copper (II) sulfate pentahydrate	*G. globosa*: Rod/hexagonal/irregular shape 345 nm *G. serrata*: Spherical 380 nm	Antibacterial, anticancer, antioxidant, photocatalytic activity	CuO NPs produced by *G. globosa* at 125 µg/mL demonstrated antibacterial activity, with the zone of inhibition measuring between 14 ± 1.41 and 13 ± 1.41 mm. NPs produced by *G. serrata* and *G. globosa* showed IC_{50} values of 85.14 and 77.75 µg/mL, respectively	[98]

Table 1 (continued)

MNPs/MONPs	Plant/part used	Metal precursor used	Morphology	Biomedical application	Findings	References
TiO_2	*Andrographis paniculata* leaves extract	Titanium (IV) oxide	Spherical 50 nm	Antibacterial, antifungal, anti-diabetic, antioxidant	*E. Coli* and *Bacillus spp*. showed a lower zone of inhibition. *Salmonella spp*. showed a higher zone of inhibition. LD_{50} value of TiO_2 NPs was 250 µg/L	[99]
	Psidium guajava (Aqueous leaf extract)	Titanium dioxide	Spherical 32.58 nm	Antibacterial, antioxidant activity	TiO_2 NPs (20 µg/mL) showed maximum zone of inhibition against *E. coli* (23 mm) and *S. aureus* (25 mm). In comparison to ascorbic acid, aqueous plant extract and TiO_2 NPs exhibited the highest level of antioxidant activity	[100]
	Morinda citrifolia (Root extract)	Titanium dioxide	Spherical/oval/triangle 20.46–39.20 nm	Larvacidal activity	Maximum activity of TiO_2 NPs was shown against the larvae of *An. stephensi*, *Ae. aegypti* and *Culex. quinquefasciatus*	[101]
	Moringa oleifera (Leaf extract)	Titanium dioxide	Spherical 100 nm	Wound healing activity	Nano-sized particles significantly exhibited wound healing activity in albino rats	[102]

Table 1 (continued)

MNPs/MONPs	Plant/part used	Metal precursor used	Morphology	Biomedical application	Findings	References
Ag	*Allium cepa*	Silver nitrate	Spherical 10–23 nm	Antimicrobial, antioxidant, antitumor activity	Human breast (MCF-7), hepatocellular (HepG-2) and colon (HCT-116) carcinoma cells were susceptible to the antitumor effects of Ag NPs with IC_{50} values of 1.6, 2.3, and 2.2 µg/mL	[103]
	Indigofera tinctoria (Leaf extract)	Silver nitrate	Spherical 9–26 nm	Anticancer, antimicrobial, antioxidant activity	IC_{50} values for Ag NPs and *I. tinctoria* leaf extract were 56.62 ± 0.86 µg/mL and 71.92 ± 0.76 µg/mL, respectively	[104]
	Morinda citrifolia (Root extract)	Silver nitrate	Spherical and oval 32–55 nm	Anticancer activity	Complete cell death against HeLa cells was observed at 100 µg of Ag NPs	[105]
	Alhagi graecorum (Leaf Extract)	Silver nitrate	Spherical 22–36 nm	Antifungal, antitumor	Antifungal activity was observed against *Candida albicans, glabrata, parapsilosis, tropicales*, and *krusei*. The inhibition zone ranged from 14 to 22 mm at 0.01 mmol/ml and from 17 to 27 mm at 0.02 mmol/mL	[106]
	Azadirachta indica (Leaf and bark extract)	Silver nitrate	Spheroidal 13.01 nm (leaf) 19.30 nm (bark)	Antiplasmodial, hemolytic activity	Antiplasmodial activity against 3D7 and RKL9 P was demonstrated by IC_{50} values of 9.27 mg/mL and 11.14 mg/mL for leaf-mediated NPs and 8.10 mg/mL and 7.87 mg/mL for bark-mediated NPs. Ag NPs from the bark and leaves showed significant hemolytic activity (> 25%) at 125 µg/mL	[107]

Table 1 (continued)

MNPs/MONPs	Plant/part used	Metal precursor used	Morphology	Biomedical application	Findings	References
Au	*Allium sp.*	Chloroauric acid	Spherical 11 nm	Antiviral	At 50% effective concentration (EC_{50} of 8.829 µg/mL), Au NPs actively inhibited MeV replication in Vero cells	[108]
	Sansevieria (Leaf extract)	Chloroauric acid	Spherical 40–70 nm	Anticancer	Au NPs enhanced antiproliferative effect of Cisplatin on prostate cancer cells with minimal cytotoxicity	[109]
	Curcuma pseudomontana (rhizomes)	Chloroauric acid	Spherical 39 nm	Anti-Inflammatory, antimicrobial, antioxidant	*P. aeruginosa* exhibited largest inhibition zone (13 mm) at 100 µg/mL of Au NPs, followed by *E. coli* (12 mm), and *B. subtilis* (11 mm) and *S. aureus* (11 mm). At 25 µg/mL, NPs exhibited high level of inhibition efficiency (94%) in comparison to the standard drug (92%)	[110]
	Allium cepa (Onion peel extract)	Gold trichloride	Spherical/triangular 25–70 nm	Antibacterial, anticandidal, antioxidant, proteasome inhibitory effect	Zones of inhibition measuring 10.66 to 19.95 mm demonstrated greater efficacy of Au NPs and kanamycin mixture against the tested pathogens. Au NPs and rifampicin mixture was limited to its activity against *S. aureus* (22.49 mm) and *E. coli* (9.99 mm). At 100 µg/mL, NPs showed moderate DPPH scavenging potential of 14.44%, while BHT (the reference standard) showed 36.54% at same concentration	[111]
	Jatropha integerrima (Flower extract)	Gold trichloride	Spherical 28–43 nm	Antibacterial	*B. subtilis, S. aureus, E. coli,* and *K. pneumoniae* were found to have MICs of 5.0, 10, 2.5, and 2.5 µg/mL	[112]

Table 2 Biosynthesis of metallic NPs using various bacteria and their biomedical applications

MNPs/MONPs	Bacteria used	Metal precursor used	Morphology	Biomedical applications	Findings	References
CuO	Marine endophytic *Actinomycetes* CKV1	Copper (II) sulfate pentahydrate	Spherical shape 10–30 nm	Antibacterial, anticancer, antibiofilm activity	At 750 µg/mL, CuO NPs showed remarkable antibacterial activity against *E. Coli* and *P. mirabilis*, exhibiting 24 mm and 28 mm zones. At 500 µg/mL, 54% inhibition was recorded against A549 cells	[127]
	Streptomyces sp. MHM38	Copper (II) sulfate	Spherical 1.72–13.49 nm	Antimicrobial	CuO nanoparticles showed antibacterial efficacy against *Enterococcus faecalis*, *Salmonella typhimurium*, *E. coli*, *P. aeruginosa*, and *Candida albicans*	[128]
	Marinomonas Rhodococcus Pseudomonas Brevundimonas Bacillus	Copper (II) sulfate pentahydrate	Spherical/ovoidal shapes 40 nm	Antibacterial, antifungal	The MIC of CuO NPs ranged from 3.12 to 25 µg/mL for Gram-negative bacteria, 12.5 to 25 µg/mL for Gram-positive bacteria, and 12.5 to 25 µg/mL for fungi	[129]
	Actinomycetes	Copper (II) sulfate pentahydrate	Crystalline 198 nm	Antibacterial	*B. cereus* showed high susceptibility (25.3 mm) to CuO NPs. The CuO NPs inhibited bacterial pathogens *B. cereus*, *P. mirabilis*, and *A. caviae* at 5 µg/mL	[130]

Table 2 (continued)

MNPs/MONPs	Bacteria used	Metal precursor used	Morphology	Biomedical applications	Findings	References
ZnO	*Cyanobacterium Nostoc sp. EA03*	*Zinc acetate dihydrate*	Star-like shape 50–80 nm	Antibacterial, anticancer activity	MIC and MBC values for *E. coli, P. aeruginosa,* and *S. aureus* were found to be 2000, 2000, and 64 µg/mL, and 2500, 2500, and 128 µg/mL, respectively. ZnO NPs were less cytotoxic to MRC-5 lung fibroblast cells than to A549 cells treated with cancer	[131]
	Paraclostridium benzoelyticum strain 5610	Zinc nitrate	Spherical/rectangular shape 50 nm	Antibacterial, anti-inflammatory, antidiabetic	Inhibitory zone of *Helicobacter suis* measured 19.53 ± 0.62 mm at 5 mg/mL. After 21 days. In arthritis model the edema was inhibited by NPs by 87.62 ± 0.12%. ZnO NPs sharply reduced glucose level in STZ-induced diabetic mice	[132]
	B. subtilis ZBP4	Zinc sulfate heptahydrate	Pseudo-spherical 14–45 nm	Antibacterial	For *B. cereus, S. aureus, E. coli* O157:H7, *E. coli* Type 1, and *P. aeruginosa* the MIC was 1 mg/mL. It was 2 mg/mL for *L. monocytogenes* and *S. typhimurium*	[133]
	Saccharomyces cerevisiae	Zinc acetate dihydrate	Spherical 20–30 nm	Antioxidant, antibacterial, anticancer, photocatalytic activity	ZnO NPs showed concentration-dependent increases in anticancer activity. At 100 µg/mL, ZnO NPs inhibited 93% cells	[134]
TiO_2	*B. subtilis*	Titanium dioxide	Spherical 70.17 nm	Treatment of dental caries	Dental caries responded best to treatment with 5% TiO_2, which had no discernible cytotoxic effects	[135]
	Rummelii pycnus Acinetobacter baumanii Acinetobacter seohaensis Bacillus cereus	Titanium Oxychloride	Spherical/irregular 8 nm	Antibacterial	Maximum zone of inhibition was found at 50 mL of TiO_2 NPs	[136]
	Streptomyces sp. HC1	Titanium oxyhydroxide	Spherical 30–70 nm	Antimicrobial, antibiofilm	The highest level of antibiofilm activity was shown by 500 µL TiO_2 NPs produced by *Streptomyces sp*. HC1. Maximum zone of inhibition was recorded against *S. aureus* and *E. coli*	[137]

Table 2 (continued)

MNPs/MONPs	Bacteria used	Metal precursor used	Morphology	Biomedical applications	Findings	References
Ag	*Streptomyces rochei* MS-37	Silver nitrate	Spherical 23.2 nm	Antibacterial, anti-inflammatory, antioxidant	Ag NPs had IC_{50} value of 34.03 µg/mL in CAL27 and 81.16 µg/mL in human peripheral blood mononuclear cells, indicating CAL27 was more susceptible to the NPs cytotoxicity. Ag NPs had MIC ranging from 8 to 128 µg/mL	[138]
	Streptomyces parvus	Silver nitrate	9.7–17.25 nm	Antimicrobial, antioxidant	*K. pneumoniae* (28.33 mm) and *E. coli* (21.66 mm) were susceptible to antibacterial activity. When compared to *E. faecalis* (125 µg/mL), *S. aureus* (250 µg/mL), *P. aeruginosa* (125 µg/mL), *K. pneumoniae* (500 µg/mL), and *E. coli* (250 µg/mL), the MIC of Ag NPs was significant	[139]
	Nocardiopsis dassonvillei	Silver nitrate	Spherical 29.28 ± 2.2 and 32.13 ± 3.4 nm	Antimicrobial, antioxidant, anticancer	Ag NPs showed notable scavenging activity with IC_{50} values of 4.08 and 8.9 µg/mL against OH and DPPH radicals, respectively. Ag NPs with $CaCo_2$ cells demonstrated concentration dependent reduction in cell viability. Lactate dehydrogenase leakage increased as cell viability declined	[140]
	Bacillus amyloliquefaciens MSR5	Silver nitrate	Spherical/cubical/and regular 29.2 nm	Anticancer, catalytic activity	Using $NaBH_4$, Ag NPs demonstrated potent chemocatalytic action, completely degrading 4-NP to 4-aminophenol (4-AP) in 15 min. Ag NPs activated A549cells	[141]
	Bacillus brevis (NCIM 2533)	Silver nitrate	Spherical 41 nm	Antibacterial	Ag NPs demonstrated mean zone of inhibition 14, 15, 16, and 19 mm against *S. aureus* at 5, 10, 15, and 20 µL	[142]

Table 2 (continued)

MNPs/MONPs	Bacteria used	Metal precursor used	Morphology	Biomedical applications	Findings	References
Au	*Streptomyces sp.* NH21	Chloroauric acid	Spherical/rod 18–20 nm	Antibacterial	Ag NPs had MIC of 2.5 µg/mL against *E. coli*, 5 µg/mL against *K. pneumoniae*, *P. mirabilis*, and *S. infantis*, and 10 µg/mL against *P. aeruginosa* and *B. subtilis*. For *P. aeruginosa* and *B. subtilis* minimum bactericidal concentrations were 140 and 170 µg/mL	[143]
	Vibrio alginolyticus	Chloroauric acid	100–150 nm	Antioxidant, anticancer	Colon cancer cell growth inhibited by Au NPs in a dose-dependent manner. 25 µg/mL resulted in maximum inhibition of cell death (> 75%), with an IC_{50} of 15 µg/mL	[144]
	Paracoccus haeundaensis BC74171T	Chloroauric acid	Spherical 20.93 ± 3.46 nm	Antioxidant, anticancer	In HaCaT and HEK293 normal cells, Au NPs did not exhibit growth inhibition. Au NPs exhibited concentration dependent growth inhibition against A549 and AGS cancer cells	[145]
	Enterococcus sp. RMAA	Gold chloride	Spherical	Anticancer	Mitochondrial membrane potential was lowered, ROS and caspase-3 expressions were increased	[146]

with the mineral solution outside the fungal cell [149]. This whole process is accomplished through two distinct mechanisms. First, the fungal cell wall traps metal ions on its surface due to the electrostatic interaction of the positively charged groups in the enzymes, and then, the cell enzymes reduce the metal ions to produce NPs. Second, the method involves the reduction of nitrates using NADPH secreted by fungi, followed by its conversion into NADP to produce extracellular NPs [150]. The myogenic pathway produces better NPs than bacteria and plants because they accumulate metals more efficiently. Triangle-shaped intracellular Au NPs (20–35 nm) synthesized by *Aspergillus clavatus* isolated from *Azadirachta indica* have been explored to demonstrate mycosynthesis [151]. *Phoma glomerata* can be used to synthesize Ag NPs that are antibacterial against resistant strains of *E. coli, P. aeruginosa, and S. aureus* [152]. *Trichoderma viride, Chaetomium globosum, Aspergillus niger, and Pleurotus ostreatus* can produce selenium NPs [153]. *Cladosporium perangustum* aqueous extract-derived Ag NPs decreased MCF-7 cell viability by increasing caspase-3, caspase-7, caspase-8, and caspase-9 expression [154]. Metallic NPs derived from various fungi are presented in Table 3.

Algae

Algae have the capacity to accumulate heavy metal ions. These aquatic microorganisms have been explored to synthesize NPs [176]. Using *Tetraselmis kochinensis*, spherical Au NPs with sizes ranging from 5–35 nm were produced intracellularly [177]. *Sargassum polycystum* (a brown algae)-based CuO NPs had excellent anticancer characteristics and great potential against pathogenic bacteria [178]. Priyadharshini et al. used *Gracilaria edulis* (macroalgae) extract to synthesize Ag and ZnO NPs. The synthesized NPs exhibited excellent antitumor activity against human PC3 cells [179]. *Hypnea musciformis* (Wulfen), a red macroalga, has been explored to synthesize Au NPs for its anti-fungal activity against *Aspergillus niger* and *Mucor spp* [180]. *Ecklonia cava* extract-loaded Ag NPs have shown significant anti-bacterial activity against *E. coli* and *S. aureus*. These NPs had antioxidant properties and anti-cancer activity against human cervical (HeLa) cells [181]. Numerous algal components and precursor salts employed in the synthesis and capping of metallic NPs are shown in Table 4.

Green-synthesized metallic nanoparticles for cancer treatment

Cancer is defined as an abnormal growth of tissue or cells characterized by uncontrolled autonomous division, with the number of cell divisions rising over time [4]. More than 200 distinct cancers have been identified, and they have six common basic characteristics: replicative immortality; the ability to generate new blood vessels; the ability to invade and spread to other organs; resistance to apoptosis; proliferative signaling; and evasion of growth [198]. NPs are used to increase the compatibility and bioavailability of natural bioactives for the treatment of different chronic disorders, including cancer [199]. NPs are often considered as a possible solution for this due to evidence of their ability to induce the apoptotic pathway in vitro, which implies their anticancer effect [200]. NPs have been demonstrated to produce ROS, which can activate pro-apoptotic pathways. Different biogenic metal oxide NPs have shown promising results in the treatment of cancer by producing cytotoxicity in malignant cells while having no effect on normal cells. The specific mechanism by which various metal and metal oxide NPs kill cancer cell types is unclear [201]. It is widely believed that mitochondrial signaling pathways play a crucial role in NP-based activation of apoptosis in cancer cells. Metallic NPs usually produce ROS, which causes oxidative stress and apoptosis [202]. Apoptosis begins with apoptotic protein activation, DNA damage, mitochondrial breakdown, apoptosome formation, and cell shrinkage [203]. Prostate and lung cancer cells are sensitive to cytotoxic activities in *Pinus roxburghii* bioactive-loaded Ag NPs. The ability of mitochondrial depolarization and DNA damage to trigger apoptosis via the intrinsic route have been reported. ROS, cell cycle arrest, and caspase-3 activation cause cancer cell apoptosis [204]. A class of protease enzymes called caspases is important for the apoptotic process. By activating the executioner caspase-3 through cleavage, the initiators caspase-8 and caspase-9 specifically cause the proteolysis of poly(ADP-ribose) polymerase (PARP) and apoptosis by impairing DNA repair [205].

Breast cancer

Breast cancer has surpassed lung cancer as the most frequent cancer in the world, with 2.26 million recorded cases per year, 11.7% of all cancer cases, and 24.5% of malignancies in women. Furthermore, it is the most frequent disease among women, accounting for 15.5% of all female cancer mortality each year [206]. With an emphasis on more biologically directed medicines and treatment deescalation to lessen side effects, therapeutic approaches have evolved over the past 10–15 years to take this heterogeneity into consideration [207]. Capping ZnO NPs with *R. fairholmianus* inhibited cellular development while increasing cytotoxicity and ROS. Apoptosis was also accompanied by an increase in pro-apoptotic proteins (p53, Bax), a decrease in anti-apoptotic proteins (Bcl-2), and a marked elevation in cytoplasmic cytochrome c and caspase 3/7 (apoptosis indicators) [208]. *Calendula officinalis* leaf extract was

Table 3 Biosynthesis of metallic NPs using various fungi and their biomedical applications

MNPs/MONPs	Fungi used	Metal precursor (medium) used	Morphology	Biomedical application	Findings	References
Fe_2O_3/Fe_3O_4	*Penicillium spp.*	Iron (III) chloride	Spherical 3.31 to 10.69 nm	Antibacterial, antioxidant activity	NPs demonstrated inhibition activity at 250 µg against *S. aureus* (12 ± 0.6 nm), *E. coli* (11.3 ± 1.2 nm), *K. pneumoniae* (11.3 ± 0.6 nm), *S. sonnie* (11.3 ± 0.6 nm), and *P. aeruginosa* (11.3 ± 0.6 nm). NPs exhibited antioxidant potential against DPPH radical as compared by ascorbic acid with IC_{50} values of 12.2 µg/mL	[155]
	A. flavus	Iron (II) sulfate heptahydrate	Spherical 28.6–33.8 nm	Antimicrobial	Maximum (10 mm) inhibition of bacterial growth against *S. aureus* was demonstrated by Fe NPs. Zones of inhibition against *S. aureus* and *P. aeruginosa* were 12.3 and 10.5, respectively	[156]
	Aspergillus terreus	Iron (III) chloride	Spherical 40–100 nm	Anticancer	Cell viability dropped to 41.9%	[157]
CuO	*Trichoderma asperellum*	Copper (II) nitrate trihydrate	Spherical 110 nm	Anticancer	CuO NPs significantly increased cell death. IC_{50} for CuO NPs in A549 cell lines was 40.625 µg/mL	[158]
	Aspergillus fumigatus	Copper (II) nitrate trihydrate	Spherical 48 nm	Antibacterial	At 100 µg/mL, CuO NPs showed maximum scavenging activity against DPPH (73.65%)	[159]
	Aspergillus terreus	Copper sulfate	Less than 100 nm	Antimicrobial, antioxidant, anticancer	CuO NPs exhibited the highest activity against *P. aeruginosa, E. coli,* and *V. cholera* (50% cell inhibition at 22 µg/mL)	[160]
	Shizophyllum commune	copper (II) chloride	Spherical 22 to 60 nm	Antibacterial, antifungal	Highest antibacterial efficacy was shown against *S. aureus* followed by *E. coli*. At 150 µM, inhibition zone of 1.7 cm and 1.9 cm was recorded in *C. albicans* and *F. oxysporum, respectively*	[161]

Table 3 (continued)

MNPs/MONPs	Fungi used	Metal precursor (medium) used	Morphology	Biomedical application	Findings	References
ZnO	*Pleurotus ostreatus*	Zinc nitrate	Spherical 7.50 nm	Antibacterial, anticancer	Mushroom extract induced dose-dependent decline in cell viability for Hek293 cells. Lowest cell viability (22%) was recorded at 2000 µg/mL. ZnO NPs synthesized from mushrooms demonstrated comparable cytotoxic effects on HepG2 and Hek293 cells. A steep drop in cell viability in HepG2 cells (97% at 16 µM to 12% at 100 µM) and Hek293 cells (94% at 16 µM to 22% cells at 100 µM) was recorded	[162]
	Cladosporium tenuissimum FCBGr	Zinc nitrate	Hexagonal Less than 100 nm	Antimicrobial, antioxidant, anticancer	ZnO NPs had an IC_{50} concentration of 62 µg/mL for DPPH radical scavenging activity. At 58 µg/mL, NPs inhibited 50% of nitric oxide radicals. ZnO NPs (1 mg/mL) inhibited HeLa cell lines at a rate of 89.59% indicating their effectiveness against cervical cancer cells	[163]
	Aspergillus niger	Zinc acetate	Spherical 23.97 ± 2.29 nm	Antibacterial	MIC values for the antibacterial potential against the tested *S. aureus* ranged from 8 to 128 µg/mL	[164]
TiO_2	*Tricoderma citrinoviride*	Titanium isopropoxide	Irregular/triangular, pentagonal/spherical rod-shaped 10–400 nm	Antibacterial, antioxidant	The biogenic TiO_2 NPs (100 µg/mL) exhibited remarkable antibacterial efficacy when tested on planktonic cells of clinical isolates of *P. aeruginosa* that are highly resistant to drugs. The antioxidant potential of TiO_2 NPs was superior to gallic acid	[165]
	Fomitopsis pinicola	Titanium (IV) isopropoxide	Spherical 10–30 nm	Antibacterial, anticancer	MIC/MBC values were 62.5/125 and 62.5/125 µg/mL for *E. coli* and *S. aureus*. Strong cytotoxic effect of TiO_2 NPs was observed against HCT-116 cancer cells	[166]

Table 3 (continued)

MNPs/MONPs	Fungi used	Metal precursor (medium) used	Morphology	Biomedical application	Findings	References
Ag	*Penicillium oxalicum* (*Amoora rohituka* plant leaf)	Silver nitrate	Spherical 15–19 nm	Antimicrobial, antioxidant, anticancer	MIC_{25}, MIC_{50}, and MIC_{75} values of Ag NPs against *E. coli* were 8.710 ± 0.217, 12.369 ± 0.099, and 81.857 ± 0.453 µg/mL, respectively. The corresponding values for *S. aureus* were 14.417 ± 0.011, 20.975 ± 0.008, and 61.614 ± 1.452 µg/mL, respectively	[167]
	F. oxysporum (*Withania somnifera* leaves)	Silver nitrate	Spherical 10–50 nm	Antibacterial Cytotoxic activity	All the Gram-negative and Gram-positive organisms were found to be sensitive and to exhibit a zone of clearance	[168]
	Aspergillus brasiliensis	Silver nitrate	Spherical 6–21 nm	Antibacterial, antifungal	Ag NPs inhibited *B. subtilis, S. aureus, E. coli, P. aeruginosa,* and *C. albicans* in distinct zones, measuring 12, 15, 12, 12, and 14 mm, respectively	[169]
	Trichoderma spp.	Silver nitrate	Spherical	Antibacterial	Gram-negative bacteria (*E. coli* and *P. aeruginosa)* had lower MIC values than Gram-positive bacteria (*S. aureus and E. faecalis*)	[170]
	Alternaria sp	Silver nitrate	Spherical 3–10 nm	Antifungal	The MIC of Ag NPs was 25 µL, whereas all fungal strains grew at very low rates (50 and 100 µL)	[171]

Table 3 (continued)

MNPs/MONPs	Fungi used	Metal precursor (medium) used	Morphology	Biomedical application	Findings	References
Au	*Cladosporium species* (*C. wightii* leaves)	Chloroauric acid	Spherical (irregular morphology) 5–10 nm	Anticancer effect	IC_{50} value of the Au NPs was 38.23 µg/mL in breast cancer cell line MCF-7	[172]
	Trichoderma hamatum SU136	Gold chloride	Spherical/pentagonal/hexagonal 5–30 nm	Antibacterial	Compared to the clear zones surrounding streptomycin and gold chloride, the AuNPs' clear zone appearance was smaller and showed antibacterial activity against all tested bacterial strains; no clear zones were observed surrounding the fungal mycelial-free extract	[173]
	Alternaria alternata	Chloroauric acid	Spherical/triangular/hexagonal 2–30 nm	Antifungal	–-	[174]
	Fusarium solani	Chloroauric acid	Spindle 40–45 nm	Anticancer	IC_{50} value was found to be 1.3 ± 1.0 µg/mL followed by 0.8 ± 0.5 µg/mL against MCF-7 cell line	[175]

Table 4 Biosynthesis of metallic NPs using various algae and their biomedical applications

MNPs/MONPs	Algae used	Metal precursor (medium) used	Morphology	Biomedical application	Findings	References
Fe_2O_3/Fe_3O_4	*Ulva lactuca*	Iron (III) chloride	Spherical 20 and 40 nm	Anticancer, anti-diarrheal activity	Significant cytotoxicity was observed in cancer cell lines treated with NPs at higher concentrations (50 mg/mL and 100 mg/mL). The zone of inhibition by *Ulva lactuca*-mediated NPs against *E. coli* and *S. aureus* were 29 ± 1 mm and 17 ± 2 mm, respectively	[182]
	Colpomenia sinuosa, Pterocladia capillacea	Iron (III) chloride	Spherical 11.24–33.71 nm, 16.85–22.47 nm	Antibacterial, antifungal	Fe_3O_4 NPs demonstrated superior antifungal efficacy against *A. flavus* (9 mm) and *F. oxysporum* (6 mm) in contrast to Fe_3O_4 NPs derived from *P. capillacea* (7 & 5 mm)	[183]
	Gracilaria edulis	Iron (III) chloride	Cubic 20 nm–26 nm	Antibacterial, antifungal	NPs inhibited *P. aerogenosa* (bacteria), *A. nidulans*, and *C. albicans* (fungi)	[184]
	Oscillatoria limnetica	Iron chloride hexahydrate	Trigonal rhombohedral	Antibacterial, antioxidant, anticancer	Maximum antifungal activity was observed against *Aspergillus versicolor* (MIC value 27 µg/mL and LD_{50} value 47 µg/mL). *B. subtilis* was the most suspected (MIC: 14 µg/mL) and *E. coli* was the least suspected strain (MIC 35 µg/mL)	[185]
CuO	*Bifurcaria bifurcata*	Copper (II) sulfate	Spherical 20.66 nm	Antibacterial	Zones of inhibition for *S. aureus* and *Enterobacte aerogenes* was 14 mm and 16 mm, respectively	[186]
	Sargassum polycystum	Copper solution	–	Antibacterial, antifungal, anticancer	More antibacterial activity was shown in *P. aeruginosa* (15 ± 0.5 mm) than *Shigella dysenteriae* (6 ± 0.5 mm). IC_{50} value for NPs was 61.25 µg/mL	[178]
	Spirulina platensis	Copper (II) acetate	30–40 nm	Antibacterial	Maximum zone of inhibition (28.0 ± 0.41 mm) was shown against *P. vulgaris*	[187]

Table 4 (continued)

MNPs/MONPs	Algae used	Metal precursor (medium) used	Morphology	Biomedical application	Findings	References
ZnO	*S. marginatum*	Zinc nitrate hexahydrate	80–126 nm	Antiviral	NPs demonstrated 99.09% anti-dengue activity in C6/36 cell line	[188]
	Sargassum muticum	Zinc acetate dihydrate	–	Anticancer	> 55% cells survived at 175 µg/mL of ZnO NPs. Cell viability was < 40% 175 µg/mL. HepG2 cell survival percentage was 4.5%. Maximum radical scavenging was observed up to 89% at 2800 µg/mL with an EC_{50} value of 600 µg/mL	[189]
	Anabaena cylindrica	Zinc sulfate	Rod 40–60 nm	Anticancer, antibacterial	ZnO NPs had 50% reduction in cellular viability at 3% dose, while commercial ZnO showed an ED_{50} at 6% of doses. Zone of inhibition against *P. aeruginosa* and *S. aureus* was 10–22 mm and 9–12 mm, respectively	[190]
Ag	*Caulerpa racemosa*	Silver nitrate	Spherical/triangular 10 nm	Antibacterial	Zone of inhibition against *P. mirabilis* was 14 mm at 15 µL and 7 mm against *S. aureus* at 5 µL	[191]
	Spirulina platensis Oscillatoria sp	Silver nitrate	Spherical 14.42–48.97 nm	Antiviral	90% reduction in cytopathic effect of HSV-1 by Ag NPs, with a high reduction rate (49.23%)	[192]
	Pithophora oedogonia	Silver nitrate	Cubical/hexagonal 25–44 nm	Antibacterial	Largest zone of inhibition observed against *P. aeruginosa* (17.2 mm) followed by *E. coli* (16.8 mm)	[193]
	Caulerpa serrulata	Silver nitrate	Spherical 10 ± 2 nm	Antibacterial, catalytic	Maximum inhibition zone (21 mm at 75 µL) was observed against *E. coli*, while lowest inhibition zone (10 mm at 50 µL) was shown for *S. typhi*	[194]

Table 4 (continued)

MNPs/MONPs	Algae used	Metal precursor (medium) used	Morphology	Biomedical application	Findings	References
Au	*Spirulina platensis Oscillatoria sp.*	Tetrachloroauric (III) acid trihydrate	Octahedral/Pentagonal/triangular 15.60–77.13 nm	Antiviral	90% reduction in cytopathic effect of HSV-1 by Au NPs at 31.25 µL with a high reduction rate of Au NPs (42.75%)	[192]
	Sargassum wightii	Chloroauric acid	–	Antiviral	Au NPs showed cell viability of 93.12–85.18%	[195]
	Gracilaria corticata	Chloroauric acid	Spherical 45–57 nm	Antimicrobial, antioxidant	Antibiotic-conjugated Au NPs showed antimicrobial activity against *E. coli* (24 mm) and *E. aerogenes* (21 mm). *S. aureus* (19 mm) showed the moderate antimicrobial activity	[196]
	Padina gymnospora	Gold salt	Spherical/triangular/hexagonal 9–21 nm	Anticancer	50% reduction in cell viability in HepG2 (IC_{50} value of 51.9 nM) was recorded	[197]

used as a green reducing and stabilizing agent in the biosynthesis of Sn NPs. These NPs showed remarkable potential in breast cancer treatment. The IC_{50} values for biosynthesized Sn NPs were 132, 126, and 119 μg/mL for the MCF7, Hs 319.T, and MCF10 cell lines, respectively [209]. *Gloriosa superba* rhizome extract was used in the synthesis of biomolecule-coated nanotitania catalysts. For the MCF-7 (cancer) and L929 (normal) cell lines, the IC_{50} of nanotitania catalysts was 46.64 and 61.81 μg/mL, respectively. Figure 3A shows that when nanotitania catalysts (46.64 μg/mL) were added to MCF-7 cells, they made a lot more intracellular ROS than control cells. This demonstrated that metal and metal oxide nanoparticle exposure increased ROS levels and decreased mitochondrial membrane potential. This suggested that the NPs induced apoptotic cell death. ROS generation can stimulate cell death by apoptosis and necrosis [210].

Yugandhar et al. reported that *Syzygium alternifolium* bark extract-loaded CuO NPs reduced treated cell lines by 50% in comparison with untreated cell lines with an IC_{50} value of 50 μg/mL (Fig. 3B) [211]. *Artabotrys hexapetalus* leaf extracts loaded CeO_2 NPs potent cytotoxicity against MCF-7 cancer cells at an IC_{50} value of 48 0.05 μg/mL [212]. Al-Nuairi et al. used MTT assay to examine the effects of Ag NPs from *Cyperus conglomeratus* root extract on MCF-7 breast cancer cells and normal fibroblasts. The selective cytotoxicity was found against MCF-7 with an IC_{50} of 5 μg/mL [213]. Kabir et al. treated MCF-7 cells for 48 h with *Zizyphus mauritiana* fruit extract-loaded Ag/AgCl NPs. A real-time polymerase chain reaction (PCR) was used to monitor the expression levels of eight apoptosis-related genes. FAS, caspase-8, and FADD expression levels were increased, and PARP expression levels were decreased (Fig. 3C) [214]. To confirm the antiproliferative activity of *P. granatum* crust extract-loaded platinum NPs (Pt NPs), Sahin et al. examined nuclear densification and apoptotic alterations using the propidium iodide staining in MCF-7 cell line. Only a few control cells responded positively to propidium iodide. A progressive increase in the proportion of cells that responded favorably to propidium iodide was seen in the cells treated with 25 μg/mL of Pt NPs after 48-h exposure (Fig. 3D) [215]. Table 5 shows various plant extracts and precursor salts explored to synthesize metallic NPs for their breast cancer applications.

Lung cancer

Lung cancer is the sixth-leading cause of mortality worldwide [226]. With estimated yearly occurrences of 2.21 million (11.4% of cancer cases) and a mortality rate of 1.79 million lung cancer patients per year, lung cancer is still prevalent in all nations. Lung cancer is the second-leading cause of death in women after breast cancer [227]. Because of the long-term adaptation of cancer-causing behaviors including smoking, physical inactivity, and westernized diets, the global incidence of lung cancer is quickly rising [228]. Au NPs containing leaf extract of *Alternanthera bettzickiana* reduced cancer cell growth and triggered apoptosis, DNA breakage, and altered mitochondrial membrane potential in lung cancer cell lines. Au NPs had an impact on cellular M-phase entry. Au^+ may activate p53 and other cell cycle genes, delaying the entry of cells into the M-phase and increasing apoptosis [229].

Cleistanthus collinus extract loaded into Ag NPs has been explored as a reducing and capping agent. The scavenging of free radicals was significantly impacted by the in vitro antioxidant activity of Ag NPs. The IC_{50} for human lung cancer cells (A549) and normal cells (HBL-100) was 30 μg/mL and 60 μg/mL, respectively. Ag NPs do not have any adverse effects on mice organs [230]. A549 cells exposed to 50 μg/mL *Magnolia officinalis* extract-loaded Au NPs showed substantial cell death. TUNEL and DAPI staining of A549 lung cancer cells *Magnolia officinalis* extract-loaded Au NPs confirmed ROS-arbitrated apoptosis (Fig. 4A). The TUNEL assay stained with green fluorescence showed live cells. *Magnolia officinalis* loaded Au NPs confirmed increased apoptotic cells with DAPI staining with blue fluorescent cells [231]. MTT assay to test the anti-lung cancer activity of *Ledebouria revoluta* bulb extract-loaded TiO_2 NPs showed an IC_{50} value of 53.65 μg/mL and showed improved antitumor activity against A549 cells [232]. At 100 μg/mL, biogenic Au NPs showed that Vero cells remained alive; however, these NPs were cytotoxic (IC_{50} 60 μg/mL) against A549 lung cancer cells (Fig. 4B) [233]. The proliferative activity of A549 cells gradually decreased over time in proportion to the increasing concentration of the test substance during the biological synthesis of Pt NPs using *Ononidis radix* extract. The mortality of cells cultured with platinum NPs increased [234]. *Lonicera japonica* extract-loaded Ag NPs at 75 μg/mL concentration showed 52% cell viability (Fig. 4C) [235]. In a xenograft severe combined immunodeficient mouse model, H1299 tumor growth was inhibited by Ag NPs synthesized from longan peel powder. After 36 days of treatment, the lung tumor size was 1.13 ± 0.21 mm^2 and 0.49 ± 0.07 mm^2 in the control and Ag NP-treated groups, respectively [236]. Valodkar et al. conducted in vitro toxicity research on human lung cancer cells using plant latex-capped Ag NPs. At the higher dose, more dead cells (in red) and very few live cells (in green) were seen, indicating a dose-dependent mortality of the cells ranging from 20 to 80% (Fig. 4D) [237]. Table 6 shows various plant extracts and precursor salts explored to synthesize metallic NPs for their lung cancer applications.

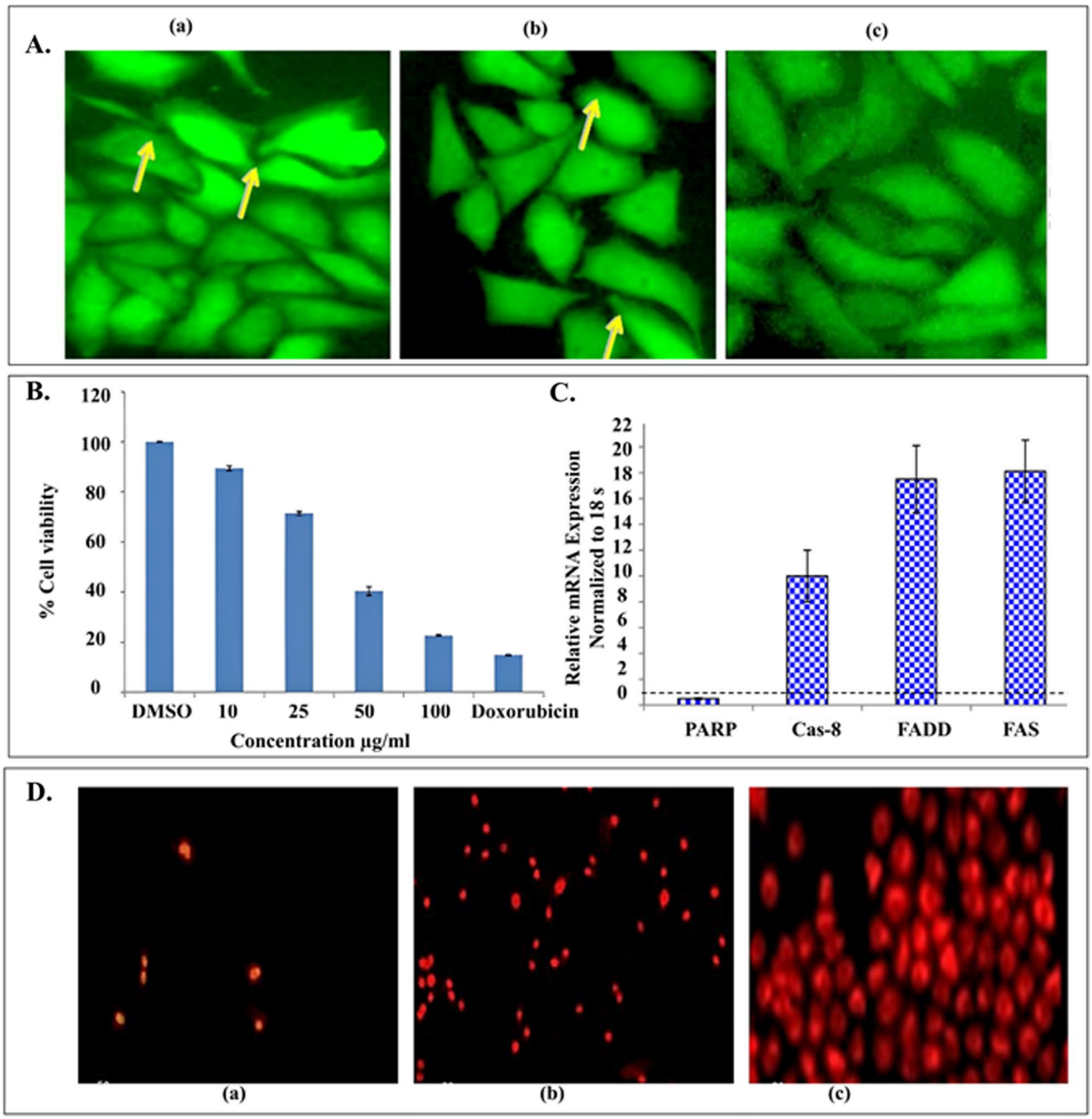

Fig. 3 **A** Effects of *Gloriosa superba* rhizome and *Gloriosa superba* rhizome extract mediated titanium dioxide nanoparticles on intracellular ROS generation in treated MCF-7 cells, shown as follows: (a) nanotitania catalyst-treated cells, (b) rhizome extract, (c) control cells, **B** anticancer activity of CuO NPs synthesized from *S. alternifolium* stem bark extract, **C** Relative mRNA expression percentages following treatment of MCF7 cells with *Z. mauritiana* fruit extract-mediated Ag/AgCl NPs. A dashed line denotes an expression level of 1.0, **D** Pt NPs containing *P. granatum* stained by propidium iodide (a) control; (b) IC_{50} molarity (25 µg/mL); (c) maximum molarity (100 µg/mL). (**A**: under copyright (CC BY) from Taylor and Francis, **B**: under copyright (CC BY) from Springer, **C**: under copyright (CC BY) from ACS publication, and **D**: under copyright (CC BY) from Elsevier)

Cervical cancer

About 604,127 new cases and 341,831 fatalities from cervical cancer are reported in 2020 [253]. *Solanum nigrum* leaf extract-loaded ZnO NPs inhibited β-catenin, increased the levels of p53, caspase-3, and caspase-9, and showed a dose-dependent cytotoxic effect against HeLa cell lines [254]. After 24 h of treatment, *Catharanthus roseus* extract (5 µg/mL) loaded in Au NPs induced

Table 5 Various plant extracts and precursor salts explored to synthesize metallic NPs for their breast cancer applications

Plant used	Metal precursor	Morphology	Cell line	Techniques used	IC_{50} value	Impact	References
Silver							
Tamarindus indica Fruit shell extract	Silver nitrate	Spherical 20–52 nm	MCF7	MTT assay, Dual staining (Ao/EtBr), DCFH-DA staining, Rhodamine 123 staining	20 µg/mL	More nuclear morphological changes significant induction in MMP level compared to control	[216]
Buchanania axillaris leaves	Silver nitrate	Spherical 17–80 nm	MCF7	MTT assay	31 µg/mL	The percent inhibitions of cell growth were found to increase with the increasing concentrations of the nanoparticle	[217]
Cyperus conglomeratus Root Extracts	Silver nitrate	Spherical 70–100 nm	MCF7	MTT assay, Flow cytometry, rtPCR	5 µg/mL	The IC_{50} concentration of synthesized Ag NPs after 24 h treatment of MCF-7 cells significantly reduced the mRNA levels of Bcl2, survivin, and YAP genes compared with control untreated MCF-7 cells	[213]
Phoenix dactylifera root extract	Silver nitrate	Spherical 21.65–41.05 nm	MCF-7	MMTT assay, AO/EtBr staining, Flow cytometry	29.6 µg/mL	At S-phase, it was discovered that the cell cycle is arrested, significantly slowing down the rate of cell division	[218]
Conocarpus Lancifolius fruits extract	Silver nitrate	Spherical 5–30 nm	MDA-MB-231	MMTT assay, DCFH-DA staining, Hoechst blue staining, Rhodamine 123	16.8 µg/mL	Observed dose-dependent cytotoxicity against MDA-MB-231 cells through activation of reactive oxygen species (ROS) generation	[219]
Gold							
Mentha Longifolia leaf extract	Chloroauric acid	Spherical 36.4 nm	MCF7 Hs578Bst Hs319.T UACC-3133	MTT assay	MCF7: 274 µg/mL Hs 578Bst: 279 µg/mL Hs 319.T: 274 µg/mL UACC-3133: 201 µg/mL	The biosynthesized nanoparticles had effective antibreast cancer effects against MCF7, Hs 578Bst, Hs 319.T, UACC-3133 cell lines without any cytotoxicity activity against normal cell line i.e., HUVEC	[220]

Table 5 (continued)

Plant used	Metal precursor	Morphology	Cell line	Techniques used	IC_{50} value	Impact	References
Tecoma capensis (L.) leaves extract	Gold tetrachloroaurate	Spherical 10–35 nm	MCF7	MTT assay, DPPH assay	*T. capensis* extract: 23.3 µg/mL *T. capensis* Au NPs: 9.6 µg/mL	Both *T. capensis* Au NPs and *T. capensis* extract showed significant antioxidant activity with DPPH scavenging percentages of 70.73% for *T. capensis* Au NPs and 85.62% for *T. capensis* extract	[221]
Copper oxide							
Prunus nepalensis Fruit	Copper sulfate	Crystalline 42.5 nm	MCF7 Human normal cell line: MCF10A	MTT assay, Quantitative RT-PCR	158.5 µg/mL	RT-PCR results showed upregulation in p53, caspase-3, Bax, and caspase-9. Down regulation of mRNA expression recorded in Myc and Ras genes in MCF-7 cells	[222]
Acalypha indica leaf extract	Copper sulfate	Spherical 26–30 nm	MCF7	MTT assay	56.16 µg/mL	Plant-mediated copper oxide NPs showed best anticancer activity	[223]
Syzygium alternifolium stem bark	Copper sulfate pentahydrate	Spherical 5–13 nm	MDA-MB-231	MTT assay	50 µg/mL	From 10, 25, 50, and 100 µg/mL, the concentration of CuONPs increased	[211]
Wrightia tinctoria (Wt) extract	Copper sulfate pentahydrate	Spherical 15–40 nm	MCF-7	MTT assay	119.23 µg/mL	The release of copper ions from the nanoparticles, which bind to the cell's DNA, is the primary cause of Cu NPs harmful effects on cancer cells. As a result, it damages DNA and induces cell death	[224]
Titanium oxide							
Gloriosa superba rhizome extract	Titanium hydroxide	Spherical 20–100 nm	MCF7 Normal fibroblast mouse cells: L929	MMTT assay, AO/EtBr and Hoechst staining, DCFH-DA staining, Rhodamine 123, Comet assay	MCF-7: 46.64 µg/mL L929: 61.81 µg/mL	COMET assay confirmed the DNA destruction in the nanotitania-treated cancer cells. The biomolecule-coated nanotitania catalysts could be used as potential and novel comp	[210]

Table 5 (continued)

Plant used	Metal precursor	Morphology	Cell line	Techniques used	IC_{50} value	Impact	References
Zanthoxylum armatum leaf extract	Titanium tetra butoxide	Spherical 15–50 nm	murine 4T1 mammary carcinoma cells	RPMI-1640 assay, Flow cytometry, TBARS assay, Hemolysis assay	4.11 µg/mL	*Z. armatum*-derived NPs are as efficient as doxorubicin toward breast carcinoma with no symptoms of cardio toxicity and alteration in the body weight making them safer than doxorubicin	[225]

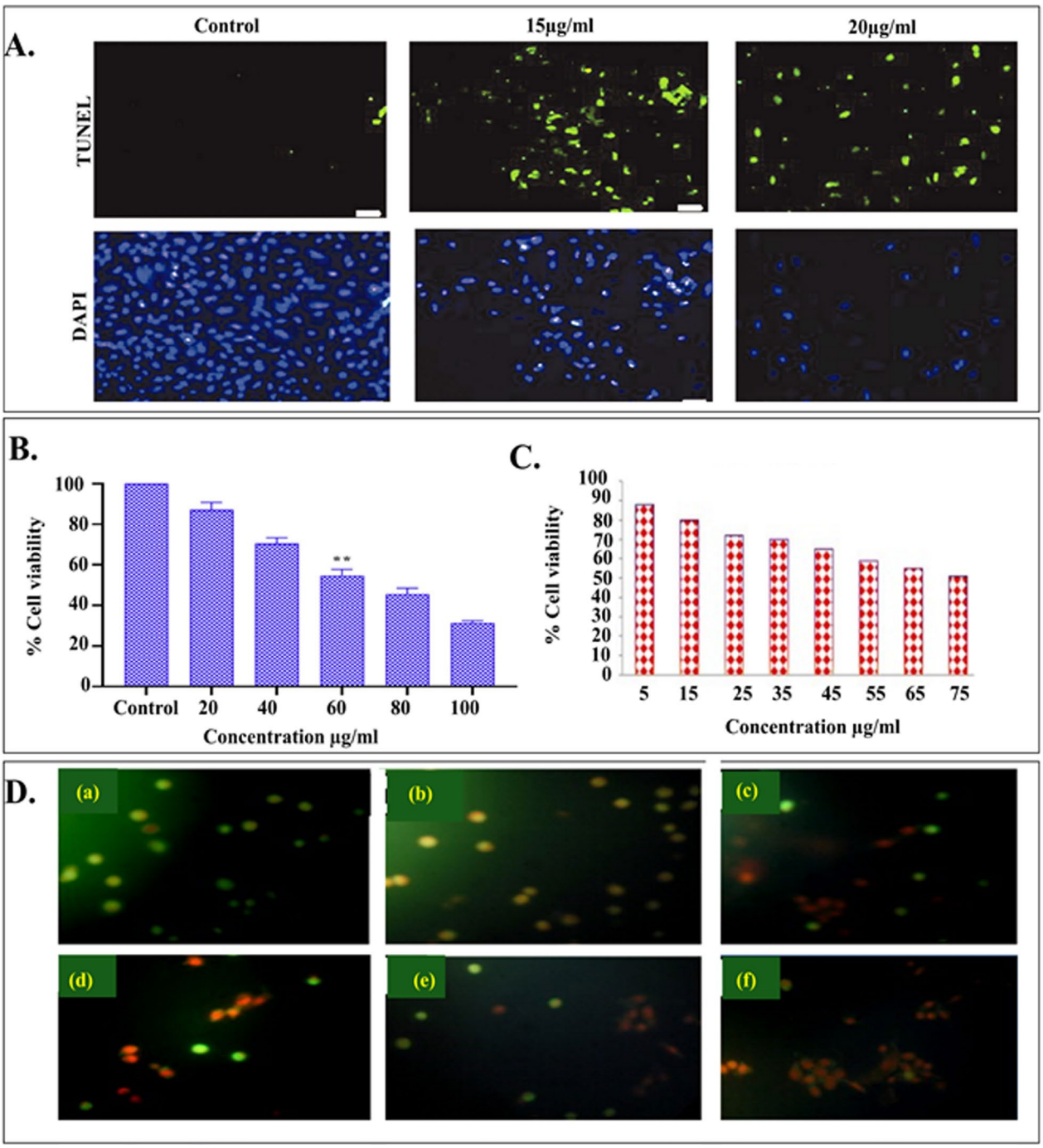

Fig. 4 **A** By using DAPI/TUNEL dual staining, Au NPs synthesized by Magnolia officinalis were determined to increase ROS-arbitrated apoptosis. **B** The cytotoxicity of biogenic Au NPs using bael fruit juice was studied against A549. **C** Anti-cancer ability of synthesized silver nanoparticle (Ag NPs) using phytochemical rich medicinal plant *Lonicera japonica* proved against A549 lung cancer cells by cell viability assay. **D** AO/EB staining of plant latex-capped silver nanoparticles in A549 (cells more dead cells (in red) and very few live cells (in green) in highest dose of LAgNP) exposed to (a) 0 µg/mL LAg NPs, (b) 1 µg/mL LAg NPs, (c) 10 µg/mL LAg NPs, (d) 20 µg/mL LAg NPs,(e) 50 µg/mL LAg NPs and (f) 100 µg/mL LAg NPs (**A:** under copyright (CC BY) from Taylor and Francis, **B**, **C** and **D** under copyright (CC BY) from Elsevier)

Table 6 Various plant extracts and precursor salts explored to synthesize metallic NPs for their lung cancer applications

Plant used	Metal precursor	Morphology	Cell line	Techniques used	IC_{50} value	Impact	References
Silver							
Citrus sinensis leaf aqueous extract	Silver nitrate	Spherical 78.12 nm	NCI-H661, HLC-1, NCI-H1563, LC-2/ad, NCI-H1299, PC-14, HUVEC	DPPH assay, MTT assay	NCI-H661: 82 µg/mL HLC-1: 139 µg/mL NCI-H1563:170 µg/mL LC-2/ad: 66 µg/mL NCI-H1299: 62 µg/mL PC-14: 50 µg/mL	Dose-dependent decrease in human lung cancer cell viability reported	[238]
Leucus aspera leaf extract	Silver nitrate	Spherical 40.67–8.17 nm	A549 HUVEC	DPPH assay, MTT assay	328 µg/mL	No cytotoxicity on the normal cell line (HUVEC) and very low cell viability against the A549 cell line	[239]
Avicennia marina leaf extract	Silver nitrate	Spherical 10–100 nm	A549	MTT assay, DCFH-DA assay, Rhodamine 123	50 µg/mL	High damages in mitochondrial membrane	[240]
Cleome viscosa L fruit extract	Silver nitrate	Spherical 20–50 nm	A549	MTT assay	28 µg/mL	The ability of green-synthesized silver nanoparticles to inhibit cancer cells growth in vitro could be taken as an indicator of potential anticancer effect	[241]
Lonicera japonica leaves extract	Silver nitrate	Spherical	A549	MTT assay	75 µg/mL	At very low concentration- sAg NPs altered the shape of A549 human lung cancer cells	[235]
Gold							
Rabdosia rubescens	Gold (III) chloride trihydrate	Spherical 130 nm	A549	MTT assay, DAPI staining, TUNEL assay, Western blotting analysis	50 µg/mL	Caspase levels were found to be 1.5 times higher in the cells treated with 25 µg/mL of RR-AuNP	[242]
Musa paradisiaca peel extract against	Chloroauric acid	Spherical to triangular 50 nm	A549	MTT assay	58 µg/mL	Nuclear morphological changes, such as cell clumping and a lack of membrane stability, after 24 h at 100 µg/mL	[243]
Marsdenia tenacissima plant extracts	Chloroauric acid	Spherical 40–50 nm	A549	MTT assay, AO/EtBr staining, Western blotting	15 µg/mL	Modulates the levels of the proteins Bax and Bcl-2 to cause apoptosis in the lung cancer cell line A549	[244]
Magnolia officinalis extract	–	Oval, spherical, hexagonal, and triangular 70–10 nm	A549	MTT assay, DCFH-DA, TUNEL assay, Western blotting	50 µg/mL	In A549 cells, Au NPs made from Magnolia officinalis increased the expression of Bax, Beclin-1, and caspase-3 while decreasing the expression of Bcl-2 and Bid	[231]
Zinc oxide							
Azadirachta indica leaf extract	Zinc sulfate heptahydrate	Ribbon/strip shaped	A549	MTT assay, Crystal violet assay, AO/PI staining, Flow cytometry	138.50 µg/mL	Apoptosis was observed in cells treated with IC_{50} dose G1 phase accounted for 76.9% cells get arrested in A549 cells after treatment	[245]

Table 6 (continued)

Plant used	Metal precursor	Morphology	Cell line	Techniques used	IC_{50} value	Impact	References
Euphorbia fischeriana root extract	Zinc acetate dehydrate	Spherical 30 nm	A549	MTT assay, AO/EtBr fluorescence staining, DCFH-DA assay, Rhodamine 123, Cell migration assay, Western blotting analysis	14.5 µg/mL	EF-ZnO NPs induced cytotoxicity also activated apoptosis during increased ROS formation, decreased MMP, inhibited cell migration, altered AO/EtBr staining and induced pro-apoptotic and inhibited anti-apoptotic protein were observed	[246]
Mangifera indica leaf extract	Zinc nitrate	Spherical/hexagonal quartzite 45–60 nm	A549	MTT assay	25 µg/mL	Anticancer activity of ZnO NPs increased with the increasing concentration of NPs and is comparable to the cytotoxic effects of cyclophosphamide in low doses	[247]
Copper oxide							
Calendula officinalis aqueous leaf extract	Copper (II) Nitrate Trihydrate	Spherical 19.64–39.15 nm	LC-2/ad PC-14 HLC-1	DPPH assay, MTT assay	PC-14: 297 µg/mL LC-2/ad:328 µg/mL HLC-1:514 µg/mL	The viability of malignant lung cell line reduced dose-dependently	[248]
Ficus religiosa leaf extract	Cupric sulfate	Spherical	A549	MTT assay, AO/EtBr fluorescence staining, DCFH-DA assay, Rhodamine 123	200 µg/mL	When compared to control, A549 cells treated with copper oxide nanoparticles showed loss of membrane integrity, apoptosis induction, and orange fragmented nuclei, all of which were consistent with low cell viability	[249]
Ilex paraguariensis	Copper(I) sulfate	Spherical 26–40 nm	A549	MTT assay	100 µg/mL	In lung cancer A549 cells, Cu NPs with a size of less than 20 nm caused cytotoxicity	[250]
Beta vulgaris extract	Cupric sulfate	Spherical 33.47 nm	A549	MTT assay, FACS analysis	25 µg/mL	In comparison to control, A549 cells decreased at the G0/G1 phase from 52.8 to 20.6%, increased at the S phase from 38.43 to 30.41%, and considerably increased at the G2/M phase from 14.56 to 52.46%	[251]
Foeniculum vulgare leaves extract	Copper (II) nitrate trihydrate	Spherical 33.62–74.81 nm	NCI-H2126, NCI-H1299, NCIH1437 Normal cell line: HUVEC	MTT assay DPPH assay	Fv-Cu NPs NCI-H2126: 122 µg/mL NCI-H1299: 168 µg/mL NCI-H1437: 108 µg/mL *F. vulgare* extract NCI-H2126: 594 µg/mL NCI-H1299: 781 µg/mL NCI-H1437: 610 µg/mL	The viability of malignant lung cell lines reduced dose-dependently in the presence of NPs. The IC_{50} of Cu NPs and BHT against DPPH free radicals were 42 and 26 µg/mL, respectively	[252]
Titanium oxide							
Ledebouria revoluta bulb extract	Titanium dioxide	Spherical 47.6 nm	A549	MTT assay	53.65 µg/mL	Highly reactive hydroxyl act as a powerful oxidant resulting in oxidative DNA-damage both single and double standard DNA	[232]

apoptosis in HeLa cells dual stained with acridine orange (AO)/ethiduim bromide (EtBr). The control cells showed homogeneous bright green nuclei and cytoplasm for AO-positive cells. In Ao/EtBr staining, the cells treated with the synthesized NPs showed characteristics of apoptosis such as nuclear condensation, cell shrinkage, and the formation of apoptosis bodies (Fig. 5A). HeLa cells were incubated with *Catharanthus roseus* extract-loaded Au NPs at different concentrations (5 and 10 μg/mL) for 24 h to measure the level of ROS production (Fig. 5B) [255]. *A. officinalis* root extract-loaded Ag NPs are toxic to SiHa cell lines, with an IC_{50} of 44 μg/mL. The biosynthesized Ag NPs arrested cell division in the G2/M phases and accelerated the cell cycle in the G1 and S phases [256]. Extract of *Euphorbia antiquorum* L. latex loaded in Ag NPs inhibited the growth of HeLa cell line with an IC_{50} value of 28 μg/mL [257]. After 24 h of incubation, Au NPs containing an aqueous extract of *Alternanthera sessilis* (1–15 μg/mL) showed cytotoxicity against HeLa cells (Fig. 5C) [258]. CuO NPs containing dry black beans (0.5 μg/mL and 1 μg/mL) have shown cytotoxic effects against HeLa cells. CuO NPs inhibited cervical carcinoma colonies and influenced the generation of ROS. The number of cervical carcinoma cell colonies was much lower in CuO NPs-treated cells than in the control group (Fig. 5D) [259]. Table 7 shows various plant extracts and precursor salts explored to synthesize metallic NPs for their cervical cancer applications.

Colorectal cancer

Colorectal cancer (CRC) is the second most lethal and third-most prevalent cancer worldwide. It accounts for 9.2% of all cancer-related deaths and 10.2% of all new cases. Aqueous extract of *Allium cepa* loaded in Ag NPs promotes apoptosis by suppressing expression of Bcl2 family genes [267]. *Albizia lebbeck* extract (40 and 60 μg/mL)-loaded CuO NPs showed early apoptosis (orange stained) and late apoptosis (red stained) apoptotic cells (Fig. 6A) for 24 h through the activation of a dual staining method by AO/EtBr in HCT-116 colon cancer cells [268]. Ag NPs containing *Pimpinella anisum* seed extract showed cytotoxicity against CRC cells. Ag NPs destroyed cancer cells through cell growth inhibition, cell cycle arrest in the G2/M phase, and induction of apoptosis [269]. AO/EtBr staining assay in HCT-116 cells showed that the *Trichosanthes kirilowii* extract loaded in Au NPs increased ROS production, damaged mitochondrial membrane, induced morphological alterations (Fig. 6B), induced G0/G1 phase cell-cycle arrest (Fig. 6C), activated caspase expression, and downregulated anti-apoptotic expression [270]. The cytotoxic effect of lead oxide and CeO_2 NPs synthesized using an aqueous extract of *Prosopis fracta* fruit was investigated in colon (HT-29) cancer cell lines. These NPs were not harmful at 500 μg/mL and 62.5 μg/mL [271]. Ag NPs containing *Curcuma longa* and *Zingiber officinale* rhizomes extract had an IC_{50} of 150.8 μg/mL. At a 25–500 μg/mL dose, the synthesized NPs were cytotoxic to HT-29 cells (Fig. 6D) [272]. Table 8 shows various plant extracts and precursor salts explored to synthesize metallic NPs for their colorectal cancer applications.

Prostate cancer

Prostate cancer is the second most common cancer in men, with 1.41 million incidences annually (14.1% of all cancer cases in men) [275]. Green-synthesized nanosilver containing *Rosmarinus officinalis* extract exhibited cytotoxic effects against prostate cancer cells through the activation of caspase 3 and caspase 9 mRNA [276]. Firdhouse et al. examined the cytotoxic effect of nanosilver containing *Alternanthera sessilis* extract against prostate cancer cells (PC3) at 1.56, 3.12, 6.25, 12.5, and 25 μL/mL doses. The highest concentration (12.5 and 25 μL/mL) of Ag NPs showed a decrease in PC3 cancer cells (Fig. 7A) [277]. *Camellia sinensis L* extract loaded in Au NPs reduced PC-3 cell growth with an IC_{50} of 19.71 μg/mL. Surface detachment, cell shrinkage, and body distortion were observed in PC-3 cells. This demonstrated the cytotoxic effect of green tea extract containing Au NPs [278]. The cytotoxic effect of Au NPs containing an extract of desert truffles (*Tirmania nivea*) against normal human prostate cell lines and prostate cancer cell lines is shown in Fig. 7B [279]. *Salvia miltiorrhiza* extract has been used as a capping agent to synthesize Ag NPs to explore its cytotoxic property against PCa LNcap cell lines. The proliferation of LNcap cells was dramatically inhibited for 24 h with increasing concentration of Ag NPs (Fig. 7C) [280]. The IC_{50} for the PC3 cell line treated with green-synthesized ZnO NPs made from *Hyssopus officinalis* extract for 24 h and 48 h was 8.07 μg/mL and 5 μg/mL, respectively. The percentage of PC3 cells that underwent induced apoptosis was 26.6% ± 0.05, 44% ± 0.12, and 80% ± 0.07 [281]. The Trypan blue exclusion test was used to assess in vitro cytotoxicity in PC-3 cells. Ag NPs of *Dimocarpus longan Lour*. peel extract showed cytotoxic effect at a dose between 5 to 10 μg/mL with an IC_{50} value less than 10 μg/mL (about 50% of PC-3 cells died) (Fig. 7D) [282]. Table 9 shows various plant extracts and precursor salts explored to synthesize metallic NPs for their prostate cancer applications.

Skin cancer

In a study by Wu et al., aqueous *Siberian ginseng* extract was used as an organic reducing agent to biosynthesize Au NPs. These Au NPs were then tested against murine melanoma B16 cells for their anticancer properties.

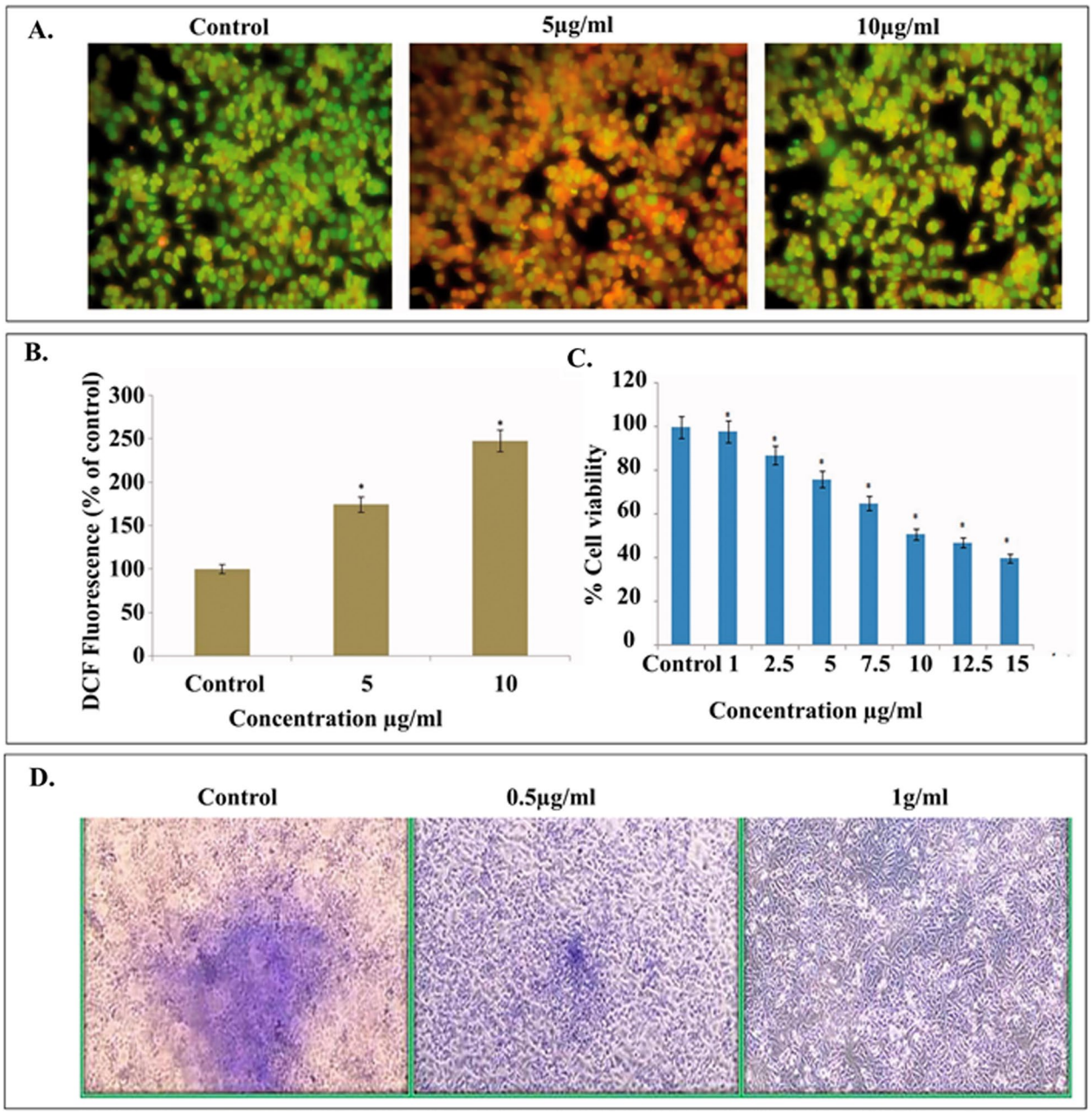

Fig. 5 **A** Ao/EtBr staining after 24 h of treatment with various concentrations (5 and 10 µg/mL) of photosynthesized Au NPs from *Catharanthus roseus*. **B** Using DCFH-DA staining assay photosynthesized Au NPs from *Catharanthus roseus* induces ROS production in HeLa cells. **C** The ability of Au NPs from *A. sessilis* to cause cytotoxicity in HeLa cervical cancer cell lines. **D** Clonogenic survival assay on HeLa cells following incubation with CuO NPs synthesized using an aqueous black bean extract NPs (**A**, **B** and **C** under copyright (CC BY) from Taylor and Francis, **D**. under copyright (CC BY) from Elsevier)

The results demonstrated that the synthesized Au NPs increased ROS levels and decreased mitochondrial membrane potential (Fig. 8A). The BH3 mimics by biosynthesized Au NPs increased the expression of pro-apoptotic proteins while decreasing the expression of anti-apoptotic proteins in melanoma cells [287]. *Cassia fistula* leaf extract reduced silver ions to Ag NPs. The estimated IC_{50} values for the leaf extract, Ag NPs, and $AgNO_3$ were 96.36 1.01 µg/mL, 92.207 1.24 µg/mL, and 84.246 2.41 µg/mL, respectively. The percentage cell viability in Fig. 8B shows the dose-dependent effect of synthesized Ag NPs against cancer cell line [288]. The in vivo

Table 7 Various plant extracts and precursor salts explored to synthesize metallic NPs for their cervical cancer applications

Plant used	Metal precursor	Morphology	Cell line	Techniques used	IC_{50} value	Impact	References
Silver							
Nepeta deflersiana aerial part	Silver nitrate	Spherical 33 nm	HeLa cells	MTT assay, Neutral red uptake assay, DCFH-DA, rhodamine-123	5 µg/mL	ND-Ag NPs have the capacity of inducing apoptosis and necrosis cell death of HeLA cells through SubG1 cell cycle arrest	[260]
Moringa olifera stem bark extract	Silver nitrate	Spherical 40 nm	HeLa cells	Annexin V/PI double-staining assay NRU, DCFH-DA, DAPI staining	–	The increased level of ROS revealed that most of the cells underwent induction of early apoptosis caused by oxidative stress, while many of the inhibitors that induce apoptosis show antioxidant activity	[261]
Detarium microcarpum leaf extract	Silver nitrate	Spherical/rectangular 81 nm–84 nm	HeLa cells	Presto blue cell viability assay	31.5 µg/mL	The synthesized NPs had inhibitory effect on cervical cancer cells	[262]
Gold							
Catharanthus roseus leaf extract	$HAuCl_4$	Spherical 25–35 nm	HeLa3T3 cell lines	MTT assay, AO/EtBr staining, DCFH-DA staining, Rhodamine 123 Caspases activity assay, Western blotting	5 µg/mL	The cytotoxicity and apoptosis of human cervical carcinoma (HeLa) cells increased Caspase-3 was cleaved after being exposed Biosynthesized NPs for 24 h	[255]
Pongamia pinnata leaf extract	$HAuCl_4$	Spherical 55 nm	HeLa cells Human embryonic kidney cell line: HEK293	MTT assay, Flow cytometry, Rhodamine 123, Wound healing/cell migration assay	200 µg/mL	Au NPs gets internalized into HeLa cells by endocytosis. Inside the cytosol, it exhibited cytotoxic effect by elevating intracellular ROS, perturbing the MMP, arresting cells at S-phase of the cell cycle and finally inducing cell death by apoptosis	[263]
Copper oxide							
Brassica oleracea var acephala leaf extract	Copper sulfate	Spherical 60–100 nm	HeLa cells	MTT assay	119.0805 µg/mL	The vitality of cancer cells declines as sample concentration rises, whereas cytotoxicity against HeLa cell lines rises as sample concentration rises	[264]
Phaseolus vulgaris	Copper sulfate	Spherical, hexagonal 26.6 nm	HeLa	SRB assay, Hoechst 33,258 staining, DCFH-DA, Clonogenic assay	0.5 and 1 µg/mL	In a dose-dependent manner Induced intracellular ROS generation	[259]

Table 7 (continued)

Plant used	Metal precursor	Morphology	Cell line	Techniques used	IC_{50} value	Impact	References
Houttuynia cordata	Copper sulfate	Spherical 40–45 nm	HeLa	MTT assay, DCFH-DA, EtBr/AO staining, DAPI staining, Pi stainin, Q-RT-PCR	5 µg/mL	Biosynthesized NPs inhibited cell proliferation and promoted apoptosis by targeting PI3K/Akt signaling pathways in HeLa cells	[265]
Titanium oxide							
Coleus aromaticus leaf extract	TiO_2	Hexagonal shape 12–33 nm	HeLa	MTT assay	34.45 µg/mL	Increased oxidative stress, destroyed the cell membrane, enhanced lipid peroxidation, lowered the level of glutathione (GSH), and eventually contributed to cells' death	[266]

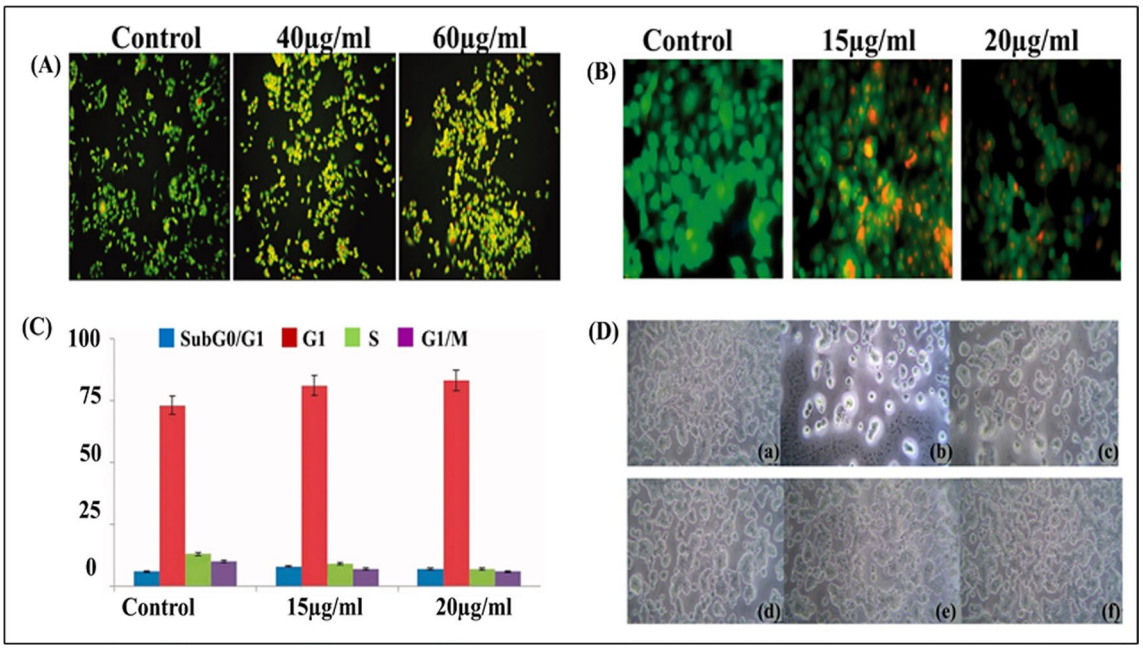

Fig. 6 **A** Dual staining method by AO/EtBr in HCT-116 colon cancer cells. **B** Induction of apoptosis on HCT-116 cells treated with Au NPs synthesized from *Trichosanthes kirilowii* at various concentrations upto 24 h studied using AO/EB staining assay. **C** Cell-cycle analysis of HCT-116 cells treatment with Au NPs (15 and 20 µg/mL) synthesized from *Trichosanthes kirilowii*. **D** Anticancer activity of *Zingiber officinale* and *Curcuma longa* synthesized Ag NPs at different concentrations (a) control, (b) 500 µg/mL, (c) 250 µg/mL, (d) 100 µg/mL, (e) 50 µg/mL and (f) 25 µg/mL (**A**, **B** and **C** under copyright (CC BY) from Taylor and Francis, **D** under copyright (CC BY) from Elsevier)

therapeutic efficacy of *Quisqualis indica* flower extract-derived Cu NPs was investigated by Mukhopadhyay et al. in mice carrying B16F10 melanoma tumors. A substantial reduction in tumor development was recorded. Quisqualis indica flower extract-derived Cu NPs triggered cytotoxicity and death in melanoma cells due to the gene expression [289]. In a study, polyphenols from *Vitis vinifera L.* (grape) peels were used as reducing and stabilizing agents for the synthesis of Au NPs. The IC_{50} value for *V. vinifera* peel extract was 319.14 µg/mL. The IC_{50} values of *V. vinifera* peel loaded Au NPs and fluorouracil (standard drug) were 23.6 µM and 23.43 µM, respectively. Figure 8C displays the percentage of inhibition plotted against the concentration of fluorouracil and peel extract-loaded Au NPs [290]. Ag NPs of *Indigofera longeracemosa* leaf extract revealed a dose–response relationship with an IC_{50} value of 48 µg/mL against the human skin cancer cell line SK MEL-28. Biosynthesized NPs upregulated the tumor suppressor gene p53 and significantly downregulated the anti-apoptotic gene Bcl-2 [291]. *Elephantopus scaber*-loaded Ag NPs were more effective against the A375 skin carcinoma cell line than its pure extract. After 48 h of incubation, morphological changes in treated A375 cells were observed under an inverted phase contrast tissue culture microscope (Fig. 8D) [292]. Table 10 shows various plant extracts and precursor salts explored to synthesize metallic NPs for their skin cancer applications.

Liver cancer

Liver cancer is the sixth-most common primary malignancy and the fourth-leading cause of cancer-related deaths in the world. Cholangiocarcinoma (CCA) and hepatocellular carcinoma (HCC) are the two most common histologic types of primary liver cancer, accounting for more than 80% of all cases. Liver fibrosis and inflammation-induced necrosis are the major causes of malignancy [296]. The effect of *Cordyceps militaris*-loaded Au NPs on the mitochondrial membrane potential of HepG2 cells revealed a strong green fluorescence in untreated cells with high membrane potential. Green fluorescence intensity decreased in HepG2 cells treated to 10 and 12.5 µg/mL Au NPs. The mitochondrial membrane potential remained intact in untreated cells (Fig. 9A). Untreated cells did not exhibit apoptosis, as shown by green fluorescence staining in Fig. 9B. HepG2 cells treated with Au NPs (10 and 12.5 µg/mL) showed a substantial increase in apoptotic cells as visualized by orange fluorescence staining. HepG2 cells were found to undergo apoptosis after being exposed to Au NPs coated with an extract of Cordyceps militaris [297]. *Coriandrum sativum* leaf aqueous extract-loaded iron

Table 8 Various plant extracts and precursor salts explored to synthesize metallic NPs for their colorectal cancer applications

Plant used	Metal precursor	Morphology	Cell line	Techniques used	IC_{50} value	Impact	References
Silver							
Allium cepa L (*A. cepa*) extract	Silver nitrate	Cubic shapes 150–250 nm	HT-29 and 0SW620 cells	DPPH scavenging, activity, TAA, FRAP, MTT assay, RT-PCR, Flow cytometry	*A. cepa* TAA: 55.49 ± 0.91 DPPH-SA: 2.23 ± 0.36 FRAP:14.78 ± 0:20 Ag NPs-CEPA TAA: 58.85 ± 4.39 DPPH-SA: 1.91 ± 0.20 FRAP: 13.37 ± 0.17	The synthesized NPs inhibited cell proliferation and induced apoptosis by inhibiting Bcl2 family gene expression hence act as a promising anticancer agent for treating colorectal cancer	[267]
Anthemis atropatana aerial parts	Silver nitrate	Spherical 38.89 nm	HT29 cancer cell	MTT assay, RT-PCR, Flow cytometry, DNA fragmentation assay	100 µg/mL	Caused the cell to undergo early and delayed apoptosis by 15.64 and 21.32%, respectively	[273]
Vitex negundo L. leaves extract	Silver nitrate	Spherical 5–47 nm	HCT15	MTT assay, Propidium iodide staining, Flow cytometry, Comet assay	20 µg/mL	Ag NPs exerted antiproliferative effects on colon cancer cell line by suppressing its growth, arresting G0/G1-phase, inhibited DNA synthesis and induced apoptosis	[274]
Gold							
Albizia lebbeck leaf extract	$HAuCl_3$	Spherical 20 and 30 nm	HCT-116 colon cancer cell lines	MTT assay, AO/EtBr staining, DCFH-DA staining, Rhodamine 123, Caspases activity assay, Western blotting	48 µg/mL	HCT-116 cells improved the activity of caspase-9 and caspase-3 in a dose-dependent manner	[268]

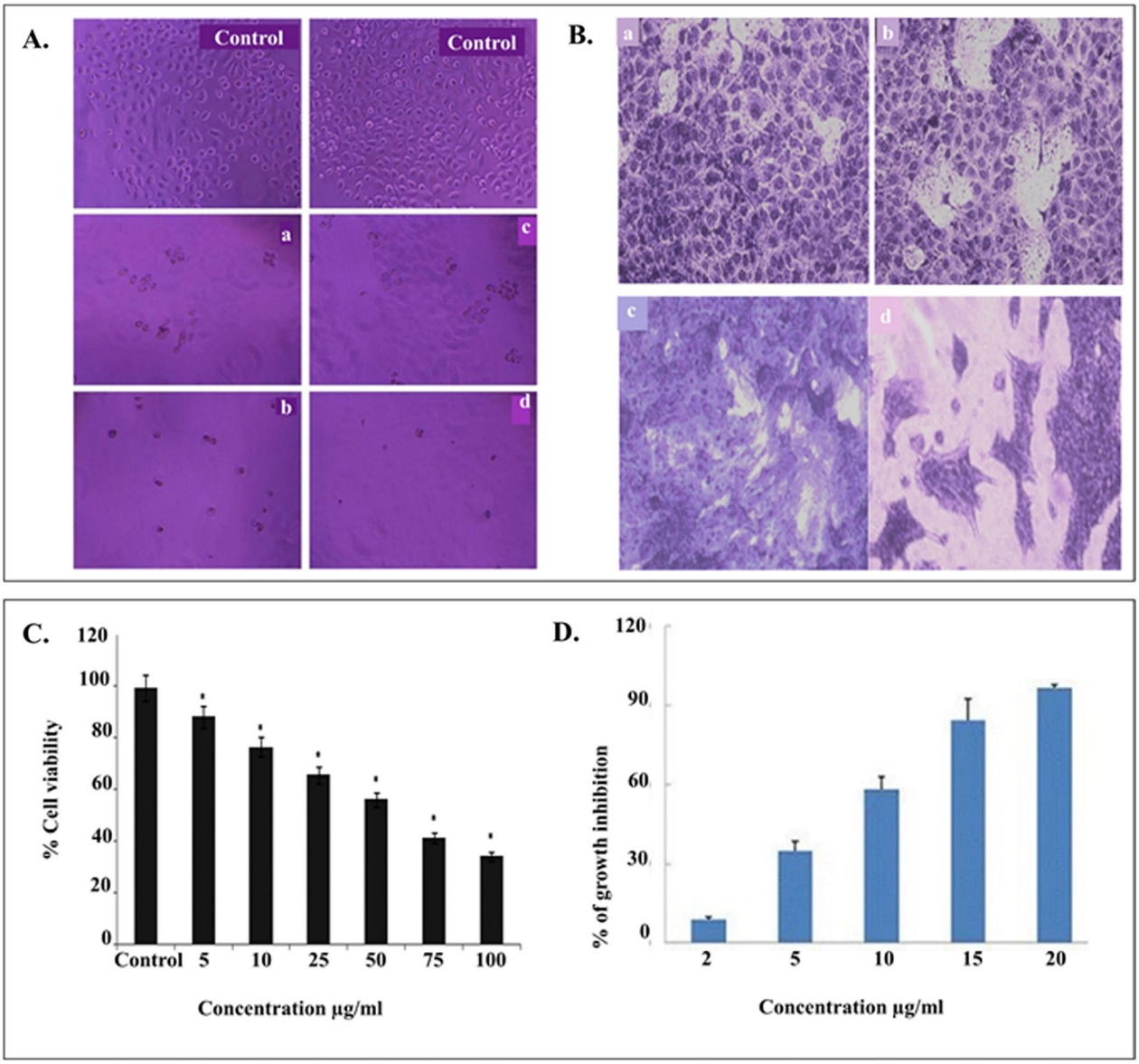

Fig. 7 **A** Cytomorphological changes such as cancer cell membrane lyses, coiling with the addition of silver (a, b) and nanosilver synthesized using *Alternanthera sessilis* in (d, e) after 48 h compared to that of control. **B** The cytotoxicity of Au NPs synthesized using extract of desert truffles (*Tirmania nivea*) against normal human cell line (a) untreated cells, (b) treated cells with synthesized Au NPs, and against cancer cell line (c) control untreated VCaP cells, (d) Treated VCaP cells with synthesized Au NPs. **C** Cytotoxic potential of Ag NPs from leaf extract of *Salvia miltiorrhiza* in prostate cancer LNcap cell. **D** Dose-dependent cytotoxic effects of Ag NPs biosynthesized using *Dimocarpus Longan Lour*. Peel Extract on prostate cancer PC-3 cells in vitro (**A** and **D** under copyright (CC BY) from Springer, **B** under copyright (CC BY) from Elsevier, **C** under copyright (CC BY) from Taylor and Francis)

NPs were green-synthesized by Zhan et al., and they demonstrated dose-dependent anticancer activity and very poor cell viability against LMH/2A, McA-RH7777, N1-S1 Fudr, and SNU-387 cell lines while having no cytotoxicity on the normal cell line (HUVEC) [298]. The MTT assay was used to test the in vitro cytotoxicity of Ag NPs loaded with extract from the *Punica granatum* leaf against the HepG2 cell line. This study found that Ag NPs had substantial anti-cancer efficacy at a dosage of 70 µg/mL, causing 50% cell death (Fig. 9C). Ag NPs significantly inhibited cell growth by more than 90% [299]. With an IC_{50} value of 93.75 µg/mL, *Morinda pubescens* extract-loaded Ag NPs have been shown to exhibit considerable cytotoxic effect against HEPG2 cell lines [300]. In a time- and dose-dependent manner, *Artemisia scoparia* extract and its biosynthesized ZnO NPs decreased

Table 9 Various plant extracts and precursor salts explored to synthesize metallic NPs for their prostate cancer applications

Plants used	Metal precursor	Morphology	Cell line	Techniques used	IC_{50} value	Impact	References
Silver							
Carica papaya leaf extract	Silver nitrate	Spherical 10–20 nm	DU145	MTT assay, DCFH-DA, Flow cytometry, AO/EtBr staining	5 µg/mL	G1-S phase cell cycle check point marker, cyclin D1 was down-regulated along with an increase in cip1/p21 and kip1/p27 tumor suppressor proteins by Ag NPs-PLE	[283]
Dimocarpus Longan Lour. Peel Extract	Silver nitrate	Spherical 9–32 nm	PC-3	Trypan Blue, Exclusion assay, Western blot analysis	Between 5 and 10 µg/mL	An increase in caspase-3 was seen along with a decrease in stat 3, bcl-2, and survivin	[282]
Dovyalis caffra fruit extract	Silver nitrate	Spherical 12–53 nm	PC-3	Sulforhodamine B (SRB) assay	–	At 100 µg/mL, microscopic observations revealed membrane shrinkage, failure of cell adhesion, blebbing of the cell membrane, lyses of the cell membrane, the emergence of unique cellular crinkle, and cell death	[284]
Indigofera hirsute L. leaf extract	Silver nitrate	Spherical 5–10 nm	PC-3	MTT assay	68.5 µg/mL	As the concentration of increases, the cells become clustered and exhibited morphological alterations which eventually leads to cell death or apoptosis	[285]
Salvia miltiorrhiza	Silver nitrate	Spherical, oval, hexagonal and triangular 80 and 12 nm	LNcap cells	MTT assay, DCFH-DA, TUNEL assay, AO/EtBr staining, Caspase-8, 9 and 3 activity assay, Western Blot Analysis	50 µg/mL	Ag NPs effectively causes cytotoxicity, ROS, and apoptosis in LNCap cell lines by altering the expression of intrinsic apoptotic genes	[280]
Gold							
Alhagi maurorum leaf aqueous extract	$HAuCl_4 \cdot H_2O$	Spherical less than 100 nm	DU 145, NCI-H660, 22Rv1, and LNCaP clone FGC)	MTT assay	DU 145: 229 µg/mL NCI-H660: 368 µg/mL 22Rv1: 298 µg/mL LNCaP clone: 222 µg/mL	The viability of malignant prostate cell lines reduced dose-dependently in the presence of Au NPs	[286]

Table 9 (continued)

Plants used	Metal precursor	Morphology	Cell line	Techniques used	IC_{50} value	Impact	References
Titanium oxide							
Coleus *aromaticus* leaf extract	TiO_2	Hexagonal shape 12–33 nm	HeLa	MTT assay	34.45 µg/mL	Increased oxidative stress, destroyed the cell membrane, enhanced lipid peroxidation, lowered the level of glutathione (GSH), and eventually contributed to cells' death	[266]

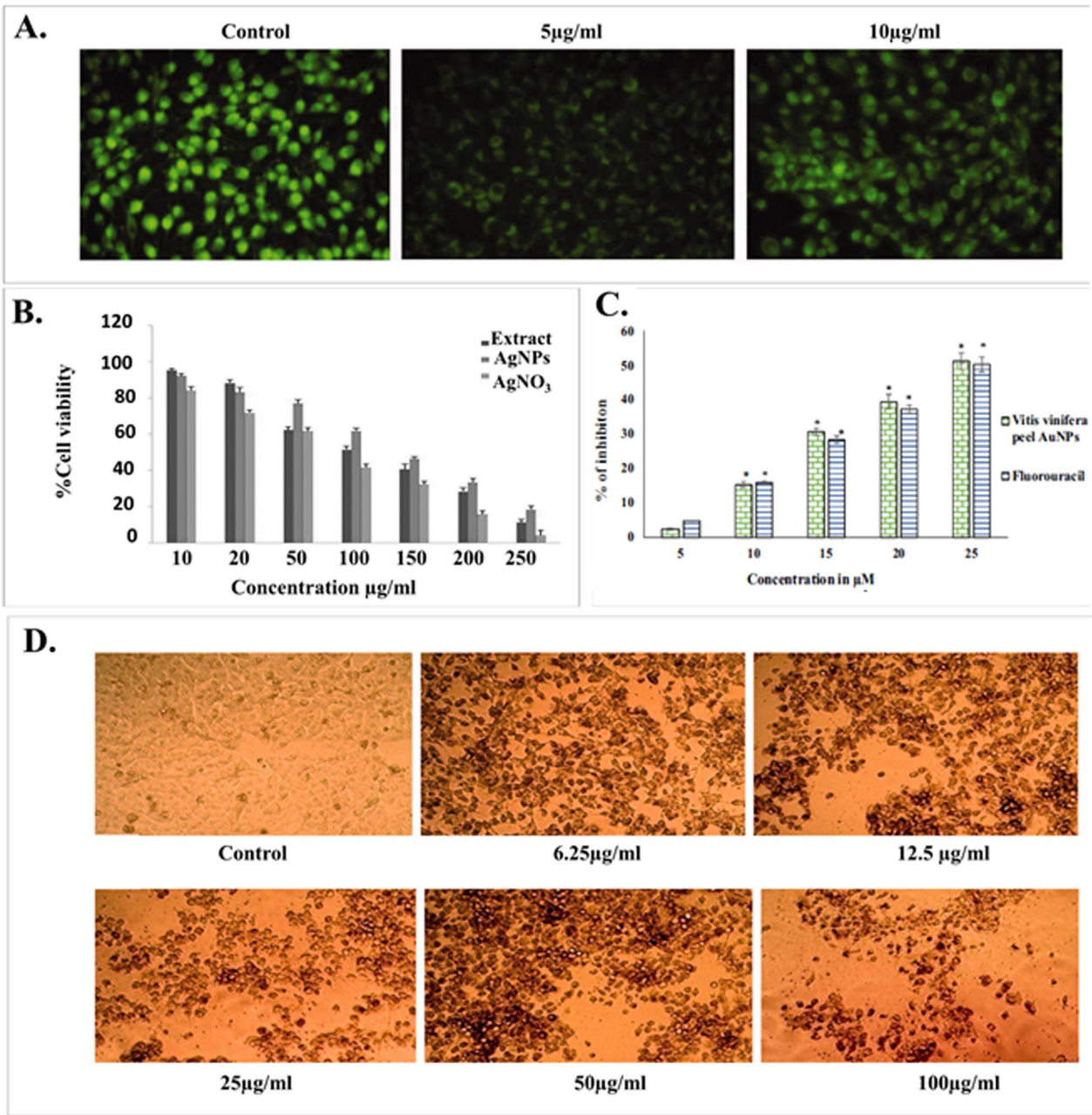

Fig. 8 **A** Using a 1-mM Rhodamine 123 staining approach, the apoptotic effect of *Siberian ginseng* synthesized Au NPs on the mitochondrial membrane permeability in murine melanoma cell line B16 was evaluated. **B** Ag NPs from the leaf extracts of *Cassia fistula* have been shown to be toxic to A-431 epidermal cancer cells (IC_{50} values for the leaf extract, Ag NPs, and $AgNO_3$ are anticipated to be 96.36 ± 1.01, 92.207 ± 1.24, and 84.246 ± 2.41 µg/mL, respectively). **C** Fluorouracil and *Vitis vinifera* peel Au NPs had an inhibitory effect on A431 cells 24 h after incubation. **D** Morphological changes induced on treated A375 cells by Ag NPs using the phytoreducing agent *Elephantopus scaber* (**A** and **D** under copyright (CC BY) from Taylor and Francis, **B** under copyright (CC BY) from Wiley Online Library, **C** under copyright (CC BY) from Elsevier)

cell proliferation and induced apoptosis in Huh-7 cancer cells. *Artemisia scoparia* extract and its biosynthesized ZnO NPs had IC_{50} values of 10.26 and 310.24 µg/mL, respectively. Figure 9D shows that the anti-apoptotic genes were downregulated while the pro-apoptotic genes were upregulated by the *Artemisia scoparia* extract-loaded ZnO NPs [301]. With an IC_{50} value of 62.5 µg/mL, *Seripheidium quettense*-mediated green synthesis

Table 10 Various plant extracts and precursor salts explored to synthesize metallic NPs for their skin cancer applications

Plant used	Metal precursor	Morphology	Cell line	Techniques used	IC_{50} value	Impact	References
Silver							
Petals of *C. maxima*, Leaves of *M. oleifera* and the rhizome of *A. calamus*	Silver nitrate	*C. maxima*: Spherical 19 nm *A. calamus*: spherical 19 nm *M. oleifera*: rectangular 11 nm	A431	MTT assay	*C. maxima*: 82.39 ± 3.1 µg/mL *M. oleifera*: 83.57 ± 3.9 µg/mL *A. calamus*: 78.58 ± 2.7 µg/mL	Ag NPs synthesized using petal extract have a higher IC_{50} value than those using rhizome extract	[293]
Trapa natans extract leaf extract	Silver nitrate	Spherical 30–90 nm	A431	MTT assay	64.2 µg/mL	Glycosides, amino acids, flavonoids, and polyphenols as well as nano-sized silver particles may be responsible for anticancer activity of bio-synthesized Ag NPs	[294]
Cassia fistula leaf extract	Silver nitrate	Spherical 40–50 nm	A-431	MTT assay	92.2 ± 1.2 µg/mL	The DLS findings showed that synthesized Ag NPs can also be utilized in conjunction with conventional medications to increase their efficacy	[288]
Gold							
Vitis vinifera L (grapes) peel extract	Hydrogen tetrachloroaurate (III) trihydrate	Spherical 20–40 nm	A-431	MTT assay DCFH-DA assay Tunel assay Rhodamine 123 AO/EtBr fluorescence staining	23.6 µM	Peel gold nanoparticle treatment resulted in a percentage of apoptotic cells of 10.02% and secondary necrotic cells of 55.5%	[290]
Siberian ginseng aqueous extract	HAuCl4	Spherical 200 nm	B16	MTT assay DCFH-DA assay Rhodamine 123 AO/EtBr fluorescence staining qPCR	10 µg/mL	In 10 µg/mL SG-GNPs treated cells compared to the control, more late apoptotic cells colored orange by EtBr were found	[287]
Zinc oxide							
Limonium pruinosum	Zinc acetate dihydrate	Hexagonal/cubic 41 nm	A-431	MTT assay	409.7 µg/mL	The green-synthesized ZnO NPs in the current study showed higher toxicity toward cancer cells compared to normal cells (WI-38)	[91]

Table 10 (continued)

Plant used	Metal precursor	Morphology	Cell line	Techniques used	IC_{50} value	Impact	References
Acorus calamus	Zinc acetate	Irregular/oval 50 – 100 nm	SK-MEL-3	MTT assay	17.50 µg/mL	Morphological alterations like cell shrinkage, detachment, rounding, and irregular shape were noted in the AC-ZnO NPs challenged cells, thus proving its cytotoxicity against SK-MEL-3 cells	[295]

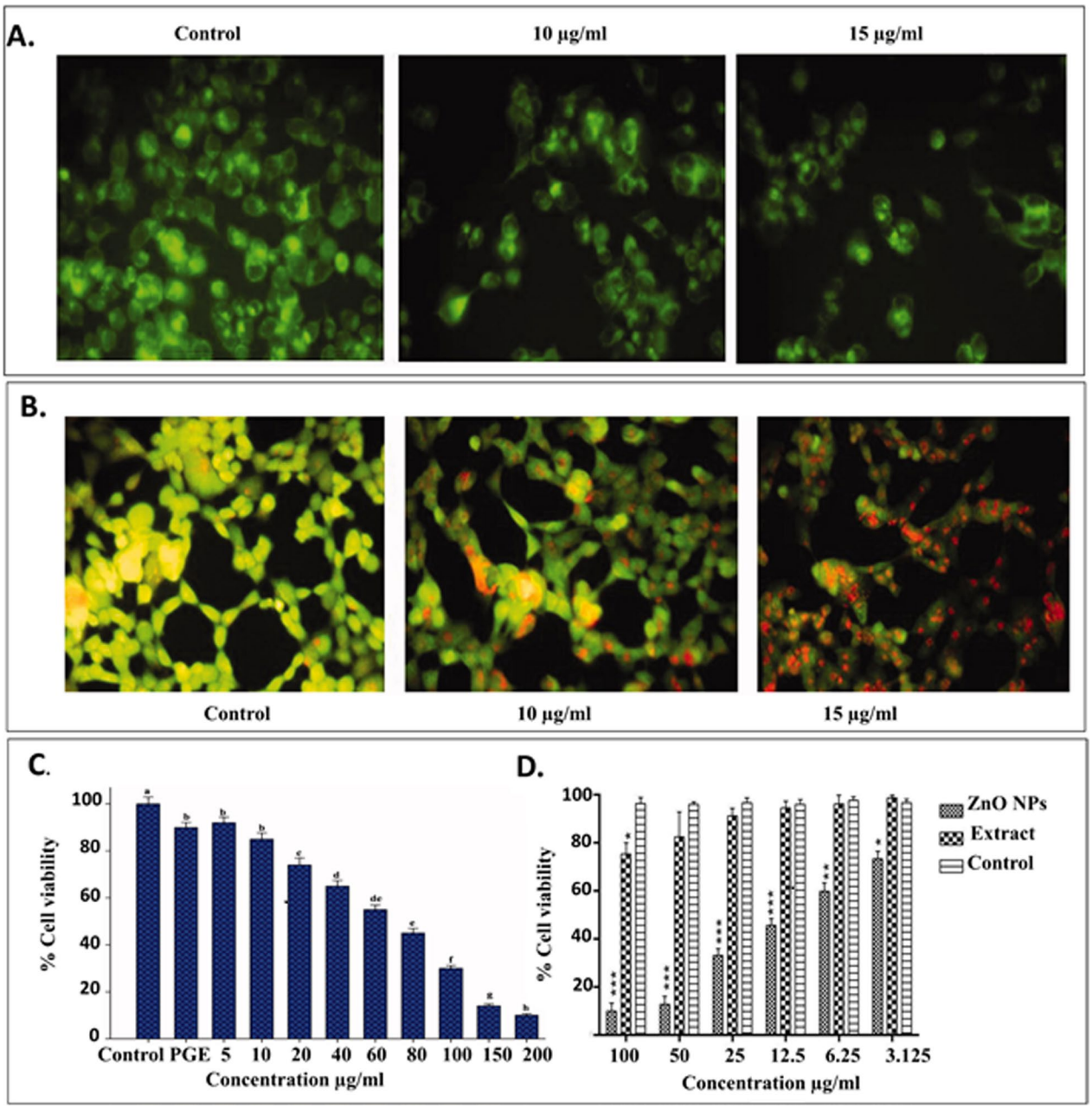

Fig. 9 **A** Represents that the mitochondrial membrane permeability of *Cordyceps militaris* extract synthesized Au NPs, **B** effect of Au NPs from *C. militaris* induces apoptotic morphological changes in HepG2 cells. Green fluorescence labeling revealed that apoptosis had not occurred in the untreated cells. Orange fluorescence staining in HepG2 cells at 10 mg and 12.5 µg/mL shows that the Au NPs treatment dramatically boosted the apoptotic cells. **C** anticancer activity of various concentrations of synthesized Ag NPs synthesized using *Punica granatum* leaves against the liver cancer cell line—HepG2, and **D** cytotoxic effects of biosynthesized ZnO NPs using *Artemisia scoparia* leaf extract against Huh-7 liver cancer cells (under copyright (CC BY) from Taylor and Francis online)

of biogenic Ag NPs inhibited the proliferation of HepG2 cells [302]. Table 11 shows various plant extracts and precursor salts explored to synthesize metallic NPs for their liver cancer applications.

Theranostic applications of green-synthesized nanoparticles

Theranostics is a multidisciplinary scientific field focused on creating a wide range of complex diagnostic and

Table 11 Various plant extracts and precursor salts explored to synthesize metallic NPs for their liver cancer applications

Plant used	Metal precursor	Morphology	Cell line	Techniques used	IC_{50} value	Impact	References
Silver							
Punica granatum leaf extract	Silver nitrate	Spherical 20–45 nm	HepG2	MTT assay, DPPH assay	70 µg/mL	It was hypothesized that Ag NPs could inhibit the function of abnormally increased signaling proteins or interact with functional groups of intracellular proteins and enzymes, as well as with the nitrogen bases in DNA, causing cell death	[299]
Artemisia kopetdaghensis shoot extract	Silver nitrate	Spherical 3–35 nm	HepG2	MTT assay	0.125 µg/mL	Due to Ak-Ag NPs' increased cellular uptake and retention, the NPs were highly cytotoxic to HepG2 cell lines	[303]
Gold							
Cajanus cajan seed coat	$AuCl_4$	Spherical 9–41 nm	HepG2	MTT assay, Flow cytometry, Comet assay, Annexin-V/PI double-staining assay	6 µg/mL	decrease in DNA amount and appearance in the sub-G0/G1 area, both of which are signs of apoptosis	[304]
Zinc oxide							
Artemisia scoparia leaf extract	Zinc acetate dihydrate	Spherical 9.00 ± 4.00 nm	Huh-7	MTT assay, Flow cytometry, DAPI staining, RT-PCR, Propidium iodide staining	ZnO NPs: 10.26 Extract: 310.24 µg/mL	Anticancer effect was stronger in the synthesized ZnO NPs than the extract	[301]
Lawsonia inermis leaf extract	Zinc nitrate	Cubic, rod, Triangular, spherical 5–35 nm	Hep-G2	MTT assay, DCFH-DA	21.63 µg/mL	DNA damage and the stimulation of intrinsic mitochondrial pathways were two ways that ZnO NPs triggered apoptosis	[305]
Eclipta prostrata leaf extract	Zinc nitrate	Triangle, radial, hexagonal, rod, and rectangle 16–85 nm	Hep-G2		100 µg/mL	ZnO NPs can potentially change apoptotic protein expression and trigger apoptosis in mitochondria-dependent pathways in Hep-G2 cells	[306]
Copper oxide							
Eclipta prostrata leaves extract		Spherical 28–45 nm	HepG2	DPPH assay, MTT assay	–	Cu NPs were tested for in vitro cytotoxicity against HepG2 cell lines at 1, 10, 100, 250, and 500 µg/mL; these concentrations resulted in cellular toxicity values of 3.0, 15.5, 28.5, 44.5, and 54.5%, respectively	[307]

therapeutic agents. By utilizing nanotechnology, theranostics enhance bioavailability by delivering bioactives to the sites of absorption. Theranostics utilizing metallic NPs could be useful in treating a wide range of conditions, including cancer, malaria, microbial infections, and cardiovascular disorders [308]. There has been a significant increase in the production of metallic NPs from medicinal plants. These metallic NPs play a crucial role in the advancement of theranostics. Anisotropic Au NPs were produced by an aqueous method employing cocoa extract. These NPs exhibited favorable biocompatibility when subjected to in vitro testing utilizing A431, MDA-MB231, L929, and NIH-3T3 cell lines, at doses of up to 200 μg/mL. The use of green-synthesized NIR absorbing anisotropic Au NPs was effective in causing cell death in epidermoid carcinoma A431 cells when irradiated with a femtosecond laser at 800 nm with a low power density of 6 W/cm^2. This demonstrates the suitability of NPs for photothermal ablation of cancer cells. These Au NPs exhibited high X-ray contrast during computed tomography testing, thus confirming their suitability as a contrast agent [309].

The synthesis of Au NPs using cinnamon proved to be an effective diagnostic agent for imaging both in laboratory settings and within living organisms. These NPs possess both biocompatibility and purity, making them suitable for use in in vivo applications. Photoacoustic emissions based in vitro study confirmed internalization of NPs in PC-3 and MCF-7 cells. Additionally, biodistribution investigations conducted on healthy mice demonstrated that these Au NPs accumulated in the lungs. This finding further supports the potential of using Au NPs as contrast agents for targeting [310]. In a radiotherapy investigation, thymoquinone-loaded green-synthesized Ag NPs in combination with the MDA-MB-231 mammary adenocarcinoma cells showed improved radiotherapy, significantly increased cancer cell killing, and DNA damage in comparison to the radiation alone. This was carried out via radiotherapy enhancement and the delivery of thymoquinone to the cancer cells. The developed system is proposed to be a promising combined regimen for efficient cancer therapy [311].

Rutin-loaded $CoFe_2O_4$ and $ZnFe_2O_4$ NPs (29 nm and 25 nm) displayed ferromagnetic and superparamagnetic properties. The saturation magnetization values were measured to be 56.2 emu/g and 6 emu/g, respectively. Thus, these NPs exhibited exceptional and efficient magnetic properties, making them crucial for magnetic hyperthermia therapy. Significant photothermal efficacy of green-synthesized $CoFe_2O_4$ and $ZnFe_2O_4$ NPs combined with laser radiation against MCF-7 cells was indicated by the results of the inverted stage microscopy and MTT assay [312]. The Fe_3O_4 NPs produced utilizing the fruit peel of *P. granatum*, exhibited an excellent relaxivity rate and generated strong magnetic resonance imaging (MRI) signals in the study. NPs containing 2% *P. granatum* fruit peel extract were loaded with 5-FU, which displayed 62 ± 0.3% entrapment efficiency. Based on in vitro cytotoxicity studies conducted on CCD112 normal and HCT116 colorectal cancer cell lines, it was observed that the 5-Fluorouracil loaded in the *P. granatum* fruit peel extract-based Fe_3O_4 NPs at 15.62% μg/mL resulted in a 11% and 29% reduction in cell viability in healthy and colorectal cancer cells, respectively. In the future, green-synthesized Fe_3O_4 NPs may play an important role as an eco-friendly nanocarrier in thermo-chemotherapy and MRI for the treatment of cancer [313].

Future perspectives

The subject of biosynthesized metallic NPs loaded with plant extracts is a novel and intriguing area of study. These NPs, often called "green nanoparticles," are extensively explored in the fields of drug delivery. Biosynthesized metallic nanoparticles loaded with plant extracts hold significant promise in medicine. Researchers are investigating their potential as drug delivery systems, where these nanoparticles can be loaded with therapeutic compounds and targeted to specific cells or tissues in the body. They might also be utilized for imaging purposes, such as in cancer detection or tracking the progression of diseases. These NPs can be designed to release drugs in a controlled and sustained manner. This characteristic permits for prolonged drug action, reducing the frequency of dosing and enhancing patient compliance with medication regimens. Biosynthesized metallic NPs loaded with plant extracts can be engineered to deliver drugs to specific cells or tissues in the body with high precision. This targeted drug delivery approach minimizes the side effects associated with conventional drug delivery methods and improves the therapeutic efficacy of medications. Drug resistance is a major challenge in many diseases. By using biosynthesized NPs, it might be possible to enhance the effectiveness of existing drugs against resistant strains of pathogens or cancer cells. Some drugs have low bioavailability, meaning that they are poorly absorbed by the body. Biosynthesized metallic NPs loaded with plant extracts can improve the solubility and bioavailability of such drugs, leading to more efficient therapeutic outcomes. Green nanoparticles derived from plant extracts generally exhibit lower toxicity compared to synthetic nanoparticles. By using biocompatible and biodegradable materials, the risk of adverse reactions and long-term side effects can be minimized. Researchers can combine the unique properties of metallic nanoparticles with the medicinal

properties of plant extracts. This results in multifunctional nanoparticles that not only deliver drugs but also possess inherent therapeutic effects derived from the plant extracts, such as anti-inflammatory or antioxidant properties. Despite the promising future of biosynthesized metallic NPs loaded with plant extracts, comprehensive safety evaluations and regulation will be required. It will be of the uttermost importance to ensure that these nanoparticles are safe for human health, the environment, and non-target organisms. The commercialization and scalability of the production of these nanoparticles will be one of the most significant future challenges as research in this field advances. To make these technologies accessible and practical for a variety of applications, it will be necessary to develop large-scale, cost-effective production methods.

Conclusions

Cancer remains one of the most prevalent causes of mortality across the world, despite recent advances in diagnosis and treatment. No effective cancer treatment has been identified to date, and all the anticancer medications now on the market have the potential to cause negative effects. Nanotechnology has the potential to significantly improve current methods for diagnosing and treating cancer patients. To find better diagnostics and therapies that are as effective, specific, and low-toxic as feasible, researchers are currently attempting to develop novel approaches. Recent biomedical research has focused extensively on biological, or "green," synthesis of NPs. Green synthesis is less expensive, less toxic, and more ecologically friendly than conventional methods of producing NPs. This article will assist formulation scientists and nanotechnologists working on the green production of metal or metal oxide NPs by utilizing plant extracts. It also explored their therapeutic potential of plant extracts against various cancers. The science of metallic NPs is one of the most intriguing areas of study for cutaneous or transdermal drug administration. Thus, lipid nanocarriers are predicted to open new avenues in biomedical science while also improving an essential area of dermatologic literature.

Acknowledgements
Authors are thankful to the UPES University for providing all necessary facilities to write this communication.

Author contributions
MT was involved in the methodology, software, data curation and writing-original draft, DM assisted in conceptualization of work, RA was involved in the visualization, supervision, validation, writing-reviewing and editing.

Funding
This work was not funded or supported by any persons or group.

Availability of data and materials
This work is not an original research paper but a review paper. Availability of data is not applicable.

Declarations

Ethics approval and consent to participate
No animal or human tissue was used in this work, and ethics approval and consent were not applicable.

Consent for publication
All authors gave their full consent for publication of this work.

Competing interests
The authors declare that they have no competing interests.

Received: 4 December 2023 Accepted: 15 February 2024
Published online: 22 February 2024

References

1. Iqbal J, Abbasi BA, Mahmood T, Kanwal S, Ali B, Shah SA, Khalil AT (2017) Plant-derived anticancer agents: a green anticancer approach. Asian Pac J Trop Biomed 7:1129–1150. https://doi.org/10.1016/j.apjtb.2017.10.016
2. Biswas AK, Islam MR, Choudhury ZS, Mostafa A, Kadir MF (2014) Nanotechnology based approaches in cancer therapeutics. Adv Nat Sci Nanosci Nanotechnol 5:043001. https://doi.org/10.1088/2043-6262/5/4/043001
3. Menon S, Ks SD, Santhiya R, Rajeshkumar S, Kumar V (2018) Selenium nanoparticles: a potent chemotherapeutic agent and an elucidation of its mechanism. Colloids Surf B Biointerfaces 170:280–292. https://doi.org/10.1016/j.colsurfb.2018.06.006
4. Vinardell MP, Mitjans M (2015) Antitumor activities of metal oxide nanoparticles. Nanomaterials 5:1004–1021. https://doi.org/10.3390/nano5021004
5. Racca L, Cauda V (2021) Remotely activated nanoparticles for anticancer therapy. Nanomicro Lett 13:11. https://doi.org/10.1007/s40820-020-00537-8
6. Caputo F, De Nicola M, Ghibelli L (2014) Pharmacological potential of bioactive engineered nanomaterials. Biochem Pharmacol 92:112–130. https://doi.org/10.1016/j.bcp.2014.08.015
7. Narayanan KB, Sakthivel N (2011) Green synthesis of biogenic metal nanoparticles by terrestrial and aquatic phototrophic and heterotrophic eukaryotes and biocompatible agents. Adv Colloid Interface Sci 169:59–79. https://doi.org/10.1016/j.cis.2011.08.004
8. Pamkhande PG, Ghule NW, Bamer AH, Kalaskar MG (2019) Metal nanoparticles synthesis: an overview on methods of preparation, advantages and disadvantages, and applications. J Drug Deliv Sci Technol 53:101174. https://doi.org/10.1016/j.jddst.2019.101174
9. Namvar F, Moniri M, Tahir M, Azizi S, Mohamad R (2015) Nanoparticles biosynthesized by fungi and yeast: a review of their preparation, properties, and medical applications. Molecules 20:16540–16565. https://doi.org/10.3390/molecules200916540
10. Patil SP, Chaudhari RY, Nemade MS (2022) *Azadirachta indica* leaves mediated green synthesis of metal oxide nanoparticles: a review. Talanta Open 5:100083. https://doi.org/10.1016/j.talo.2022.100083
11. Khan M, Albalawi GH, Shaik MR, Khan M, Adil SF, Kuniyil M, Alkhathlan HZ, Al-Warthan A, Siddiqui MR (2017) Miswak mediated green synthesized palladium nanoparticles as effective catalysts for the Suzuki coupling reactions in aqueous media. J Saudi Chem Soc 21:450–457. https://doi.org/10.1016/j.jscs.2016.03.008
12. Khatami M, Sharifi I, Nobre MA, Zafarnia N, Aflatoonian MR (2018) Waste-grass-mediated green synthesis of silver nanoparticles and evaluation of their anticancer, antifungal and antibacterial activity. Green Chem Lett Rev 11:125–134. https://doi.org/10.1080/17518253.2018.1444797

13. Mohanpuria P, Rana NK, Yadav SK (2008) Biosynthesis of nanoparticles: technological concepts and future applications. J Nanopart Res 10:507–517. https://doi.org/10.1007/s11051-007-9275-x
14. Hutchison JE (2008) Greener nanoscience: a proactive approach to advancing applications and reducing implications of nanotechnology. ACS Nano 2:395–402. https://doi.org/10.1021/nn800131j
15. Cheng J, Wang X, Qiu L, Li Y, Marraiki N, Elgorban AM, Xue L (2020) Green synthesized zinc oxide nanoparticles regulates the apoptotic expression in bone cancer cells MG-63 cells. J Photochem Photobiol B. https://doi.org/10.1016/j.jphotobiol.2019.111644
16. Deepika S, Selvaraj CI, Roopan SM (2020) Screening bioactivities of *Caesalpinia pulcherrima L. swartz* and cytotoxicity of extract synthesized silver nanoparticles on HCT116 cell line. Mater Sci Eng. https://doi.org/10.1016/j.msec.2019.110279
17. Mousavi B, Tafvizi F, Zaker Bostanabad S (2018) Green synthesis of silver nanoparticles using *Artemisia turcomanica* leaf extract and the study of anti-cancer effect and apoptosis induction on gastric cancer cell line (AGS). Artif Cells Nanomed Biotechnol 46:499–510. https://doi.org/10.1080/21691401.2018.1430697
18. Das B, Dash SK, Mandal D, Ghosh T, Chattopadhyay S, Tripathy S, Das S, Dey SK, Das D, Roy S (2017) Green synthesized silver nanoparticles destroy multidrug resistant bacteria via reactive oxygen species mediated membrane damage. Arab J Chem 10(6):862–876. https://doi.org/10.1016/j.arabjc.2015.08.008
19. Andra S, Balu SK, Jeevanandham J, Muthalagu M, Vidyavathy M, Chan YS, Danquah MK (2019) Phytosynthesized metal oxide nanoparticles for pharmaceutical applications. Naunyn Schmiedebergs Arch Pharmacol 392:755–771. https://doi.org/10.1007/s00210-019-01666-7
20. Shreyash N, Sonker M, Bajpai S, Tiwary SK (2021) Review of the mechanism of nanocarriers and technological developments in the field of nanoparticles for applications in cancer theragnostics. ACS Appl Bio Mater 4:2307–2334. https://doi.org/10.1021/acsabm.1c00020
21. Peng H, Xu Z, Wang Y, Feng N, Yang W, Tang J (2020) Biomimetic mesoporous silica nanoparticles for enhanced blood circulation and cancer therapy. ACS Appl Bio Mater 3:7849–7857. https://doi.org/10.1021/acsabm.0c01014
22. Bagalkot V, Zhang L, Levy-Nissenbaum E, Jon S, Kantoff PW, Langer R, Farokhzad OC (2007) Quantum dot-aptamer conjugates for synchronous cancer imaging, therapy, and sensing of drug delivery based on Bi-fluorescence resonance energy transfer. Nano Lett 7:3065–3070. https://doi.org/10.1021/nl071546n
23. Xu ZP, Zeng QH, Lu GQ, Yu AB (2006) Inorganic nanoparticles as carriers for efficient cellular delivery. Chem Eng Sci 61:1027–1040. https://doi.org/10.1016/j.ces.2005.06.019
24. Zhao X, Hilliard LR, Mechery SJ, Wang Y, Bagwe RP, Jin S, Tan W (2004) A rapid bioassay for single bacterial cell quantitation using bioconjugated nanoparticles. Proc Natl Acad Sci 101(42):15027–15032. https://doi.org/10.1073/pnas.0404806101
25. Mousa SA, Bharali DJ (2011) Nanotechnology-based detection and targeted therapy in cancer: nano-bio paradigms and applications. Cancers (Basel) 3:2888–2903. https://doi.org/10.3390/cancers3032888
26. Schroeder A, Heller DA, Winslow MM, Dahlman JE, Pratt GW, Langer R, Jacks T, Anderson DG (2012) Treating metastatic cancer with nanotechnology. Nat Rev Cancer 12:39–50. https://doi.org/10.1038/nrc3180
27. Singh AK (2017) Comparative therapeutic effects of plant-extract synthesized and traditionally synthesized gold nanoparticles on alcohol-induced inflammatory activity in sh-sy5y cells *in vitro*. Biomedicines. https://doi.org/10.3390/biomedicines5040070
28. Slavin YN, Asnis J, Hńfeli UO, Bach H (2017) Metal nanoparticles: understanding the mechanisms behind antibacterial activity. J Nanobiotechnol. https://doi.org/10.1186/s12951-017-0308-z
29. Ouyang L, Shi Z, Zhao S, Wang FT, Zhou TT, Liu B, Bao JK (2012) Programmed cell death pathways in cancer: a review of apoptosis, autophagy and programmed necrosis. Cell Prolif 45:487–498. https://doi.org/10.1111/j.1365-2184.2012.00845.x
30. Odeyemi SW, De La Mare J, Edkins AL, Afolayan AJ (2019) *In vitro* and *in vivo* toxicity assessment of biologically synthesized silver nanoparticles from *Elaeodendron croceum*. J Complement Integr Med 16(3):20180184. https://doi.org/10.1515/jcim-2018-0184
31. Anand K, Gengan RM, Phulukdaree A, Chuturgoon A (2015) Agroforestry waste *Moringa oleifera* petals mediated green synthesis of gold nanoparticles and their anti-cancer and catalytic activity. J Ind Eng Chem 21:1105–1111. https://doi.org/10.1016/j.jiec.2014.05.021
32. Rao PV, Nallappan D, Madhavi K, Rahman S, Jun Wei L, Gan SH (2016) Phytochemicals and biogenic metallic nanoparticles as anticancer agents. Oxid Med Cell Longev. https://doi.org/10.1155/2016/3685671
33. Wason MS, Colon J, Das S, Seal S, Turkson J, Zhao J, Baker CH (2013) Sensitization of pancreatic cancer cells to radiation by cerium oxide nanoparticle-induced ROS production. Nanomedicine 9:558–569. https://doi.org/10.1016/j.nano.2012.10.010
34. Nikolova MP, Chavali MS (2020) Metal oxide nanoparticles as biomedical materials. Biomimetics 5(2):27. https://doi.org/10.3390/BIOMIMETICS5020027
35. Kim YJ, Perumalsamy H, Castro-Aceituno V, Kim D, Markus J, Lee S, Kim S, Liu Y, Yang DC (2019) Photoluminescent and self-assembled hyaluronic acid-zinc oxide-ginsenoside rh2 nanoparticles and their potential caspase-9 apoptotic mechanism towards cancer cell lines. Int J Nanomed 14:8195–8208. https://doi.org/10.2147/IJN.S221328
36. Zhang XF, Liu ZG, Shen W, Gurunathan S (2016) Silver nanoparticles: Synthesis, characterization, properties, applications, and therapeutic approaches. Int J Mol Sci 17:1534. https://doi.org/10.3390/ijms17091534
37. Greulich C, Diendorf J, Simon T, Eggeler G, Epple M, Köller M (2011) Uptake and intracellular distribution of silver nanoparticles in human mesenchymal stem cells. Acta Biomater 7:347–354. https://doi.org/10.1016/j.actbio.2010.08.003
38. Raj S, Trivedi R, Soni V (2021) Biogenic synthesis of silver nanoparticles, characterization and their applications—a review. Surfaces 5(1):67–90. https://doi.org/10.3390/surfaces5010003
39. Bardania H, Mahmoudi R, Bagheri H, Salehpour Z, Fouani MH, Darabian B et al (2020) Facile preparation of a novel biogenic silver-loaded Nanofilm with intrinsic anti-bacterial and oxidant scavenging activities for wound healing. Sci Rep. https://doi.org/10.1038/s41598-020-63032-5
40. Ekram B, Tolba E, El-Sayed AF, Müller WEG, Schröder HC, Wang X et al (2024) Cell migration, DNA fragmentation and antibacterial properties of novel silver doped calcium polyphosphate nanoparticles. Sci Rep. https://doi.org/10.1038/s41598-023-50849-z
41. Kaur N, Kumar R, Alhan S, Sharma H, Singh N, Yogi R et al (2024) *Lycium shawii* mediated green synthesis of silver nanoparticles, characterization and assessments of their phytochemical, antioxidant, antimicrobial properties. Inorg Chem Commun 1:159. https://doi.org/10.1016/j.inoche.2023.111735
42. Miranda RR, Sampaio I, Zucolotto V (2022) Exploring silver nanoparticles for cancer therapy and diagnosis. Colloids Surf B 210:112254. https://doi.org/10.1016/j.colsurfb.2021.112254
43. Datta LP, Chatterjee A, Acharya K, De P, Das M (2017) Enzyme responsive nucleotide functionalized silver nanoparticles with effective antimicrobial and anticancer activity. New J Chem 41(4):1538–1548. https://doi.org/10.1039/C6NJ02955H
44. Guo D, Dou D, Ge L, Huang Z, Wang L, Gu N (2015) A caffeic acid mediated facile synthesis of silver nanoparticles with powerful anti-cancer activity. Colloids Surf B 134:229–234. https://doi.org/10.1016/j.colsurfb.2015.06.070
45. He J, Feizipour S, Veisi H, Amraii SA, Zangeneh MM, Hemmati S (2024) Panax ginseng root aqueous extract mediated biosynthesis of silver nanoparticles under ultrasound condition and investigation of the treatment of human lung adenocarcinoma with following the PI3K/AKT/mTOR signaling pathway. Inorg Chem Commun 160:11. https://doi.org/10.1016/j.inoche.2024.112021
46. Chen Y, Yang T, Chen S, Qi S, Zhang Z, Xu Y (2020) Silver nanoparticles regulate autophagy through lysosome injury and cell hypoxia in prostate cancer cells. J Biochem Mol Toxicol 34:1–9. https://doi.org/10.1002/jbt.22474
47. Sharma N, Bhatt G, Kothiyal P (2015) Gold nanoparticles synthesis, properties, and forthcoming applications—a review. Indian J Pharm Biol Res. https://doi.org/10.30750/IJPBR.3.2.3
48. Zhang Q, Yang M, Zhu Y, Mao C (2017) Metallic nanoclusters for cancer imaging and therapy. Curr Med Chem 25:1379–1396. https://doi.org/10.2174/0929867324666170331122757
49. Murawala P, Tirmale A, Shiras A, Prasad BL (2014) *In situ* synthesized BSA capped gold nanoparticles: effective carrier of anticancer

drug methotrexate to MCF-7 breast cancer cells. Mater Sci Eng C 34:158–167. https://doi.org/10.1016/j.msec.2013.09.004
50. Devi L, Gupta R, Jain SK, Singh S, Kesharwani P (2020) Synthesis, characterization and *in vitro* assessment of colloidal gold nanoparticles of Gemcitabine with natural polysaccharides for treatment of breast cancer. J Drug Deliv Sci Technol. https://doi.org/10.1016/j.jddst.2020.101565
51. Akrami M, Samimi S, Alipour M, Bardania H, Ramezanpour S, Najafi N, Hosseinkhani S, Kamankesh M, Haririan I, Hassanshahi F (2021) Potential anticancer activity of a new pro-apoptotic peptide–thioctic acid gold nanoparticle platform. Nanotechnology 32(14):145101. https://doi.org/10.1088/1361-6528/abd3cb
52. Niculescu AG, Chircov C, Grumezescu AM (2022) Magnetite nanoparticles: synthesis methods—a comparative review. Methods 199:16–27. https://doi.org/10.1016/j.ymeth.2021.04.018
53. Yusefi M, Shameli K, Ali RR, Pang SW, Teow SY (2020) Evaluating anticancer activity of plant-mediated synthesized iron oxide nanoparticles using *Punica Granatum* fruit peel extract. J Mol Struct. https://doi.org/10.1016/j.molstruc.2019.127539
54. Murthy S, Effiong P, Fei CC (2020) Metal oxide nanoparticles in biomedical applications. In: Al-Douri Y (ed) Metal oxide powder technologies: fundamentals, processing methods and applications. Elsevier, pp 233–251. https://doi.org/10.1016/b978-0-12-817505-7.00011-7
55. Attia NF, Abd El-Monaem EM, El-Aqapa HG, Elashery SE, Eltaweil AS, El Kady M, Khalifa SA, Hawash HB, El-Seedi HR (2022) Iron oxide nanoparticles and their pharmaceutical applications. Appl Surf Sci Adv. https://doi.org/10.1016/j.apsadv.2022.100284
56. Zanganeh S, Hutter G, Spitler R, Lenkov O, Mahmoudi M, Shaw A, Pajarinen JS, Nejadnik H, Goodman S, Moseley M, Coussens LM (2016) Iron oxide nanoparticles inhibit tumour growth by inducing pro-inflammatory macrophage polarization in tumour tissues. Nat Nanotechnol 11:986–994. https://doi.org/10.1038/nnano.2016.168
57. Das RK, Pachapur VL, Lonappan L, Naghdi M, Pulicharla R, Maiti S, Cledon M, Dalila LM, Sarma SJ, Brar SK (2017) Biological synthesis of metallic nanoparticles: plants, animals and microbial aspects. Nanotechnol Environ Eng 2:18. https://doi.org/10.1007/s41204-017-0029-4
58. Sun C, Fang C, Stephen Z, Veiseh O, Hansen S, Lee D, Ellenbogen RG, Olson J, Zhang M (2008) Tumor-targeted drug delivery and MRI contrast enhancement by chlorotoxin-conjugated iron oxide nanoparticles. Nanomedicine 3:495–505. https://doi.org/10.2217/17435889.3.4.495
59. Singh TA, Das J, Sil PC (2020) Zinc oxide nanoparticles: A comprehensive review on its synthesis, anticancer and drug delivery applications as well as health risks. Adv Colloid Interface Sci. https://doi.org/10.1016/j.cis.2020.102317
60. Wahab R, Siddiqui MA, Saquib Q, Dwivedi S, Ahmad J, Musarrat J, Al-Khedhairy AA, Shin HS (2014) ZnO nanoparticles induced oxidative stress and apoptosis in HepG2 and MCF-7 cancer cells and their antibacterial activity. Colloids Surf B Biointerfaces 117:267–276. https://doi.org/10.1016/j.colsurfb.2014.02.038
61. Fortunato E, Figueiredo V, Barquinha P, Elamurugu E, Barros R, Gonçalves G, Park SH, Hwang CS, Martins R (2010) Thin-film transistors based on p-type Cu_2O thin films produced at room temperature. Appl Phys Lett. https://doi.org/10.1063/1.3428434
62. Xia T, Kovochich M, Nel AE (2007) Impairment of mitochondrial function by particulate matter (PM) and their toxic components: Implications for PM-induced cardiovascular and lung disease. Front Biosci 12:1238–1246. https://doi.org/10.2741/2142
63. Wang Y, Yang F, Zhang HX, Zi XY, Pan XH, Chen F, Luo WD, Li JX, Zhu HY, Hu YP (2013) Cuprous oxide nanoparticles inhibit the growth and metastasis of melanoma by targeting mitochondria. Cell Death Dis 4:e783. https://doi.org/10.1038/cddis.2013.314
64. Anandgaonker P, Kulkarni G, Gaikwad S, Rajbhoj A (2019) Synthesis of TiO_2 nanoparticles by electrochemical method and their antibacterial application. Arab J Chem 12:1815–1822. https://doi.org/10.1016/j.arabjc.2014.12.015
65. Nadeem M, Tungmunnithum D, Hano C, Abbasi BH, Hashmi SS, Ahmad W, Zahir A (2018) The current trends in the green syntheses of titanium oxide nanoparticles and their applications. Green Chem Lett Rev 11(4):492–502. https://doi.org/10.1080/17518253.2018.1538430
66. Tadele KT, Abire TO, Feyisa TY (2021) Green synthesized silver nanoparticles using plant extracts as promising prospect for cancer therapy: a review of recent findings. J Nanomed 4:1040
67. Shafey AM (2020) Green synthesis of metal and metal oxide nanoparticles from plant leaf extracts and their applications: a review. Green Process Synth 9:304–339. https://doi.org/10.1515/gps-2020-0031
68. Singh KR, Nayak V, Sarkar T, Singh RP (2020) Cerium oxide nanoparticles: properties, biosynthesis and biomedical application. RSC Adv 10(45):27194–27214. https://doi.org/10.1039/D0RA04736H
69. Usman AI, Aziz AA, Khaniabadi PM (2020) Sonochemical synthesis of gold nanoparticles via palm oil fronds extracts for cytotoxicity assay. IOP Conf Ser Mater Sci Eng. https://doi.org/10.1088/1757-899X/839/1/012004
70. Gittins DI, Bethell D, Schiffrin DJ, Nichols RJ (2000) A nanometre-scale electronic switch consisting of a metal cluster and redox-addressable groups. Nature 408(6808):67–69
71. Shyam A, Chandran SS, George B, Sreelekha E (2021) Plant mediated synthesis of AgNPs and its applications: an overview. Inorg Nano-Met Chem 51:1646–1662. https://doi.org/10.1080/24701556.2020.1852254
72. Armendariz V, Herrera I, Peralta-Videa JR, Jose-Yacaman M, Troiani H, Santiago P, Gardea-Torresdey JL (2004) Size controlled gold nanoparticle formation by *Avena sativa* biomass: use of plants in nanobiotechnology. J Nanopart Res. https://doi.org/10.1007/s11051-004-0741-4
73. Sathishkumar M, Sneha K, Won SW, Cho CW, Kim S, Yun YS (2009) *Cinnamon zeylanicum* bark extract and powder mediated green synthesis of nano-crystalline silver particles and its bactericidal activity. Colloids Surf B Biointerfaces 73(2):332–338. https://doi.org/10.1016/j.colsurfb.2009.06.005
74. Prathna TC, Chandrasekaran N, Raichur AM, Mukherjee A (2011) Kinetic evolution studies of silver nanoparticles in a bio-based green synthesis process. Colloids Surf A Physicochem Eng Asp 377(1–3):212–216. https://doi.org/10.1016/j.colsurfa.2010.12.047
75. Augustine R, Hasan A (2020) Emerging applications of biocompatible phytosynthesized metal/metal oxide nanoparticles in healthcare. J Drug Deliv Sci Technol 56:101516. https://doi.org/10.1016/j.jddst.2020.101516
76. Hu J, Xianyu Y (2021) When nano meets plants: a review on the interplay between nanoparticles and plants. Nano Today. https://doi.org/10.1016/j.nantod.2021.101143
77. Velusamy P, Kumar GV, Jeyanthi V, Das J, Pachaiappan R (2016) Bio-inspired green nanoparticles: synthesis, mechanism, and antibacterial application. Toxicol Res 32:95–102. https://doi.org/10.5487/TR.2016.32.2.095
78. Kumar V, Yadav SK (2009) Plant-mediated synthesis of silver and gold nanoparticles and their applications. J Chem Technol Biotechnol 84:151–157. https://doi.org/10.1002/jctb.2023
79. Karmous I, Pandey A, Haj KB, Chaoui A (2020) Efficiency of the green synthesized nanoparticles as new tools in cancer therapy: insights on plant-based bioengineered nanoparticles, biophysical properties, and anticancer roles. Biol Trace Elem Res 196:330–342. https://doi.org/10.1007/s12011-019-01895-0
80. Marshall AT, Haverkamp RG, Davies CE, Parsons JG, Gardea-Torresdey JL, van Agterveld D (2007) Accumulation of gold nanoparticles in *Brassic juncea*. Int J Phytoremediat 9:197–206. https://doi.org/10.1080/15226510701376026
81. El-Seedi HR, El-Shabasy RM, Khalifa SA, Saeed A, Shah A, Shah R, Iftikhar FJ, Abdel-Daim MM, Omri A, Hajrahand NH, Sabir JS (2019) Metal nanoparticles fabricated by green chemistry using natural extracts: biosynthesis, mechanisms, and applications. RSC Adv 9:24539–24559. https://doi.org/10.1039/c9ra02225b
82. Govindarajan M, Rajeswary M, Veerakumar K, Muthukumaran U, Hoti SL, Benelli G (2016) Green synthesis and characterization of silver nanoparticles fabricated using *Anisomeles indica*: mosquitocidal potential against malaria, dengue and *Japanese encephalitis* vectors. Exp Parasitol 161:40–47. https://doi.org/10.1016/j.exppara.2015.12.011
83. Lee SY, Krishnamurthy S, Cho CW, Yun YS (2016) Biosynthesis of gold nanoparticles using *Ocimum sanctum* extracts by solvents with different polarity. ACS Sustain Chem Eng 4:2651–2659. https://doi.org/10.1021/acssuschemeng.6b00161
84. Patil MP, Kim GD (2017) Eco-friendly approach for nanoparticles synthesis and mechanism behind antibacterial activity of silver and anticancer

activity of gold nanoparticles. Appl Microbiol Biotechnol 101:79–92. https://doi.org/10.1007/s00253-016-8012-8
85. Mohamed HE, Afridi S, Khalil AT, Ali M, Zohra T, Salman M, Ikram A, Shinwari ZK, Maaza M (2020) Bio-redox potential of *Hyphaene thebaica* in bio-fabrication of ultrafine maghemite phase iron oxide nanoparticles (Fe_2O_3 NPs) for therapeutic applications. Mater Sci Eng C 112:110890. https://doi.org/10.1016/j.msec.2020.110890
86. Üstün E, Önbaş SC, Çelik SK, Ayvaz MÇ, Şahin N (2022) Green synthesis of iron oxide nanoparticles by using *Ficus carica* leaf extract and its antioxidant activity. Biointerface Res Appl Chem 12:2108–2116. https://doi.org/10.33263/BRIAC122.21082116
87. Velsankar K, Parvathy G, Mohandoss S, Krishna Kumar M, Sudhahar S (2022) *Celosia argentea* leaf extract-mediated green synthesized iron oxide nanoparticles for bio-applications. J Nanostruct Chem 12:625–640. https://doi.org/10.1007/s40097-021-00434-5
88. Devi HS, Boda MA, Shah MA, Parveen S, Wani AH (2019) Green synthesis of iron oxide nanoparticles using *Platanus orientalis* leaf extract for antifungal activity. Green Process Synth 8:38–45. https://doi.org/10.1515/gps-2017-0145
89. Usha V, Amutha E, Pushpalaksmi E, Samraj JJ, Rajaduraipandian S, Gandhimathi S, Annadurai G (1970) Green synthesis and characterization of antibacterial studies by iron oxide nanoparticles using *Carica papaya* leaf extract. J Appl Sci Environ Manag 26:421–427. https://doi.org/10.4314/jasem.v26i3.8
90. Padalia H, Chanda S (2017) Characterization, antifungal and cytotoxic evaluation of green synthesized zinc oxide nanoparticles using *Ziziphus nummularia* leaf extract. Artif Cells Nanomed Biotechnol 45:1751–1761. https://doi.org/10.1080/21691401.2017.1282868
91. Naiel B, Fawzy M, Halmy MW, Mahmoud AE (2022) Green synthesis of zinc oxide nanoparticles using Sea Lavender (*Limonium pruinosum L. Chaz.*) extract: characterization, evaluation of anti-skin cancer, antimicrobial and antioxidant potentials. Sci Rep 12:1–12. https://doi.org/10.1038/s41598-022-24805-2
92. Gharpure S, Yadwade R, Ankamwar B (2022) Non-antimicrobial and non-anticancer properties of ZnO nanoparticles biosynthesized using different plant parts of *Bixa orellana*. ACS Omega 7:1914–1933. https://doi.org/10.1021/acsomega.1c05324
93. Shnawa BH, Hamad SM, Barzinjy AA, Kareem PA, Ahmed MH (2022) Scolicidal activity of biosynthesized zinc oxide nanoparticles by *Mentha longifolia L.* leaves against *Echinococcus granulosus protoscolices*. Emergent Mater 5:683–693. https://doi.org/10.1007/s42247-021-00264-9
94. Faisal S, Jan H, Abdullah AI, Rizwan M, Hussain Z, Sultana K, Ali Z, Uddin MN (2022) In vivo analgesic, anti-inflammatory, and anti-diabetic screening of *Bacopa monnieri*-synthesized copper oxide nanoparticles. ACS Omega 7:4071–4082. https://doi.org/10.1021/acsomega.1c05410
95. Qamar H, Rehman S, Chauhan DK, Tiwari AK, Upmanyu V (2020) Green synthesis, characterization and antimicrobial activity of copper oxide nanomaterial derived from *Momordica charantia*. Int J Nanomed 15:2541–2553. https://doi.org/10.2147/IJN.S240232
96. Al-Khafaji MA, Al-Refai'a RA, Al-Zamely OM (2021) Green synthesis of copper nanoparticles using *Artemisia* plant extract. Mater Today Proc 49:2831–2835. https://doi.org/10.1016/j.matpr.2021.10.067
97. Pillai RR, Sreelekshmi PB, Meera AP (2020) Enhanced biological performance of green sythesized copper oxide nanoparticles using *Pimenta dioica* leaf extract. Mater Today Proc 50:163–172. https://doi.org/10.1016/j.matpr.2021.11.547
98. Chandrasekar A, Vasantharaj S, Jagadeesan NL, Shankar SN, Pannerselvam B, Bose VG, Arumugam G, Shanmugavel M (2021) Studies on phytomolecules mediated synthesis of copper oxide nanoparticles for biomedical and environmental applications. Biocatal Agric Biotechnol 33:101994. https://doi.org/10.1016/j.bcab.2021.101994
99. Rajeshkumar S, Santhoshkumar J, Jule LT, Ramaswamy K (2021) Phytosynthesis of titanium dioxide nanoparticles using king of bitter *Andrographis paniculata* and its embryonic toxicology evaluation and biomedical potential. Bioinorg Chem Appl. https://doi.org/10.1155/2021/6267634
100. Santhoshkumar T, Rahuman AA, Jayaseelan C, Rajakumar G, Marimuthu S, Kirthi AV, Velayutham K, Thomas J, Venkatesan J, Kim SK (2014) Green synthesis of titanium dioxide nanoparticles using *Psidium guajava* extract and its antibacterial and antioxidant properties. Asian Pac J Trop Med 7:968–976. https://doi.org/10.1016/S1995-7645(14)60171-1
101. Suman TY, Ravindranath RR, Elumalai D, Kaleena PK, Ramkumar R, Perumal P, Aranganathan L, Chitrarasu PS (2015) Larvicidal activity of titanium dioxide nanoparticles synthesized using *Morinda citrifolia* root extract against *Anopheles stephensi*, *Aedes aegypti* and *Culex quinquefasciatus* and its other effect on non-target fish. Asian Pac J Trop Dis 5:224–230. https://doi.org/10.1016/S2222-1808(14)60658-7
102. Sivaranjani V, Philominathan PJ (2016) Synthesize of Titanium dioxide nanoparticles using *Moringa oleifera* leaves and evaluation of wound healing activity. Wound Med 12:1–5. https://doi.org/10.1016/j.wndm.2015.11.002
103. Gomaa EZ (2017) Antimicrobial, antioxidant and antitumor activities of silver nanoparticles synthesized by *Allium cepa* extract: a green approach. J Genet Eng Biotechnol 15:49–57. https://doi.org/10.1016/j.jgeb.2016.12.002
104. Vijayan R, Joseph S, Mathew B (2018) *Indigofera tinctoria* leaf extract mediated green synthesis of silver and gold nanoparticles and assessment of their anticancer, antimicrobial, antioxidant and catalytic properties. Artif Cells Nanomed Biotechnol 46:861–871. https://doi.org/10.1080/21691401.2017.1345930
105. Suman TY, Rajasree SR, Kanchana A, Elizabeth SB (2013) Biosynthesis, characterization and cytotoxic effect of plant mediated silver nanoparticles using *Morinda citrifolia* root extract. Colloids Surf B Biointerfaces 106:74–78. https://doi.org/10.1016/j.colsurfb.2013.01.037
106. Hawar SN, Al-Shmgani HS, Al-Kubaisi ZA, Sulaiman GM, Dewir YH, Rikisahedew JJ (2022) Green synthesis of silver nanoparticles from *Alhagi graecorum* leaf extract and evaluation of their cytotoxicity and antifungal activity. J Nanomater. https://doi.org/10.1155/2022/1058119
107. Hawadak J, Kojom Foko LP, Pande V, Singh V (2022) *In vitro* antiplasmodial activity, hemocompatibility and temporal stability of *Azadirachta indica* silver nanoparticles. Artif Cells Nanomed Biotechnol 50:286–300. https://doi.org/10.1080/21691401.2022.2126979
108. Meléndez-Villanueva MA, Morán-Santibañez K, Martínez-Sanmiguel JJ, Rangel-López R, Garza-Navarro MA, Rodríguez-Padilla C, Zarate-Triviño DG, Trejo-Ávila LM (2019) Virucidal activity of gold nanoparticles synthesized by green chemistry using garlic extract. Viruses 11:1–13. https://doi.org/10.3390/v11121111
109. Peivandi S, Dehghanzadeh H, Baghizadeh A (2023) Biosynthesis of gold nanoparticles using sansevieria plant extract and its biomedical application. Inorg Nano-Met Chem 53(5):482–489. https://doi.org/10.1080/24701556.2022.2078355
110. Muniyappan N, Pandeeswaran M, Amalraj A (2021) Green synthesis of gold nanoparticles using *Curcuma pseudomontana* isolated curcumin: Its characterization, antimicrobial, antioxidant and anti- inflammatory activities. Environ Toxicol Chem 3:117–124. https://doi.org/10.1016/j.enceco.2021.01.002
111. Patra JK, Kwon Y, Baek KH (2016) Green biosynthesis of gold nanoparticles by onion peel extract: synthesis, characterization and biological activities. Adv Powder Technol 27:2204–2213. https://doi.org/10.1016/j.apt.2016.08.005
112. Suriyakala G, Sathiyaraj S, Babujanarthanam R, Alarjani KM, Hussein DS, Rasheed RA, Kanimozhi K (2022) Green synthesis of gold nanoparticles using *Jatropha integerrima Jacq*. flower extract and their antibacterial activity. J King Saud Univ Sci 34:101830. https://doi.org/10.1016/j.jksus.2022.101830
113. Gu H, Chen X, Chen F, Zhou X, Parsaee Z (2018) Ultrasound-assisted biosynthesis of CuO-NPs using brown alga *Cystoseira trinodis*: characterization, photocatalytic AOP, DPPH scavenging and antibacterial investigations. Ultrason Sonochem 41:109–119. https://doi.org/10.1016/j.ultsonch.2017.09.006
114. Gahlawat G, Choudhury AR (2019) A review on the biosynthesis of metal and metal salt nanoparticles by microbes. RSC Adv 9(23):12944–12967. https://doi.org/10.1039/C8RA10483b
115. Jain N, Bhargava A, Majumdar S, Tarafdar JC, Panwar J (2011) Extracellular biosynthesis and characterization of silver nanoparticles using *Aspergillus flavus NJP08*: a mechanism perspective. Nanoscale 3:635–641. https://doi.org/10.1039/c0nr00656d
116. Das VL, Thomas R, Varghese RT, Soniya EV, Mathew J, Radhakrishnan EK (2014) Extracellular synthesis of silver nanoparticles by the *Bacillus strain* CS 11 isolated from industrialized area. Biotech 4:121–126. https://doi.org/10.1007/s13205-013-0130-8

117. Prasad R, Pandey R (2016) Barman I (2016) Engineering tailored nanoparticles with microbes: Quo vadis? Wiley Interdiscip Rev Nanomed Nanobiotechnol 8(2):316–330. https://doi.org/10.1002/wnan.1363
118. Durán N, Marcato PD, Alves OL, De Souza GI, Esposito E (2005) Mechanistic aspects of biosynthesis of silver nanoparticles by several *Fusarium oxysporum* strains. J Nanobiotechnol 3:1–7. https://doi.org/10.1186/1477-3155-3-8
119. Kalimuthu K, Babu RS, Venkataraman D, Bilal M, Gurunathan S (2008) Biosynthesis of silver nanocrystals by *Bacillus licheniformis*. Colloids Surf B Biointerfaces 65:150–153. https://doi.org/10.1016/j.colsurfb.2008.02.018
120. Klaus T, Joerger R, Olsson E, Granqvist CG (1999) Silver-based crystalline nanoparticles, microbially fabricated. Proc Natl Acad Sci 96(24):13611–13614. https://doi.org/10.1073/pnas.96.24.13611
121. Khalil AT, Ovais M, Iqbal J, Ali A, Ayaz M, Abbas M, Ahmad I, Devkota HP (2022) Microbes-mediated synthesis strategies of metal nanoparticles and their potential role in cancer therapeutics. Semin Cancer Biol 86:693–705. https://doi.org/10.1016/j.semcancer.2021.06.006
122. Ali J, Ali N, Wang L, Waseem H, Pan G (2019) Revisiting the mechanistic pathways for bacterial mediated synthesis of noble metal nanoparticles. J Microbiol Methods 159:18–25. https://doi.org/10.1016/j.mimet.2019.02.010
123. Fariq A, Khan T, Yasmin A (2017) Microbial synthesis of nanoparticles and their potential applications in biomedicine. J Appl Biomed 15:241–248. https://doi.org/10.1016/j.jab.2017.03.004
124. Gurunathan S, Kalishwaralal K, Vaidyanathan R, Venkataraman D, Pandian SR, Muniyandi J, Hariharan N, Eom SH (2009) Biosynthesis, purification and characterization of silver nanoparticles using *Escherichia coli*. Colloids Surf B Biointerfaces 74:328–335. https://doi.org/10.1016/j.colsurfb.2009.07.048
125. Koul B, Poonia AK, Yadav D, Jin JO (2021) Microbe-mediated biosynthesis of nanoparticles: applications and future prospects. Biomolecules. https://doi.org/10.3390/biom11060886
126. Nangia Y, Wangoo N, Goyal N, Shekhawat G, Suri CR (2009) A novel bacterial isolate *Stenotrophomonas maltophilia* as living factory for synthesis of gold nanoparticles. Microb Cell Fact. https://doi.org/10.1186/1475-2859-8-39
127. Zhao H, Maruthupandy M, Al-mekhlafi FA, Chackaravarthi G, Ramachandran G, Chelliah CK (2022) Biological synthesis of copper oxide nanoparticles using marine endophytic actinomycetes and evaluation of biofilm producing bacteria and A549 lung cancer cells. J King Saud Univ Sci 34:101866. https://doi.org/10.1016/j.jksus.2022.101866
128. Bukhari SI, Hamed MM, Al-Agamy MH, Gazwi HS, Radwan HH, Youssif AM (2021) Biosynthesis of copper oxide nanoparticles using *Streptomyces* MHM38 and its biological applications. J Nanomater. https://doi.org/10.1155/2021/6693302
129. John MS, Nagoth JA, Zannotti M, Giovannetti R, Mancini A, Ramasamy KP, Miceli C, Pucciarelli S (2021) Biogenic synthesis of copper nanoparticles using bacterial strains isolated from an antarctic consortium associated to a psychrophilic marine ciliate: characterization and potential application as antimicrobial agents. Mar Drugs. https://doi.org/10.3390/md19050263
130. Nabila MI, Kannabiran K (2018) Biosynthesis, characterization and antibacterial activity of copper oxide nanoparticles (CuO NPs) from actinomycetes. Biocatal Agric Biotechnol 15:56–62. https://doi.org/10.1016/j.bcab.2018.05.011
131. Ebadi M, Zolfaghari MR, Aghaei SS, Zargar M, Shafiei M, Zahiri HS, Noghabi KA (2019) A bio-inspired strategy for the synthesis of zinc oxide nanoparticles (ZnO NPs) using the cell extract. RSC Adv 9(41):23508–23525. https://doi.org/10.1039/c9ra03962g
132. Faisal S, Rizwan M, Ullah R, Alotaibi A, Khattak A, Bibi N, Idrees M (2022) Paraclostridium benzoelyticum bacterium-mediated zinc oxide nanoparticles and their *in vivo* multiple biological applications. Oxid Med Cell Longev. https://doi.org/10.1155/2022/5994033
133. Hamk M, Akçay FA, Avcı A (2022) Green synthesis of zinc oxide nanoparticles using *Bacillus subtilis* ZBP4 and their antibacterial potential against foodborne pathogens. Prep Biochem Biotechnol. https://doi.org/10.1080/10826068.2022.2076243
134. Motazedi R, Rahaiee S, Zare M (2020) Efficient biogenesis of ZnO nanoparticles using extracellular extract of *Saccharomyces cerevisiae*: evaluation of photocatalytic, cytotoxic and other biological activities. Bioorg Chem 101:103998. https://doi.org/10.1016/j.bioorg.2020.103998
135. Mansoor A, Khan MT, Mehmood M, Khurshid Z, Ali MI, Jamal A (2022) Synthesis and characterization of titanium oxide nanoparticles with a novel biogenic process for dental application. Nanomaterials. https://doi.org/10.3390/nano12071078
136. Meenatchisundaram N, Chellamuthu J, Jeyaraman AR, Arjunan N, Muthuramalingam JB, Karuppuchamy S (2022) Biosynthesized TiO_2 nanoparticles an efficient biogenic material for photocatalytic and antibacterial applications. Energy Environ 33:377–398. https://doi.org/10.1177/0958305X211000261
137. Agceli GK, Hammachi H, Kodal SP, Cihangir N, Aksu Z (2020) A Novel approach to synthesize TiO_2 nanoparticles: biosynthesis by using *Streptomyces sp*. HC1. J Inorg Organomet Polym Mater 30:3221–3229. https://doi.org/10.1007/s10904-020-01486-w
138. Elsilk SE, Khalil MA, Aboshady TA, Alsalmi FA, Ali SS (2022) *Streptomyces rochei* MS-37 as a novel marine actinobacterium for green biosynthesis of silver nanoparticles and their biomedical applications. Molecules 27:7296. https://doi.org/10.3390/molecules27217296
139. Al-Dhabi NA, Ghilan AK, Esmail GA, Arasu MV, Duraipandiyan V, Ponmurugan K (2019) Environmental friendly synthesis of silver nanomaterials from the promising *Streptomyces parvus* strain Al-Dhabi-91 recovered from the Saudi Arabian marine regions for antimicrobial and antioxidant properties. J Photochem Photobiol B 197:111529. https://doi.org/10.1016/j.jphotobiol.2019.111529
140. Khalil MA, El-Shanshoury AE, Alghamdi MA, Alsalmi FA, Mohamed SF, Sun J, Ali SS (2022) Biosynthesis of silver nanoparticles by marine *Actinobacterium Nocardiopsis dassonvillei* and exploring their therapeutic potentials. Front Microbiol. https://doi.org/10.3389/fmicb.2021.705673
141. Samuel MS, Jose S, Selvarajan E, Mathimani T, Pugazhendhi A (2020) Biosynthesized silver nanoparticles using *Bacillus amyloliquefaciens*; application for cytotoxicity effect on A549 cell line and photocatalytic degradation of p-nitrophenol. J Photochem Photobiol B 202:111642. https://doi.org/10.1016/j.jphotobiol.2019.111642
142. Saravanan M, Barik SK, MubarakAli D, Prakash P, Pugazhendhi A (2018) Synthesis of silver nanoparticles from *Bacillus brevis* (NCIM 2533) and their antibacterial activity against pathogenic bacteria. Microb Pathog 116:221–226. https://doi.org/10.1016/j.micpath.2018.01.038
143. Składanowski M, Wypij M, Laskowski D, Golińska P, Dahm H, Rai M (2017) Silver and gold nanoparticles synthesized from *Streptomyces sp.* isolated from acid forest soil with special reference to its antibacterial activity against pathogens. J Clust Sci 28:59–79. https://doi.org/10.1007/s10876-016-1043-6
144. Shunmugam R, Balusamy SR, Kumar V, Menon S, Lakshmi T, Perumalsamy H (2021) Biosynthesis of gold nanoparticles using marine microbe (*Vibrio alginolyticus*) and its anticancer and antioxidant analysis. J King Saud Univ Sci. https://doi.org/10.1016/j.jksus.2020.101260
145. Patil MP, Kang MJ, Niyonizigiye I, Singh A, Kim JO, Seo YB, Kim GD (2019) Extracellular synthesis of gold nanoparticles using the marine bacterium *Paracoccus haeundaensis* BC74171T and evaluation of their antioxidant activity and antiproliferative effect on normal and cancer cell lines. Colloids Surf B Biointerfaces. https://doi.org/10.1016/j.colsurfb.2019.110455
146. Vairavel M, Devaraj E, Shanmugam R (2020) An eco-friendly synthesis of *Enterococcus sp.*—mediated gold nanoparticle induces cytotoxicity in human colorectal cancer cells. Environ Sci Pollut Res 27:8166–8175. https://doi.org/10.1007/s11356-019-07511-x
147. Bowman SM, Free SJ (2006) The structure and synthesis of the fungal cell wall. BioEssays 28:799–808. https://doi.org/10.1002/bies.20441
148. Jhansi K, Jayarambabu N, Reddy KP, Reddy NM, Suvarna RP, Rao KV, Kumar VR, Rajendar V (2017) Biosynthesis of MgO nanoparticles using mushroom extract: effect on peanut (*Arachis hypogaea* L.) seed germination. 3 Biotech. https://doi.org/10.1007/s13205-017-0894-3
149. Yadav A, Kon K, Kratosova G, Duran N, Ingle AP, Rai M (2015) Fungi as an efficient mycosystem for the synthesis of metal nanoparticles: progress and key aspects of research. Biotechnol Lett 37:2099–2120. https://doi.org/10.1007/s10529-015-1901-6
150. Kashyap PL, Kumar S, Srivastava AK, Sharma AK (2013) Myconanotechnology in agriculture: a perspective. World J Microbiol Biotechnol 29:191–207. https://doi.org/10.1007/s11274-012-1171-6

151. Verma VC, Singh SK, Solanki R, Prakash S (2011) Biofabrication of anisotropic gold nanotriangles using extract of endophytic *Aspergillus clavatus* as a dual functional reductant and stabilizer. Nanoscale Res Lett 6:1–7. https://doi.org/10.1007/s11671-010-9743-6
152. Birla SS, Tiwari VV, Gade AK, Ingle AP, Yadav AP, Rai MK (2009) Fabrication of silver nanoparticles by *Phoma glomerata* and its combined effect against *Escherichia coli*, *Pseudomonas aeruginosa* and *Staphylococcus aureus*. Lett Appl Microbiol 48:173–179. https://doi.org/10.1111/j.1472-765X.2008.02510.x
153. Sarkar J, Dey P, Saha S, Acharya K (2011) Mycosynthesis of selenium nanoparticles. Micro Nano Lett 6:599–602. https://doi.org/10.1049/mnl.2011.0227
154. Govindappa M, Lavanya M, Aishwarya P, Pai K, Lunked P, Hemashekhar B, Arpitha BM, Ramachandra YL, Raghavendra VB (2020) Synthesis and characterization of endophytic fungi, *Cladosporium perangustum* mediated silver nanoparticles and their antioxidant, anticancer and nano-toxicological study. Bionanoscience 10:928–941. https://doi.org/10.1007/s12668-020-00719-z
155. Zakariya NA, Majeed S, Jusof WH (2022) Investigation of antioxidant and antibacterial activity of iron oxide nanoparticles (IONPS) synthesized from the aqueous extract of *Penicillium spp*. Sens Int 3:1–9. https://doi.org/10.1016/j.sintl.2022.100164
156. Sidkey NB (2020) Biosynthesis, characterization and antimicrobial activity of iron oxide nanoparticles synthesized by fungi. Al-Azhar J Pharm Sci 62(2):164–179. https://doi.org/10.21608/AJPS.2020.118382
157. Baskar G, Chandhuru J, Praveen AS, Sheraz Fahad K (2017) Anticancer activity of iron oxide nanobiocomposite of fungal asparaginase. Int J Mod Sci Technol 2:98–104
158. Saravanakumar K, Shanmugam S, Varukattu NB, MubarakAli D, Kathiresan K, Wang MH (2019) Biosynthesis and characterization of copper oxide nanoparticles from indigenous fungi and its effect of photothermolysis on human lung carcinoma. J Photochem Photobiol B 190:103–109. https://doi.org/10.1016/j.jphotobiol.2018.11.017
159. Ghareib M, Abdallah W, Tahon M, Tallima A (2019) Biosynthesis of copper oxide nanoparticles using the preformed biomass of *Aspergillus fumigatus* and their antibacterial and photocatalytic activities. Dig J Nanomater Biostruct 14(2):291–303
160. Mani VM, Kalaivani S, Sabarathinam S, Vasuki M, Soundari AJ, Das MA, Elfasakhany A, Pugazhendhi A (2021) Copper oxide nanoparticles synthesized from an endophytic fungus *Aspergillus terreus*: bioactivity and anti-cancer evaluations. Environ Res. https://doi.org/10.1016/j.envres.2021.111502
161. Fatima F, Wahid I (2022) Eco-friendly synthesis of silver and copper nanoparticles by *Shizophyllum* commune fungus and its biomedical applications. Int J Environ Sci Technol 19:7915–7926. https://doi.org/10.1007/s13762-021-03517-6
162. Mkhize SS, Pooe OJ, Khoza S, Mongalo IN, Khan R, Simelane MB (2022) Characterization and biological evaluation of zinc oxide nanoparticles synthesized from *Pleurotus ostreatus* mushroom. Appl Sci (Switzerland). https://doi.org/10.3390/app12178563
163. Mani VM, Nivetha S, Sabarathinam S, Barath S, Das MA, Basha S, Elfasakhany A, Pugazhendhi A (2022) Multifunctionalities of mycosynthesized zinc oxide nanoparticles (ZnO NPs) from *Cladosporium tenuissimum* FCBGr: antimicrobial additives for paints coating, functionalized fabrics and biomedical properties. Prog Org Coat. https://doi.org/10.1016/j.porgcoat.2021.106650
164. Abdelkader DH, Negm WA, Elekhnawy E, Eliwa D, Aldosari BN, Almurshedi AS (2022) Zinc oxide nanoparticles as potential delivery carrier: green synthesis by *Aspergillus niger* endophytic fungus, characterization, and *in vitro/in vivo* antibacterial activity. Pharmaceuticals. https://doi.org/10.3390/ph1091057
165. Arya S, Sonawane H, Math S, Tambade P, Chaskar M, Shinde D (2021) Biogenic titanium nanoparticles (TiO_2 NPs) from *Tricoderma citrinoviride* extract: synthesis, characterization and antibacterial activity against extremely drug-*resistant Pseudomonas aeruginosa*. Int Nano Lett 11:35–42. https://doi.org/10.1007/s40089-020-00320-y
166. Rehman S, Jermy R, Asiri SM, Shah MA, Farooq R, Ravinayagam V, Ansari MA, Alsalem Z, Al Jindan R, Reshi Z, Khan FA (2020) Using *Fomitopsis pinicola* for bioinspired synthesis of titanium dioxide and silver nanoparticles, targeting biomedical applications. RSC Adv 10:32137–32147. https://doi.org/10.1039/d0ra02637a
167. Gupta P, Rai N, Verma A, Saikia D, Singh SP, Kumar R, Singh SK, Kumar D, Gautam V (2022) Green-based approach to synthesize silver nanoparticles using the fungal endophyte. ACS Omega 7(50):46653–46673. https://doi.org/10.1021/acsomega.2c05605
168. Vijayan S, Divya K, George TK, Jisha MS (2016) Biogenic synthesis of silver nanoparticles using endophytic fungi *Fusarium oxysporum* isolated from *Withania somnifera (L.),* its antibacterial and cytotoxic activity. J Bionanosci 10:369–376. https://doi.org/10.1166/jbns.2016.1390
169. Omran BA, Nassar HN, Fatthallah NA, Hamdy A, El-Shatoury EH, El-Gendy NS (2018) Characterization and antimicrobial activity of silver nanoparticles mycosynthesized by *Aspergillus brasiliensis*. J Appl Microbiol 125:370–382. https://doi.org/10.1111/jam.13776
170. Ramos MM, Morais EDS, Sena IDS, Lima AL, de Oliveira FR, de Freitas CM, Fernandes CP, de Carvalho JC, Ferreira IM (2020) Silver nanoparticle from whole cells of the fungi *Trichoderma spp*. isolated from Brazilian Amazon. Biotechnol Lett 42:833–843. https://doi.org/10.1007/s10529-020-02819-y
171. Win TT, Khan S, Fu P (2020) Fungus- (*Alternaria* sp) mediated silver nanoparticles synthesis, characterization, and screening of antifungal activity against some phytopathogens. J Nanotechnol. https://doi.org/10.1155/2020/8828878
172. Munawer U, Raghavendra VB, Ningaraju S, Krishna KL, Ghosh AR, Melappa G, Pugazhendhi A (2020) Biofabrication of gold nanoparticles mediated by the endophytic *Cladosporium* species: photodegradation, *in vitro* anticancer activity and *in vivo* antitumor studies. Int J Pharm 588:119729. https://doi.org/10.1016/j.ijpharm.2020.119729
173. Abdel-Kareem MM, Zohri AA (2018) Extracellular mycosynthesis of gold nanoparticles using *Trichoderma hamatum*: optimization, characterization and antimicrobial activity. Lett Appl Microbiol 67:465–475. https://doi.org/10.1111/lam.13055
174. Sarkar J, Ray S, Chattopadhyay D, Laskar A, Acharya K (2012) Mycogenesis of gold nanoparticles using a phytopathogen *Alternaria alternata*. Bioprocess Biosyst Eng 35:637–643. https://doi.org/10.1007/s00449-011-0646-4
175. Clarance P, Luvankar B, Sales J, Khusro A, Agastian P, Tack JC, Al Khulaifi MM, Al-Shwaiman HA, Elgorban AM, Syed A, Kim HJ (2020) Green synthesis and characterization of gold nanoparticles using endophytic fungi *Fusarium solani* and its *in-vitro* anticancer and biomedical applications. Saudi J Biol Sci 27:706–712. https://doi.org/10.1016/j.sjbs.2019.12.026
176. Shah M, Fawcett D, Sharma S, Tripathy SK, Poinern GE (2015) Green synthesis of metallic nanoparticles via biological entities. Materials 8:7278–7308. https://doi.org/10.3390/ma8115377
177. Senapati S, Syed A, Moeez S, Kumar A, Ahmad A (2012) Intracellular synthesis of gold nanoparticles using alga *Tetraselmis kochinensis*. Mater Lett 79:116–118. https://doi.org/10.1016/j.matlet.2012.04.009
178. Ramaswamy SV, Narendhran S, Sivaraj R (2016) Potentiating effect of ecofriendly synthesis of copper oxide nanoparticles using brown alga: antimicrobial and anticancer activities. Bull Mater Sci 39:361–364
179. Priyadharshini RI, Prasannaraj G, Geetha N, Venkatachalam P (2014) Microwave-mediated extracellular synthesis of metallic silver and zinc oxide nanoparticles using macro-algae (*Gracilaria edulis)* extracts and its anticancer activity against human PC3 cell lines. Appl Biochem Biotechnol 174:2777–2790. https://doi.org/10.1007/s12010-014-1225-3
180. Murugesan S, Bhuvaneswari S, Shanthi N, Murugakoothan P, Sivamurugan V (2015) Red alga *Hypnea musciformis* (Wulf) lamour mediated environmentally benign synthesis and antifungal activity of gold nano particles. Int J Nanosci Nanotechnol 6:71–83
181. Venkatesan J, Kim SK, Shim MS (2016) Antimicrobial, antioxidant, and anticancer activities of biosynthesized silver nanoparticles using marine algae *Ecklonia cava*. Nanomaterials 6(12):235. https://doi.org/10.3390/nano6120235
182. Bensy AD, Christobel GJ, Muthusamy K, Alfarhan A, Anantharaman P (2022) Green synthesis of iron nanoparticles from *Ulva lactuca* and bactericidal activity against enteropathogens. J King Saud Univ Sci 34:101888. https://doi.org/10.1016/j.jksus.2022.101888
183. Salem DM, Ismail MM, Aly-Eldeen MA (2019) Biogenic synthesis and antimicrobial potency of iron oxide (Fe_3O_4) nanoparticles using algae harvested from the Mediterranean Sea. Egypt Egypt J Aquat Res 45:197–204. https://doi.org/10.1016/j.ejar.2019.07.002

184. Subhashini G, Ruban P, Daniel T (2018) Biosynthesis and characterization of magnetic (Fe_3O_4) iron oxide nanoparticles from a red seaweed *Gracilaria edulis* and its antimicrobial activity. Int J Adv Sci Res Manag 3:184–189
185. Haris M, Fatima N, Iqbal J, Chalgham W, Mumtaz AS, El-Sheikh MA, Tavafoghi M (2023) *Oscillatoria limnetica* mediated green synthesis of iron oxide (Fe_2O_3) nanoparticles and their diverse *in vitro* bioactivities. Molecules. https://doi.org/10.3390/molecules28052091
186. Abboud Y, Saffaj T, Chagraoui A, El Bouari A, Brouzi K, Tanane O, Ihssane B (2014) Biosynthesis, characterization and antimicrobial activity of copper oxide nanoparticles (CONPs) produced using brown alga extract (*Bifurcaria bifurcata*). Appl Nanosci (Switzerland) 4:571–576. https://doi.org/10.1007/s13204-013-0233-x
187. Saran S, Sharma G, Kumar M, Ali MI (2017) Biosynthesis of copper oxide nanoparticles using cyanobacteria *Spirulina platensis* and its antibacterial activity. Int J Pharm Sci Res 8:3887–3892. https://doi.org/10.13040/IJPSR.0975-8232.8(9).3887-92
188. Kothai R, Arul B, Anbazhagan V (2022) Anti-dengue activity of ZnO nanoparticles of crude fucoidan from brown seaweed *S. marginatum*. Appl Biochem Biotechnol. https://doi.org/10.1007/s12010-022-03966-w
189. Sanaeimehr Z, Javadi I, Namvar F (2018) Antiangiogenic and antiapoptotic effects of green-synthesized zinc oxide nanoparticles using *Sargassum muticum* algae extraction. Cancer Nanotechnol. https://doi.org/10.1186/s12645-018-0037-5
190. Bhattacharya P, Chatterjee K, Swarnakar S, Banerjee S (2020) Green synthesis of zinc oxide nanoparticles via algal route and its action on cancerous cells and pathogenic microbes. Adv Nano Res 3:15–27. https://doi.org/10.21467/anr.3.1.15-27
191. Kathiraven T, Sundaramanickam A, Shanmugam N, Balasubramanian T (2015) Green synthesis of silver nanoparticles using marine algae *Caulerpa racemosa* and their antibacterial activity against some human pathogens. Appl Nanosci (Switzerland) 5:499–504. https://doi.org/10.1007/s13204-014-0341-2
192. El-Sheekh MM, Shabaan MT, Hassan L, Morsi HH (2020) Antiviral activity of algae biosynthesized silver and gold nanoparticles against Herpes Simplex (HSV-1) virus *in vitro* using cell-line culture technique. Int J Environ Health Res 32:1–12. https://doi.org/10.1080/09603123.2020.1789946
193. Sinha SN, Paul D, Halder N, Sengupta D, Patra SK (2015) Green synthesis of silver nanoparticles using fresh water green alga *Pithophora oedogonia* (Mont.) Wittrock and evaluation of their antibacterial activity. Appl Nanosci (Switzerland) 5:703–709. https://doi.org/10.1007/s13204-014-0366-6
194. Aboelfetoh EF, El-Shenody RA, Ghobara MM (2017) Eco-friendly synthesis of silver nanoparticles using green algae (*Caulerpa serrulata*): reaction optimization, catalytic and antibacterial activities. Environ Monit Assess. https://doi.org/10.1007/s10661-017-6033-0
195. Dhanasezhian A, Srivani S, Govindaraju K, Parija P, Sasikala S, Kumar MR (2019) Anti-herpes simplex virus (HSV-1 and HSV-2) activity of biogenic gold and silver nanoparticles using seaweed *Sargassum wightii*. Indian J Mar Sci 48:1252–1257
196. Naveena BE, Prakash S (2013) Biological synthesis of gold nanoparticles using marine algae *Gracilaria corticata* and its application as a potent antimicrobial and antioxidant agent. Asian J Pharm Clin Res 6:179–182
197. Singh M, Saurav K, Majouga A, Kumari M, Kumar M, Manikandan S, Kumaraguru AK (2015) The cytotoxicity and cellular stress by temperature-fabricated polyshaped gold nanoparticles using marine macroalgae, *Padina gymnospora*. Biotechnol Appl Biochem 62:424–432. https://doi.org/10.1002/bab.1271
198. Singh KR, Nayak V, Singh J, Singh AK, Singh RP (2021) Potentialities of bioinspired metal and metal oxide nanoparticles in biomedical sciences. RSC Adv 11:24722–24746. https://doi.org/10.1039/d1ra04273d
199. Al-kawmani AA, Alanazi KM, Farah MA, Ali MA, Hailan WA, Al-Hemaid FM (2020) Apoptosis-inducing potential of biosynthesized silver nanoparticles in breast cancer cells. J King Saud Univ Sci 32(4):2480–2488. https://doi.org/10.1016/j.jksus.2020.04.002
200. Eid AM, Fouda A, Niedbała G, Hassan SE, Salem SS, Abdo AM, F. Hetta H, Shaheen TI, (2020) Endophytic *Streptomyces laurentii* mediated green synthesis of Ag-NPs with antibacterial and anticancer properties for developing functional textile fabric properties. Antibiotics 9:1–18. https://doi.org/10.3390/antibiotics9100641
201. Biswas AK, Islam MR, Choudhury ZS, Mostafa A, Kadir MF (2014) Nanotechnology based approaches in cancer therapeutics. Adv Nat Sci J Nanosci Nanotechnol 5(4):043001. https://doi.org/10.1088/2043-6262/5/4/043001
202. Ullah I, Khalil AT, Ali M, Iqbal J, Ali W, Alarifi S, Shinwari ZK (2020) Green-synthesized silver nanoparticles induced apoptotic cell death in MCF-7 breast cancer cells by generating reactive oxygen species and activating caspase 3 and 9 enzyme activities. Oxid Med Cell Longev 1215395:1–14. https://doi.org/10.1155/2020/1215395
203. Jain N, Jain P, Rajput D, Patil UK (2021) Green synthesized plant-based silver nanoparticles: therapeutic prospective for anticancer and antiviral activity. Micro Nano Syst Lett. https://doi.org/10.1186/s40486-021-00131-6
204. Kumari R, Saini AK, Kumar A, Saini RV (2020) Apoptosis induction in lung and prostate cancer cells through silver nanoparticles synthesized from *Pinus roxburghii* bioactive fraction. J Biol Inorg Chem 25:23–37. https://doi.org/10.1007/s00775-019-01729-3
205. Li Y, Ke Y, Zou H, Wang K, Huang S, Rengarajan T, Wang L (2019) Gold nano particles synthesized from *Strychni semen* and its anticancer activity in cholangiocarcinoma cell (KMCH-1). Artif Cells Nanomed Biotechnol 47:1610–1616. https://doi.org/10.1080/21691401.2019.1594860
206. Sung H, Ferlay J, Siegel RL, Laversanne M, Soerjomataram I, Jemal A, Bray F (2021) Global cancer statistics 2020: GLOBOCAN estimates of incidence and mortality worldwide for 36 cancers in 185 countries. CA Cancer J Clin 71:209–249. https://doi.org/10.3322/caac.21660
207. Harbeck N, Penault-Llorca F, Cortes J, Gnant M, Houssami N, Poortmans P, Ruddy K, Tsang J, Cardoso F (2019) Breast cancer. Nat Rev Dis Primers. https://doi.org/10.1038/s41572-019-0111-2
208. George BP, Rajendran NK, Houreld NN, Abrahamse H (2022) Rubus capped zinc oxide nanoparticles induce apoptosis in MCF-7. Breast Cancer Cell Mol. https://doi.org/10.3390/molecules27206862
209. Zhai C, Shi C, Hu Y, Xu Z, Wang R (2022) Anti-breast carcinoma effects of green synthesized tin nanoparticles from *Calendula officinalis* leaf aqueous extract inhibits MCF7, Hs 319.T, and MCF10 cells proliferation. J Exp Nanosci 17:351–361. https://doi.org/10.1080/17458080.2022.2076836
210. Mahendran D, Kavi Kishor PB, Geetha N, Manish T, Sahi SV, Venkatachalam P (2021) Efficient antibacterial/biofilm, anti-cancer and photocatalytic potential of titanium dioxide nanocatalysts green synthesised using *Gloriosa superba* rhizome extract. J Exp Nanosci 16:11–31. https://doi.org/10.1080/17458080.2021.1872781
211. Yugandhar P, Vasavi T, Uma Maheswari Devi P, Savithramma N (2017) Bioinspired green synthesis of copper oxide nanoparticles from *Syzygium alternifolium* (Wt.) Walp: characterization and evaluation of its synergistic antimicrobial and anticancer activity. Appl Nanosci (Switzerland) 7:417–427. https://doi.org/10.1007/s13204-017-0584-9
212. Parvathy S, Manjula G, Balachandar R, Subbaiya R (2022) Green synthesis and characterization of cerium oxide nanoparticles from *Artabotrys hexapetalus* leaf extract and its antibacterial and anticancer properties. Mater Lett. https://doi.org/10.1016/j.matlet.2022.131811
213. Al-Nuairi AG, Mosa KA, Mohammad MG, El-Keblawy A, Soliman S, Alawadhi H (2020) Biosynthesis, characterization, and evaluation of the cytotoxic effects of biologically synthesized silver nanoparticles from *Cyperus conglomeratus* root extracts on breast cancer cell line MCF-7. Biol Trace Elem Res 194:560–569. https://doi.org/10.1007/s12011-019-01791-7
214. Kabir SR, Asaduzzaman AK, Amin R, Haque AT, Ghose R, Rahman MM, Islam J, Amin MB, Hasan I, Debnath T, Chun BS (2020) *Zizyphus mauritiana* fruit extract-mediated synthesized silver/silver chloride nanoparticles retain antimicrobial activity and induce apoptosis in MCF-7 cells through the Fas pathway. ACS Omega 5:20599–20608. https://doi.org/10.1021/acsomega.0c02878
215. Şahin B, Aygün A, Gündüz H, Şahin K, Demir E, Akocak S, Şen F (2018) Cytotoxic effects of platinum nanoparticles obtained from pomegranate extract by the green synthesis method on the MCF-7 cell line. Colloids Surf B Biointerfaces 163:119–124. https://doi.org/10.1016/j.colsurfb.2017.12.042
216. Gomathi AC, Rajarathinam SX, Sadiq AM, Rajeshkumar S (2020) Anticancer activity of silver nanoparticles synthesized using aqueous fruit shell extract of *Tamarindus indica* on MCF-7 human breast cancer cell line. J Drug Deliv Sci Technol 55:101376. https://doi.org/10.1016/j.jddst.2019.101376

217. Khateef R, Khadri H, Almatroudi A, Alsuhaibani SA, Mobeen SA, Khan RA (2019) Potential *in-vitro* anti-breast cancer activity of green-synthesized silver nanoparticles preparation against human MCF-7 cell-lines. Adv Nat Sci Nanosci Nanotechnol. https://doi.org/10.1088/2043-6254/ab47ff
218. Oves M, Aslam M, Rauf MA, Qayyum S, Qari HA, Khan MS, Alam MZ, Tabrez S, Pugazhendhi A, Ismail IM (2018) Antimicrobial and anticancer activities of silver nanoparticles synthesized from the root hair extract of *Phoenix dactylifera*. Mater Sci Eng C 89:429–443. https://doi.org/10.1016/j.msec.2018.03.035
219. Oves M, Rauf MA, Aslam M, Qari HA, Sonbol H, Ahmad I, Zaman GS, Saeed M (2022) Green synthesis of silver nanoparticles by *Conocarpus Lancifolius* plant extract and their antimicrobial and anticancer activities. Saudi J Biol Sci 29:460–471. https://doi.org/10.1016/j.sjbs.2021.09.007
220. Li S, Al-Misned FA, El-Serehy HA, Yang L (2021) Green synthesis of gold nanoparticles using aqueous extract of *Mentha Longifolia* leaf and investigation of its anti-human breast carcinoma properties in the *in vitro* condition. Arab J Chem 14:102931. https://doi.org/10.1016/j.arabjc.2020.102931
221. Hosny M, Fawzy M, El-Badry YA, Hussein EE, Eltaweil AS (2022) Plant-assisted synthesis of gold nanoparticles for photocatalytic, anticancer, and antioxidant applications. J Saudi Chem Soc. https://doi.org/10.1016/j.jscs.2022.101419
222. Biresaw SS, Taneja P (2020) Copper nanoparticles green synthesis and characterization as anticancer potential in breast cancer cells (MCF7) derived from *Prunus nepalensis* phytochemicals. Mater Today Proc 49:3501–3509. https://doi.org/10.1016/j.matpr.2021.07.149
223. Sivaraj R, Rahman PK, Rajiv P, Narendhran S, Venckatesh R (2014) Biosynthesis and characterization of *Acalypha indica* mediated copper oxide nanoparticles and evaluation of its antimicrobial and anticancer activity. Spectrochim Acta A Mol Biomol Spectrosc 129:255–258. https://doi.org/10.1016/j.saa.2014.03.027
224. Rajagopal G, Nivetha A, Sundar M, Panneerselvam T, Murugesan S, Parasuraman P, Kumar S, Ilango S, Kunjiappan S (2021) Mixed phytochemicals mediated synthesis of copper nanoparticles for anticancer and larvicidal applications. Heliyon. https://doi.org/10.1016/j.heliyon.2021.e07360
225. Iqbal H, Razzaq A, Uzair B, Ul Ain N, Sajjad S, Althobaiti NA et al (2021) Breast cancer inhibition by biosynthesized titanium dioxide nanoparticles is comparable to free doxorubicin but appeared safer in balb/c mice. Materials 14:12. https://doi.org/10.3390/ma14123155
226. Sargazi S, Laraib U, Er S, Rahdar A, Hassanisaadi M, Zafar MN, Diez-Pascual AM, Bilal M (2022) Application of green gold nanoparticles in cancer therapy and diagnosis. Nanomaterials 12(7):1102. https://doi.org/10.3390/nano12071102
227. Barta JA, Powell CA, Wisnivesky JP (2019) Global epidemiology of lung cancer. Ann Glob Health. https://doi.org/10.5334/aogh.2419
228. Jemal A, Bray F, Center MM, Ferlay J, Ward E, Forman D (2011) Global cancer statistics. CA Cancer J Clin 61:69–90. https://doi.org/10.3322/caac.20107
229. Nagalingam M, Kalpana VN, Panneerselvam A (2018) Biosynthesis, characterization, and evaluation of bioactivities of leaf extract-mediated biocompatible gold nanoparticles from *Alternanthera bettzickiana*. Biotechnol Rep. https://doi.org/10.1016/j.btre.2018.e00268
230. Kanipandian N, Kannan S, Ramesh R, Subramanian P, Thirumurugan R (2014) Characterization, antioxidant and cytotoxicity evaluation of green synthesized silver nanoparticles using *Cleistanthus collinus* extract as surface modifier. Mater Res Bull 49:494–502. https://doi.org/10.1016/j.materresbull.2013.09.016
231. Zheng Y, Zhang J, Zhang R, Luo Z, Wang C, Shi S (2019) Gold nano particles synthesized from *Magnolia officinalis* and anticancer activity in A549 lung cancer cells. Artif Cells Nanomed Biotechnol 47:3101–3109. https://doi.org/10.1080/21691401.2019.1645152
232. Aswini R, Murugesan S, Kannan K (2021) Bio-engineered TiO_2 nanoparticles using *Ledebouria revoluta* extract: Larvicidal, histopathological, antibacterial and anticancer activity. Int J Environ Anal Chem 101:2926–2936. https://doi.org/10.1080/03067319.2020.1718668
233. Devendrapandi G, Sahay MI, Padmanaban D, Panneerselvam A, Palraj R, Thanikasalam R, Sadaiyandi V, Balu R, Rajendiran N (2023) Biogenic synthesis of gold nanoparticles using bael fruit juice and its efficacy against human A-549 lung cancer cell line. Inorg Chem Commun. https://doi.org/10.1016/j.inoche.2023.110636
234. Dobrucka R, Romaniuk-Drapała A, Kaczmarek M (2019) Evaluation of biological synthesized platinum nanoparticles using *Ononidis radix* extract on the cell lung carcinoma A549. Biomed Microdev. https://doi.org/10.1007/s10544-019-0424-7
235. Rajivgandhi GN, Chackaravarthi G, Ramachandran G, Manoharan N, Ragunathan R, Siddiqi MZ, Alharbi NS, Khaled JM, Li WJ (2022) Synthesis of silver nanoparticle (Ag NPs) using phytochemical rich medicinal plant *Lonicera japonica* for improve the cytotoxicity effect in cancer cells. J King Saud Univ Sci. https://doi.org/10.1016/j.jksus.2021.101798
236. He Y, Du Z, Ma S, Liu Y, Li D, Huang H, Jiang S, Cheng S, Wu W, Zhang K, Zheng X (2016) Effects of green-synthesized silver nanoparticles on lung cancer cells in vitro and grown as xenograft tumors *in vivo*. Int J Nanomed 11:1879–1887. https://doi.org/10.2147/IJN.S103695
237. Valodkar M, Jadeja RN, Thounaojam MC, Devkar RV, Thakore S (2011) *In vitro* toxicity study of plant latex capped silver nanoparticles in human lung carcinoma cells. Mater Sci Eng C 31:1723–1728. https://doi.org/10.1016/j.msec.2011.08.001
238. Chen F, Zheng Q, Li X, Xiong J (2022) Citrus sinensis leaf aqueous extract green-synthesized silver nanoparticles: characterization and cytotoxicity, antioxidant, and anti-human lung carcinoma effects. Arab J Chem 15:103845. https://doi.org/10.1016/j.arabjc.2022.103845
239. Zhang H, Li T, Luo W, Peng GX, Xiong J (2022) Green synthesis of Ag nanoparticles from *Leucus aspera* and its application in anticancer activity against alveolar cancer. J Exp Nanosci 17:47–60. https://doi.org/10.1080/17458080.2021.2007886
240. Tian S, Saravanan K, Mothana RA, Ramachandran G, Rajivgandhi G, Manoharan N (2020) Anti-cancer activity of biosynthesized silver nanoparticles using *Avicennia marina* against A549 lung cancer cells through ROS/mitochondrial damages. Saudi J Biol Sci 27:3018–3024. https://doi.org/10.1016/j.sjbs.2020.08.029
241. Lakshmanan G, Sathiyaseelan A, Kalaichelvan PT, Murugesan K (2018) Plant-mediated synthesis of silver nanoparticles using fruit extract of *Cleome viscosa L.*: assessment of their antibacterial and anticancer activity. Karbala Int J Mod Sci 4:61–68. https://doi.org/10.1016/j.kijoms.2017.10.007
242. Zhang X, Tan Z, Jia K, Zhang W, Dang M (2019) *Rabdosia rubescens Linn*: green synthesis of gold nanoparticles and their anticancer effects against human lung cancer cells A549. Artif Cells Nanomed Biotechnol 47:2171–2178. https://doi.org/10.1080/21691401.2019.1620249
243. Vijayakumar S, Vaseeharan B, Malaikozhundan B, Gopi N, Ekambaram P, Pachaiappan R, Velusamy P, Murugan K, Benelli G, Kumar RS, Suriyanarayanamoorthy M (2017) Therapeutic effects of gold nanoparticles synthesized using *Musa paradisiaca* peel extract against multiple antibiotic resistant *Enterococcus faecalis* biofilms and human lung cancer cells (A549). Microb Pathog 102:173–183. https://doi.org/10.1016/j.micpath.2016.11.029
244. Sun B, Hu N, Han L, Pi Y, Gao Y, Chen K (2019) Anticancer activity of green synthesised gold nanoparticles from *Marsdenia tenacissima* inhibits A549 cell proliferation through the apoptotic pathway. Artif Cells Nanomed Biotechnol 47:4012–4019. https://doi.org/10.1080/21691401.2019.1575844
245. Rani N, Rawat K, Shrivastava A, Yadav S, Gupta K, Saini K (2022) *In Vitro* study of green synthesized ZnO nanoparticles on human lung cancer cell lines. Mater Today Proc 49:1436–1442. https://doi.org/10.1016/j.matpr.2021.07.203
246. Zhang H, Liang Z, Zhang J, Wang WP, Zhang H, Lu Q (2020) Zinc oxide nanoparticle synthesized from *Euphorbia fischeriana* root inhibits the cancer cell growth through modulation of apoptotic signaling pathways in lung cancer cells. Arab J Chem 13:6174–6183. https://doi.org/10.1016/j.arabjc.2020.05.020
247. Rajeshkumar S, Kumar SV, Ramaiah A, Agarwal H, Lakshmi T, Roopan SM (2018) Biosynthesis of zinc oxide nanoparticles using *Mangifera indica* leaves and evaluation of their antioxidant and cytotoxic properties in lung cancer (A549) cells. Enzyme Microb Technol 117:91–95. https://doi.org/10.1016/j.enzmictec.2018.06.009
248. Gu J, Aidy A, Goorani S (2022) Anti-human lung adenocarcinoma, cytotoxicity, and antioxidant potentials of copper nanoparticles green-synthesized by *Calendula officinalis*. J Exp Nanosci 17:285–296. https://doi.org/10.1080/17458080.2022.2066082

249. Sankar R, Maheswari R, Karthik S, Shivashangari KS, Ravikumar V (2014) Anticancer activity of *Ficus religiosa* engineered copper oxide nanoparticles. Mater Sci Eng C 44:234–239. https://doi.org/10.1016/j.msec.2014.08.030
250. Majid A, Faraj HR (2022) Green synthesis of copper nanoparticles using aqueous extract of Yerba Mate (Ilex Paraguarients St Hill) and its anticancer activity. Int J Nanosci Nanotechnol 18(2):99–108
251. Chandrasekaran R, Yadav SA, Sivaperumal S (2020) Phytosynthesis and characterization of copper oxide nanoparticles using the aqueous extract of *Beta vulgaris L* and evaluation of their antibacterial and anticancer activities. J Clust Sci 31:221–230. https://doi.org/10.1007/s10876-019-01640-6
252. Gu J, Chen F, Zheng Z, Bi L, Morovvati H, Goorani S (2023) Novel green formulation of copper nanoparticles by *Foeniculum vulgare*: Chemical characterization and determination of cytotoxicity, anti-human lung cancer and antioxidant effects. Inorg Chem Commun. https://doi.org/10.1016/j.inoche.2023.110442
253. Singh D, Vignat J, Lorenzoni V, Eslahi M, Ginsburg O, Lauby-Secretan B, Arbyn M, Basu P, Bray F, Vaccarella S (2020) Articles Global estimates of incidence and mortality of cervical cancer in 2020: a baseline analysis of the WHO Global Cervical Cancer Elimination Initiative. Lancet Glob Health 11:197–206. https://doi.org/10.1016/S2214-109X(22)00501-0
254. Thomas S, Gunasangkaran G, Arumugam VA, Muthukrishnan S (2022) Synthesis and characterization of zinc oxide nanoparticles of *Solanum nigrum* and its anticancer activity via the induction of apoptosis in cervical cancer. Biol Trace Elem Res 200:2684–2697. https://doi.org/10.1007/s12011-021-02898-6
255. Ke Y, Al Aboody MS, Alturaiki W, Alsagaby SA, Alfaiz FA, Veeraraghavan VP, Mickymaray S (2019) Photosynthesized gold nanoparticles from *Catharanthus roseus* induces caspase-mediated apoptosis in cervical cancer cells (HeLa). Artif Cells Nanomed Biotechnol 47:1938–1946. https://doi.org/10.1080/21691401.2019.1614017
256. Tripathi D, Modi A, Smita SS, Narayan G, Pandey-Rai S (2022) Biomedical potential of green synthesized silver nanoparticles from root extract of *Asparagus officinalis*. J Plant Biochem Biotechnol 31:213–218. https://doi.org/10.1007/s13562-021-00684-y
257. Rajkuberan C, Prabukumar S, Sathishkumar G, Wilson A, Ravindran K, Sivaramakrishnan S (2017) Facile synthesis of silver nanoparticles using *Euphorbia antiquorum L*. latex extract and evaluation of their biomedical perspectives as anticancer agents. J Saudi Chem Soc 21:911–919. https://doi.org/10.1016/j.jscs.2016.01.002
258. Qian L, Su W, Wang Y, Dang M, Zhang W, Wang C (2019) Synthesis and characterization of gold nanoparticles from aqueous leaf extract of *Alternanthera sessilis* and its anticancer activity on cervical cancer cells (HeLa). Artif Cells Nanomed Biotechnol 47:1173–1180. https://doi.org/10.1080/21691401.2018.1549064
259. Nagajyothi PC, Muthuraman P, Sreekanth TV, Kim DH, Shim J (2017) Green synthesis: *In-vitro* anticancer activity of copper oxide nanoparticles against human cervical carcinoma cells. Arab J Chem 10:215–225. https://doi.org/10.1016/j.arabjc.2016.01.011
260. Al-Sheddi ES, Farshori NN, Al-Oqail MM, Al-Massarani SM, Saquib Q, Wahab R, Musarrat J, Al-Khedhairy AA, Siddiqui MA (2018) Anticancer potential of green synthesized silver nanoparticles using extract of *Nepeta deflersiana* against human cervical cancer cells (HeLA). Bioinorg Chem Appl. https://doi.org/10.1155/2018/9390784
261. asanth K, Ilango K, MohanKumar R, Agrawal A, Dubey GP, (2014) Anticancer activity of *Moringa oleifera* mediated silver nanoparticles on human cervical carcinoma cells by apoptosis induction. Colloids Surf B Biointerfaces 117:354–359. https://doi.org/10.1016/j.colsurfb.2014.02.052
262. Adebayo IA, Arsad H, Gagman HA, Ismail NZ, Samian MR (2020) Inhibitory effect of eco-friendly naturally synthesized silver nanoparticles from the leaf extract of medicinal *Detarium microcarpum* plant on pancreatic and cervical cancer cells. Asian Pac J Cancer Prev 5:1247–1252. https://doi.org/10.31557/APJCP.2020.21.5.1247
263. Khatua A, Prasad A, Priyadarshini E, Patel AK, Naik A, Saravanan M, Barabadi H, Ghosh L, Paul B, Paulraj R, Meena R (2020) Emerging antineoplastic plant-based gold nanoparticle synthesis: a mechanistic exploration of their anticancer activity toward cervical cancer cells. J Clust Sci 31:329–1340. https://doi.org/10.1007/s10876-019-01742-1
264. Sundaram CS, Kumar JS, Kumar SS, Ramesh PL, Zin T, Rao UM (2020) Antibacterial and anticancer potential of *Brassica oleracea var acephala* using biosynthesised copper nanoparticles. Med J Malays 75(6):677–684
265. Chen H, Feng X, Gao L, Mickymaray S, Paramasivam A, Abdulaziz Alfaiz F et al (2021) Inhibiting the PI3K/AKT/mTOR signalling pathway with copper oxide nanoparticles from *Houttuynia cordata* plant: attenuating the proliferation of cervical cancer cells. Artif Cells Nanomed Biotechnol 49(1):240–249. https://doi.org/10.1080/21691401.2021.1890101
266. Narayanan M, Vigneshwari P, Natarajan D, Kandasamy S, Alsehli M, Elfasakhany A, Pugazhendhi A (2021) Synthesis and characterization of TiO_2 NPs by aqueous leaf extract of *Coleus aromaticus* and assess their antibacterial, larvicidal, and anticancer potential. Environ Res. https://doi.org/10.1016/j.envres.2021.111335
267. Abdellatif AA, Mahmood A, Alsharidah M, Mohammed HA, Alenize SK, Bouazzaoui A, Al Rugaie O, Alnuqaydan AM, Ahmad R, Vaali-Mohammad MA, Alfayez M (2022) Bioactivities of the green synthesized silver nanoparticles reduced using *Allium cepa L* aqueous extracts induced apoptosis in colorectal cancer cell lines. J Nanomater. https://doi.org/10.1155/2022/1746817
268. Malaikolundhan H, Mookkan G, Krishnamoorthi G, Matheswaran N, Alsawalha M, Veeraraghavan VP, Krishna Mohan S, Di A (2020) Anticarcinogenic effect of gold nanoparticles synthesized from *Albizia lebbeck* on HCT-116 colon cancer cell lines. Artif Cells Nanomed Biotechnol 48:1206–1213. https://doi.org/10.1080/21691401.2020.1814313
269. Devanesan S, Al Salhi MS, Vishnubalaji R, Alfuraydi AA, Alajez NM, Alfayez M, Murugan K, Sayed SR, Nicoletti M, Benelli G (2017) Rapid biological synthesis of silver nanoparticles using plant seed extracts and their cytotoxicity on colorectal cancer cell lines. J Clust Sci 28:595–605. https://doi.org/10.1007/s10876-016-1134-4
270. Han X, Jiang X, Guo L, Wang Y, Veeraraghavan VP, Krishna Mohan S, Wang Z, Cao D (2019) Anticarcinogenic potential of gold nanoparticles synthesized from *Trichosanthes kirilowii* in colon cancer cells through the induction of apoptotic pathway. Artif Cells Nanomed Biotechnol 47:3577–3584. https://doi.org/10.1080/21691401.2019.1626412
271. Nazaripour E, Mousazadeh F, Moghadam MD, Najafi K, Borhani F, Sarani M, Ghasemi M, Rahdar A, Iravani S, Khatami M (2021) Biosynthesis of lead oxide and cerium oxide nanoparticles and their cytotoxic activities against colon cancer cell line. Inorg Chem Commun. https://doi.org/10.1016/j.inoche.2021.108800
272. Venkatadri B, Shanparvish E, Rameshkumar MR, Arasu MV, Al-Dhabi NA, Ponnusamy VK, Agastian P (2020) Green synthesis of silver nanoparticles using aqueous rhizome extract of *Zingiber officinale* and *Curcuma longa*: *i3n-vitro* anti-cancer potential on human colon carcinoma HT-29 cells. Saudi J Biol Sci 27:2980–2986. https://doi.org/10.1016/j.sjbs.2020.09.021
273. Dehghanizade S, Arasteh J, Mirzaie A (2018) Green synthesis of silver nanoparticles using *Anthemis atropatana* extract: characterization and *in vitro* biological activities. Artif Cells Nanomed Biotechnol 46:160–168. https://doi.org/10.1080/21691401.2017.1304402
274. Prabhu D, Arulvasu C, Babu G, Manikandan R, Srinivasan P (2013) Biologically synthesized green silver nanoparticles from leaf extract of *Vitex negundo* L. induce growth-inhibitory effect on human colon cancer cell line HCT15. Process Biochem 48(2):317–324. https://doi.org/10.1016/j.procbio.2012.12.013
275. Chhikara BS, Parang K (2023) Global Cancer Statistics 2022: the trends projection analysis. Chem Biol Lett 10(1):451–451
276. Vimal TG (2022) Green synthesis of silver nanoparticles using *Rosmarinus officinalis* leaf extract and study of anticancer effect and apoptosis induction on prostate cancer cell line (PC-3). J Pharm Negat Results 13:3531–3536. https://doi.org/10.47750/pnr.2022.13.S06.472
277. Firdhouse MJ, Lalitha P (2013) Biosynthesis of silver nanoparticles using the extract of *Alternanthera sessilis*-antiproliferative effect against prostate cancer cells. Cancer Nanotechnol 4:137–143. https://doi.org/10.1007/s12645-013-0045-4
278. Prema P, Boobalan T, Arun A, Rameshkumar K, Babu RS, Veeramanikandan V, Nguyen VH, Balaji P (2022) Green tea extract mediated biogenic synthesis of gold nanoparticles with potent anti-proliferative effect against PC-3 human prostate cancer cells. Mater Lett. https://doi.org/10.1016/j.matlet.2021.130882

279. Obaid AS, Hassan KT, Hassan OM, Ali HH, Ibraheem IJ, Salih TA, Adil BH, Almoneef MM (2023) *In-vitro* antibacterial, cytotoxicity, and anti-prostate cancer effects of gold nanoparticles synthesized using extract of desert truffles (*Tirmania nivea*). Mater Chem Phys. https://doi.org/10.1016/j.matchemphys.2023.127673
280. Zhang K, Liu X, Samuel Ravi SO, Ramachandran A, Aziz Ibrahim IA, Nassir MA, Yao J (2019) Synthesis of silver nanoparticles (AgNPs) from leaf extract of *Salvia miltiorrhiza* and its anticancer potential in human prostate cancer LNCaP cell lines. Artif Cells Nanomed Biotechnol 47:2846–2854. https://doi.org/10.1080/21691401.2019.1638792
281. Rahimi Kalateh Shah Mohammad G, Karimi E, Oskoueian E, Homayouni-Tabrizi M (2020) Anticancer properties of green-synthesised zinc oxide nanoparticles using *Hyssopus officinalis* extract on prostate carcinoma cells and its effects on testicular damage and spermatogenesis in Balb/C mice. Andrologia. https://doi.org/10.1111/and.13450
282. He Y, Du Z, Ma S, Cheng S, Jiang S, Liu Y, Li D, Huang H, Zhang K, Zheng X (2016) Biosynthesis, antibacterial activity and anticancer effects against prostate cancer (PC-3) cells of silver nanoparticles using *Dimocarpus Longan Lour*. Peel Extract Nanoscale Res Lett. https://doi.org/10.1186/s11671-016-1511-9
283. Singh SP, Mishra A, Shyanti RK, Singh RP, Acharya A (2021) Silver nanoparticles synthesized using *Carica papaya* leaf extract (AgNPs-PLE) causes cell cycle arrest and apoptosis in human prostate (DU145) cancer cells. Biol Trace Elem Res 199:1316–1331. https://doi.org/10.1007/s12011-020-02255-z
284. Adeyemi JO, Onwudiwe DC, Oyedeji AO (2022) Biogenic synthesis of CuO, ZnO, and CuO–ZnO nanoparticles using leaf extracts of *Dovyalis caffra* and their biological properties. Molecules. https://doi.org/10.3390/molecules27103206
285. Netala VR, Bukke S, Domdi L, Soneya S, Reddy GS, Bethu MS, Kotakdi VS, Saritha KV, Tartte V (2018) Biogenesis of silver nanoparticles using leaf extract of *Indigofera hirsuta* L. and their potential biomedical applications (3-in-1 system). Artif Cells Nanomed Biotechnol 46:1138–1148. https://doi.org/10.1080/21691401.2018.1446967
286. Zhao W, Wang L, Chen H, Qi L, Yang R, Ouyang T, Ning L (2022) Green synthesis, characterization and determination of anti-prostate cancer, cytotoxicity and antioxidant effects of gold nanoparticles synthesized using *Alhagi maurorum*. Inorg Chem Commun. https://doi.org/10.1016/j.inoche.2022.109525
287. Wu F, Zhu J, Li G, Wang J, Veeraraghavan VP, Krishna Mohan S, Zhang Q (2019) Biologically synthesized green gold nanoparticles from *Siberian ginseng* induce growth-inhibitory effect on melanoma cells (B16). Artif Cells Nanomed Biotechnol 47:3297–3305. https://doi.org/10.1080/21691401.2019.1647224
288. Mohanta YK, Panda SK, Biswas K, Tamang A, Bandyopadhyay J, De D, Mohanta D, Bastia AK (2016) Biogenic synthesis of silver nanoparticles from *Cassia fistula (Linn.): in vitro* assessment of their antioxidant, antimicrobial and cytotoxic activities. IET Nanobiotechnol 10:438–444. https://doi.org/10.1049/iet-nbt.2015.0104
289. Mukhopadhyay R, Kazi J, Debnath MC (2018) Synthesis and characterization of copper nanoparticles stabilized with *Quisqualis indica* extract: evaluation of its cytotoxicity and apoptosis in B16F10 melanoma cells. Biomed Pharmacother 97:1373–1385. https://doi.org/10.1016/j.biopha.2017.10.167
290. Nirmala JG, Akila S, Narendhirakannan RT, Chatterjee S (2017) *Vitis vinifera* peel polyphenols stabilized gold nanoparticles induce cytotoxicity and apoptotic cell death in A431 skin cancer cell lines. Adv Powder Technol 28:1170–1184. https://doi.org/10.1016/j.apt.2017.02.003
291. Suseela V (2015) Cytotoxic effect of green synthesized silver nanoparticles using *Indigofera longeracemosa* on skin cancer SK MEL-28 cell lines. Int J Preclin Pharm Res 6(3):118–125
292. Francis S, Joseph S, Koshy EP, Mathew B (2018) Microwave assisted green synthesis of silver nanoparticles using leaf extract of *Elephantopus scaber* and its environmental and biological applications. Artif Cells Nanomed Biotechnol 46:795–804. https://doi.org/10.1080/21691401.2017.1345921
293. Nayak D, Pradhan S, Ashe S, Rauta PR, Nayak B (2015) Biologically synthesised silver nanoparticles from three diverse family of plant extracts and their anticancer activity against epidermoid A431 carcinoma. J Colloid Interface Sci 457:329–338. https://doi.org/10.1016/j.jcis.2015.07.012
294. Saber MM, Mirtajani SB, Karimzadeh K (2018) Green synthesis of silver nanoparticles using *Trapa natans* extract and their anticancer activity against A431 human skin cancer cells. J Drug Deliv Sci Technol 47:375–379. https://doi.org/10.1016/j.jddst.2018.08.004
295. Vakayil R, Muruganantham S, Kabeerdass N, Rajendran M, Mahadeo-Palve A, Ramasamy S et al (2021) *Acorus calamus*-zinc oxide nanoparticle coated cotton fabrics shows antimicrobial and cytotoxic activities against skin cancer cells. Process Biochem 111:1–8. https://doi.org/10.1016/j.procbio.2021.08.024
296. Wu H, Wang MD, Zhu JQ, Li ZL, Wang WY, Gu LH, Shen F, Yang T (2022) Mesoporous nanoparticles for diagnosis and treatment of liver cancer in the era of precise medicine. Pharmaceutics. https://doi.org/10.3390/pharmaceutics14091760
297. Ji Y, Cao Y, Song Y (2019) Green synthesis of gold nanoparticles using a *Cordyceps militaris* extract and their antiproliferative effect in liver cancer cells (HepG2). Artif Cells Nanomed Biotechnol 47:2737–2745. https://doi.org/10.1080/21691401.2019.1629952
298. Zhan Q, Han J, Sheng L (2021) Iron nanoparticles green-formulated by *Coriandrum sativum* leaf aqueous extract: investigation of its anti-liver cancer effects. Arch Med Sci. https://doi.org/10.5114/aoms/144627
299. Saratale RG, Shin HS, Kumar G, Benelli G, Kim DS, Saratale GD (2018) Exploiting antidiabetic activity of silver nanoparticles synthesized using *Punica granatum* leaves and anticancer potential against human liver cancer cells (HepG2). Artif Cells Nanomed Biotechnol 46:211–222. https://doi.org/10.1080/21691401.2017.1337031
300. Inbathamizh L, Ponnu TM, Mary EJ (2013) *In vitro* evaluation of antioxidant and anticancer potential of *Morinda pubescens* synthesized silver nanoparticles. J Pharm Res 6:32–38. https://doi.org/10.1016/j.jopr.2012.11.010
301. Mohammadi Shivyari A, Tafvizi F, Noorbazargan H (2022) Anti-cancer effects of biosynthesized zinc oxide nanoparticles using *Artemisia scoparia* in Huh-7 liver cancer cells. Inorg Nano-Met 52:375–386. https://doi.org/10.1080/24701556.2021.1980018
302. Qasim Nasar M, Zohra T, Khalil AT, Saqib S, Ayaz M, Ahmad A, Shinwari ZK (2019) *Seripheidium quettense* mediated green synthesis of biogenic silver nanoparticles and their theranostic applications. Green Chem Lett Rev 12:310–322. https://doi.org/10.1080/17518253.2019.1643929
303. Taghavizadeh Yazdi ME, Darroudi M, Amiri MS, Hosseini HA, Nourbakhsh F, Mashreghi M, Farjadi M, Mousavi Kouhi SM, Mousavi SH (2020) Anticancer, antimicrobial, and dye degradation activity of biosynthesised silver nanoparticle using *Artemisia kopetdaghensis*. Micro Nano Lett 15:1065–1070. https://doi.org/10.1049/mnl.2020.0387
304. Ashokkumar T, Prabhu D, Geetha R, Govindaraju K, Manikandan R, Arulvasu C, Singaravelu G (2014) Apoptosis in liver cancer (HepG2) cells induced by functionalized gold nanoparticles. Colloids Surf B Biointerfaces 123:549–556. https://doi.org/10.1016/j.colsurfb.2014.09.051
305. Amuthavalli P, Hwang JS, Dahms HU, Wang L, Anitha J, Vasanthakumaran M, Gandhi AD, Murugan K, Subramaniam J, Paulpandi M, Chandramohan B (2021) Zinc oxide nanoparticles using plant *Lawsonia inermis* and their mosquitocidal, antimicrobial, anticancer applications showing moderate side effects. Sci Rep. https://doi.org/10.1038/s41598-021-88164-0
306. Chung IM, Abdul Rahuman A, Marimuthu S, Vishnu Kirthi A, Anbarasan K, Rajakumar G (2015) An investigation of the cytotoxicity and caspase-mediated apoptotic effect of green synthesized zinc oxide nanoparticles using *Eclipta prostrata* on human liver carcinoma cells. Nanomaterials 5:1317–1330. https://doi.org/10.3390/nano5031317
307. Chung IM, Abdul Rahuman A, Marimuthu S, Vishnu Kirthi A, Anbarasan K, Padmini P, Rajakumar G (2017) Green synthesis of copper nanoparticles using *Eclipta prostrata* leaves extract and their antioxidant and cytotoxic activities. Exp Ther Med 14:18–24. https://doi.org/10.3892/etm.2017.4466
308. Liu L, Kshirsagar PG, Gautam SK, Gulati M, Wafa EI, Christiansen JC, White BM, Mallapragada SK, Wannemuehler MJ, Kumar S, Solheim JC (2022) Nanocarriers for pancreatic cancer imaging, treatments, and immunotherapies. Theranostics 12(3):1030. https://doi.org/10.7150/thno.64805
309. Fazal S, Jayasree A, Sasidharan S, Koyakutty M, Nair SV, Menon D (2014) Green synthesis of anisotropic gold nanoparticles for photothermal therapy of cancer. ACS Appl Mater Interfaces 11:8080–8089. https://doi.org/10.1021/am500302t

310. Chanda N, Shukla R, Zambre A, Mekapothula S, Kulkarni RR, Katti K et al (2011) An effective strategy for the synthesis of biocompatible gold nanoparticles using cinnamon phytochemicals for phantom CT imaging and photoacoustic detection of cancerous cells. Pharm Res 2:279–291. https://doi.org/10.1007/s11095-010-0276-6
311. Fathy MM (2020) Biosynthesis of silver nanoparticles using thymoquinone and evaluation of their radio-sensitizing activity. Bionanoscience 10(1):260–266. https://doi.org/10.1007/s12668-019-00702-3
312. Mosleh-Shirazi S, Kasaee SR, Dehghani F, Kamyab H, Kirpichnikova I, Chelliapan S, Firuzyar T, Akhtari M, Amani AM (2023) Investigation through the anticancer properties of green synthesized spinel ferrite nanoparticles in present and absent of laser photothermal effect. Ceram Int 49(7):11293–11301. https://doi.org/10.1016/j.ceramint.2022.11.329
313. Yusefi M, Shameli K, Hedayatnasab Z, Teow SY, Ismail UN, Azlan CA et al (2021) Green synthesis of Fe_3O_4 nanoparticles for hyperthermia, magnetic resonance imaging and 5-fluorouracil carrier in potential colorectal cancer treatment. Res Chem Intermed 47(5):1789–1808. https://doi.org/10.1007/s11164-020-04388-1

Publisher's Note